9-12-2023

Role of Copyback Viral Genomes in Activating Cellular Stress Responses During Pneumovirus and Paramyxovirus Infection

Lavinia Jose Gonzalez Aparicio
Washington University in St. Louis

WASHINGTON UNIVERSITY IN ST. LOUIS
Division of Biology and Biomedical Sciences
Molecular Microbiology and Microbial Pathogenesis

Dissertation Examination Committee:
Carolina B. López, Chair
Michael Diamond
Andrew Janowski
Deborah Lenschow
Daisy Leung
David Wang

Role of Copyback Viral Genomes in Activating Cellular Stress Responses During Pneumovirus and Paramyxovirus Infection

by
Lavinia J. González Aparicio

A dissertation presented to
Washington University in St. Louis
in partial fulfillment of the
requirements for the degree
of Doctor of Philosophy

August 2023
St. Louis, Missouri

Table of Contents

List of Figures

List of Abbreviations

cbVGs: copyback viral genomes

CHX: cycloheximide

DDO: DVG-derived oligonucleotides

FISH: Fluorescent *in situ* hybridization

G3BP1: Ras-GTPase-activating protein-binding protein 1

G3BP2: Ras-GTPase-activating protein-binding protein 2

GCN2: General control non-depressible 2

HPIV: Human Parainfluenza virus

HRI: Heme-regulated eIF2a kinase

IAV: Influenza virus

IFN: Interferon

ISGs: Interferon stimulated genes

MAVS: Mitochondrial Antiviral Signaling

MOI: Multiplicity of infection

PERK: Protein kinase R-like ER kinase

PKR: Protein Kinase R

Poly I:C: Polyinosinic:polycytidylic acid

RdRP: RNA-dependent RNA polymerase

RIG-I: Retinoic acid-inducible gene I

RLB: RNAse L-dependent bodies

RLR: RIG-I-like receptors

RSV: Respiratory syncytial virus

SeV: Sendai virus

SGs: Stress granules

stVG: Standard viral genome

$TCID_{50}$: Tissue culture infectious dose

TIAR: T-cell intracellular antigen 1 related

Acknowledgments

I would like to thank my PI, Carolina, for supporting me throughout these years from the start of my PhD at UPenn to the end here at Washu. Transferring universities during a PhD is not common, but I am glad I did it with the support of Carolina and the lab. Her excitement towards science together with her intellectual guidance made the graduate experience enjoyable. I would like to thank my thesis committee, for their support and suggestions on how to move my project forward. Their expertise made this dissertation possible.

I would like to thank my amazing lab, both Lopez lab 1.0 (UPenn) and Lopez lab 2.0 (Washu) for making my daily life in lab fun and enriching. I am lucky to be part of a lab made of incredibly intelligent, incredibly kind, and incredibly funny people. It is rare to find people that can find a balance between the seriousness of science and the absurdity of everyday life. It would have been impossible to develop this project without the constant support and intellectual contribution I received from the lab.

I want to thank all the mentors that helped me get into grad school: Dr. Reginald Morales, Dr. Orestes Quesada, Dr. Ingrid Montes, and Dr. Paul Bates. They all saw a potential in me that, at that moment, I could not see in myself. They inspired me to continue pursuing knowledge and enabled me to shoot higher than I thought I could.

I would also like to thank all the friends I have made throughout my scientific (and non-scientific) journey. From my time in the University of Puerto Rico, to The University of Pennsylvania to finally Washington University in St Louis, I was lucky enough to encounter many kindred spirits that made me not only a better scientist but also a better person.

Finally, I would like to thank my family for always supporting my nerdy behavior and always serving as my emotional safe space.

Lavinia Gonzalez Aparicio,

Washington University in St Louis

August 2023

Dedicated to my father,

for always persuading me to seek knowledge above all things.

ABSTRACT OF THE DISSERTATION

Role of Copyback Viral Genomes in Activating Cellular Stress Responses During Pneumovirus and Paramyxovirus Infection

by

Lavinia J. González Aparicio

Doctor of Philosophy in Biology and Biomedical Sciences

Molecular Microbiology and Microbial Pathogens

Washington University in St Louis, 2023

Professor Carolina B. López

The interactions that occur between a virus and the infected cell determine the success of an infection. During negative-sense single-stranded RNA virus infections, copyback viral genomes (cbVGs) drive key virus-host interactions by activating the Mitochondrial Antiviral Signaling (MAVS) pathway that induces antiviral immunity and leads to reduced levels of virus replication. Whether cbVGs induce other cellular pathways and how these relate to their immunostimulatory activity is unknown. Here we show that cbVGs also induce a cellular stress response during pneumovirus and paramyxovirus infections. cbVGs activate the cellular stress response through Protein Kinase R (PKR) signaling, triggering translation inhibition and stress granule formation. The stress response is induced independent of MAVS signaling and does not have global effects on the antiviral immunity, demonstrating that cbVGs induce both pathways independently. The translation inhibition that accompanies the stress response leads to a reduction of virus protein levels that extends for several days after the initial infection. The work presented in this dissertation reveals a new cbVG-driven mechanism of viral interference where cbVGs induce a PKR-dependent cellular stress response that leads to reduction in viral

protein expression without altering overall antiviral immunity. Elucidating the pathways that viruses activate in the cell and the effects these have in shaping the infection outcome broadens our understanding on the intricate evolutionary relationship between the pathogen and the host it infects. This knowledge will also serve as the basis for developing therapies that allow us to harness these virus-host interactions to combat RNA virus disease burden.

Chapter 1

Introduction

1.1. Impact of RNA Viruses in Human Diseases

RNA viruses are the causative agents of some of the most catastrophic pandemics humankind has faced in the last two centuries. The ability of RNA viruses to infect a broad range of hosts, together with their fast host adaptability and ease of transmission, make RNA viruses a constant threat to the human population [1]. Out of the context of pandemics, endemic RNA viruses such as Respiratory Syncytial virus (RSV), Human Parainfluenza viruses (HPIVs), Influenza virus (IAV) and others, cause tremendous disease burden annually around the world [2-5]. In addition to acute disease, infection with these viruses in early life correlates with development of severe chronic respiratory diseases and recurrent lower respiratory tract infections [6-10]. Vaccine and therapeutic effectiveness can often be hindered by the RNA virus high mutation rates and the host's inability to mount a strong immune response, as exemplified by the inconsistent effectiveness of the IAV vaccine [11, 12] and lack of vaccines for the general population for viruses like metapneumovirus, rhinovirus and the HPIVs [13]. Understanding how RNA viruses interact with the host, cause disease, and spread will allow us to design better treatments and preventive care to reduce their disease burden.

Specifically, RSV and the HPIVs are seasonal viruses that affect primarily children and older adults. RSV alone is the main cause of infant respiratory disease worldwide accounting with 3.3 million yearly hospitalizations and approximately 26,000 deaths [2, 14, 15]. It is estimated that one in 50 deaths of children aged 0-60 months are due to RSV-associated disease [2]. Moreover, approximately 4% of the deaths due to acute lower respiratory infection in children are caused by HPIV infection [16]. Currently, monoclonal antibody-based therapies against RSV work as prophylactics and are available only for high-risk cases in children [17].

Recently, an RSV vaccine was developed but is only approved for adults of 60 years and older [18]. For HPIV no vaccine or therapy is available. The impact that RSV and HPIVs have in the human population, especially in children under the age of 5, calls for increase research and development of therapies to combat the respiratory disease caused by these viruses. Understanding the molecular mechanisms RSV and the HPIVs use to infect their host can provide with the basis for developing better antiviral therapies and prophylactics to prevent RSV and HPIV-associated disease burden.

1.2. Negative-sense Single-stranded RNA Virus Replication

Within the RNA virus realm, *Riboviria*, viruses like RSV and HPIVs are part of the mononegavirales order, which include non-segmented negative-sense RNA viruses [19]. These viruses are characterized by containing an RNA genome in the 3' to 5' orientation [20]. The negative-sense RNA genome encodes for all the necessary proteins required for the virus replication, together with accessory proteins that although not essential, serve to modulate virus pathogenesis [20]. One of these essential genes encodes for the RNA-dependent RNA polymerase (RdRP), which contrary to the polymerases found in prokaryotes and eukaryotes, can synthesize RNA from an RNA template and generate RNA strands with a 3' to 5' direction [21]. Upon entry to the cell, the RdRP initiates transcription at the 3' end promoter region termed leader region to generate positive-sense viral mRNA [21]. Once viral proteins are made from the mRNA, the same RdRP begins replication of the genome by first synthesizing the anti-genome from the leader promoter. This generates a positive-sense RNA strand that is the reverse complement of the virus genome [21]. With this new anti-genome, the RdRP then binds to the 3' end of the anti-genome, termed the trailer promoter region, and begins

synthesizing the genome, generating a negative-sense RNA strand that will be eventually packaged and released to infect other neighboring cells (**Figure 1.1**).

Additional to the RdRP, negative-sense single-stranded RNA viruses encode for viral proteins that are important for replication. The virus nucleoprotein, for example, is one of the most conserved and abundant protein made during negative-sense single-stranded RNA virus infections. This protein coats the genome and anti-genome, serves to protect the RNA from cytoplasmic RNA sensors and is essential for virus replication [22, 23]. The lack of nucleoprotein expression leads to aberrant production of viral RNAs and enhanced activation of antiviral immune responses [24]. Nucleoprotein concentrations during infection has shown to be important in controlling the shift from transcription to replication [25]. The virus phosphoprotein is also important for efficient replication of the genome. The phosphoprotein plays roles in recruiting and stabilizing the RdRP and preventing the nucleoprotein from binding to non-viral RNAs [26-28]. Together, the viral RNA with the nucleoprotein, phosphoprotein and RdRP make up the ribonucleoprotein complex that allows for replication of the virus.

The fast adaptability of negative-sense RNA viruses and ease of escape from the hosts immune response is in part attributed to the high rates of mutations RNA viruses acquire from the error-prone RdRP that lacks proofreading activity [29-31] . Errors that occur during replication of negative-sense RNA viruses can cause an array of mutations and aberrations leading to the production of a diverse population of virus particles that shift the outcome of the infection. This diverse population of virus particles ultimately help the virus become more fit to

successfully spread and be maintained within the host population [31, 32]. For this reason, we describe negative-sense RNA viruses as a community, where all the members have different functions and contributions that ultimately affect the fate of both the virus and the host [33].

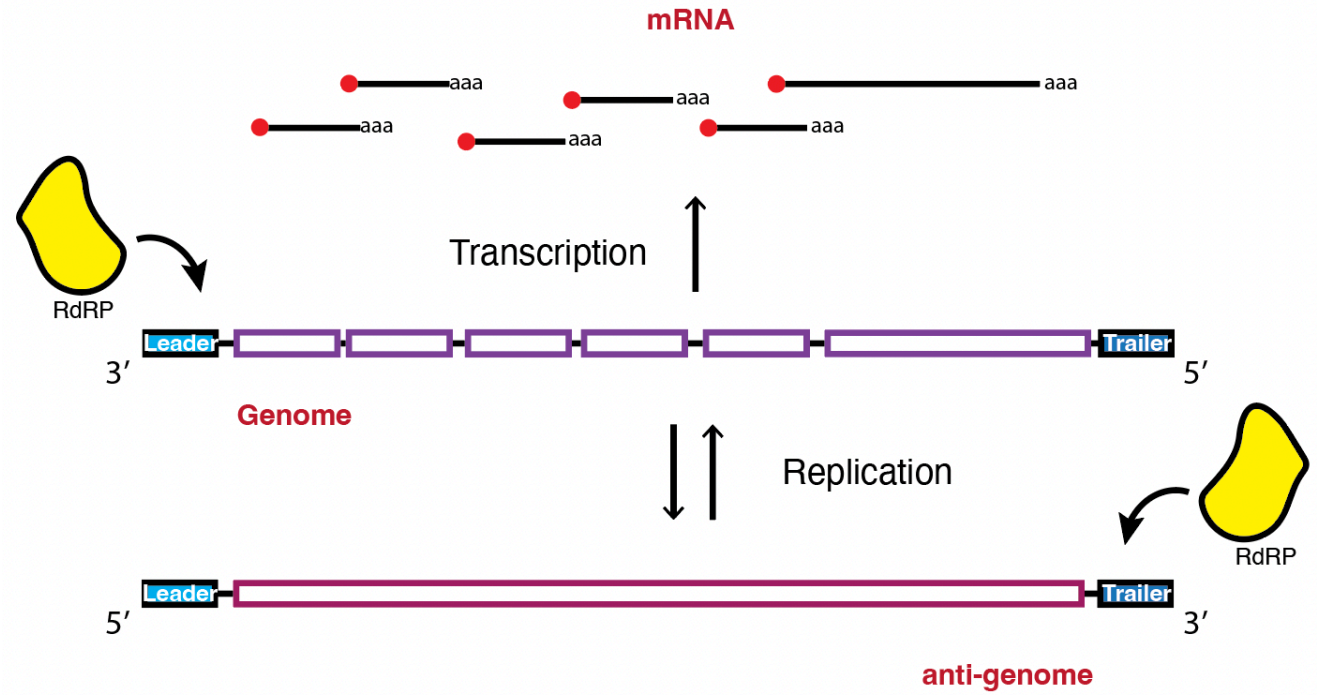

Figure 1.1. **Replication of negative-sense single-stranded RNA viruses.** The RNA-dependent RNA polymerase (RdRP) initiates transcription and replication at the leader promoter. To make genomic RNA, RdRP binds to the trailer promoter of the anti-genome and synthetizes the reverse complement strand.

1.3. Role of Non-standard Viral Genomes During RNA Virus Replication

The negative-sense RNA virus community can differ at the particle level, where different particle shape and protein composition can change the fitness of the virus by facilitating entry or by evading extracellular immune responses in the host [34-37]. At the genomic level the virus can generate variants that harbor one or more mutations acquired during multiple rounds

of replication [38]. These mutations can change the function of the viral genes to either increase fitness at the replication level or modulate the virus-host interactions within the cell [39]. Variants that are selected during infection often retain the replication capabilities of a full-length standard genome. Another type of genome, non-standard viral genomes, arise during viral replication. Non-standard viral genomes are often highly truncated and thus are replication defective because they lack genes that encode for proteins important for replication [40]. For non-standard viral genomes to replicate and spread, it is necessary that the standard viral genome is also present in the same cell [40] . The co-infecting standard viral genome provides with the necessary proteins the non-standard viral genomes need to replicate.

Within the non-standard viral genomes, two types are the most studied. The first type are deletion viral genomes, which have been identified more abundantly during replication of positive-sense single-stranded RNA viruses and negative-sense segmented RNA viruses [41]. Deletion viral genomes are predicted to arise when the virus polymerase initiates replication of the virus genome and as it elongates, falls off the template at a break point. Instead of reattaching where it fell off, it rejoins at a down-stream spot and continues replication, generating an RNA strand with missing nucleotides (**Figure 1.2A**). The second type of non-standard viral genomes are the copyback viral genomes (cbVGs), which are commonly detected in high abundance during infections with negative-sense single-stranded RNA viruses [41]. Like deletion viral genomes, cbVGs are predicted to arise as the polymerase elongates and breaks off the template but instead of re-attaching to the template, re-attaches to the nascent strand at a rejoin point and continues replicating [42]. This causes the polymerase to "copy back" the strand it began synthetizing, generating an RNA strand that contains highly

complementary ends together with a predicted “loop” containing the RNA sequence before the breaking point (**Figure 1.2B**) [42].

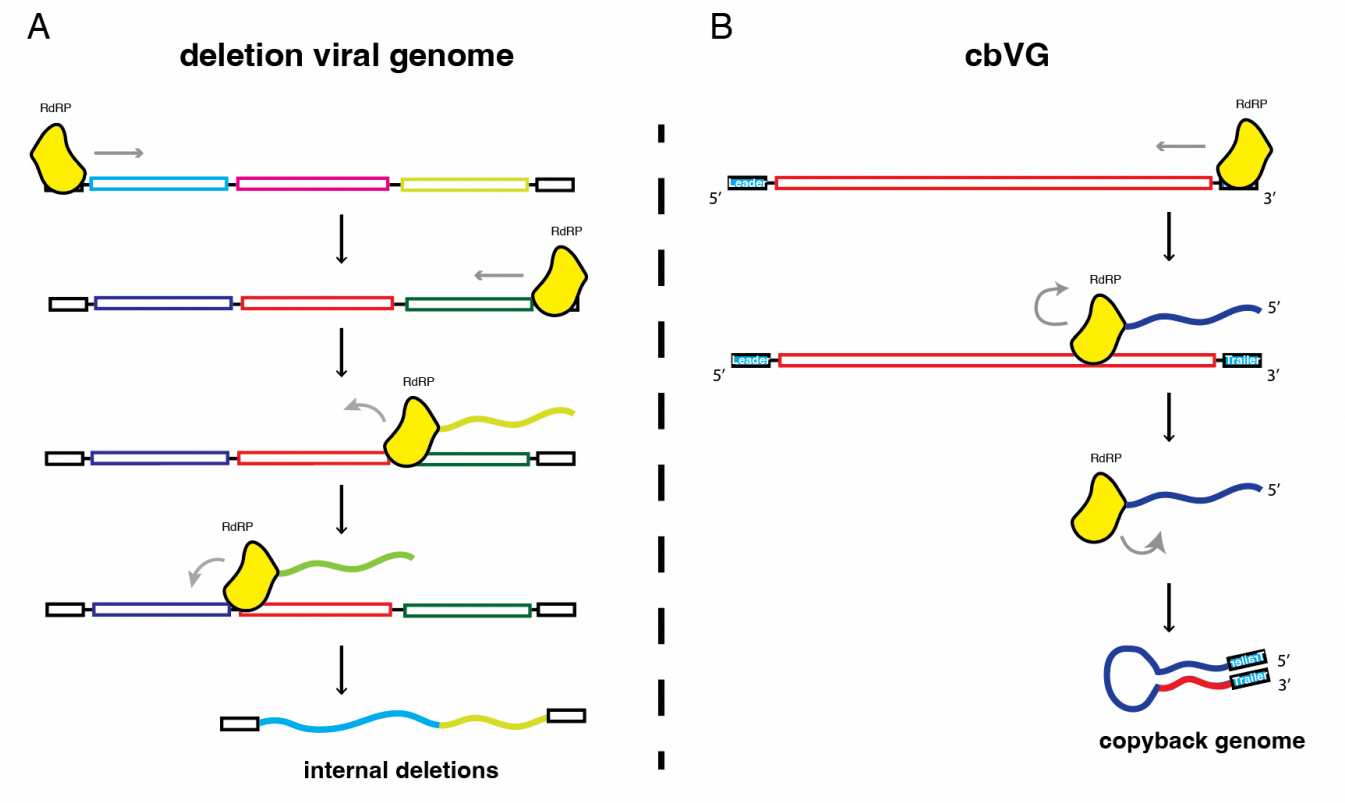

Figure 1.2. **Generation of deletion and cbVGs**. (A) Deletion viral genomes form when the polymerase initiate RNA synthesis, falls off the template, and rejoins at a downstream point. Deletion viral genomes contain internal truncations and retain both promoters. (B) cbVGs form when the polymerase falls off the template and rejoins the nascent strand to continue RNA synthesis. This generates an RNA that contains the sequence from the genome until the break point. After the breakpoint, it contains the complementary sequence of the genome. This complementarity leads to a predicted hairpin loop structure. cbVGs contain trailer promoters at both ends of the RNA strand.

cbVGs are the subject of intense research as their functions during virus replication have proven to greatly influence the outcome of the infection. Within these functions are

interfering by competing with the standard virus replication, activating cellular antiviral responses, and facilitating the establishment of persistence [40, 41, 43]. Understanding the many functions cbVGs have has allowed scientist to begin exploiting cbVG's potential for use as therapeutics [44]. Due to the great impact cbVGs have in both the virus and the host, it is of utmost importance to fully elucidate cbVGs functions to ensure the safety and efficacy of their use as therapeutics.

1.3.1 cbVGs and Virus Interference

The ability of cbVGs to compete for viral resources and reduce standard viral genome replication is the base for most on-going development of cbVG-based therapeutics. The nature of the cbVG RNA strand allows it to be selected for during replication. cbVGs are not only shorter in size compared to the standard viral genome, but also contain two trailer promoters (**Figure 1.1B**) [40]. The trailer promoter is known to have more affinity for the viral polymerase than the leader promoter [45]. This provides the cbVG RNA a replication advantage over the standard virus.

Accumulation of cbVGs leads to a reduction of standard viral genomes and therefore, reduction of factors necessary for the virus to complete its lifecycle. This way, copyback viral genomes cause the virus' demise by inhibiting production of infectious particles and virus spread. At the same time, because cbVGs do not encode for viral proteins important for replication, their own replication is eventually blocked. This mechanism of interference with the standard genome has provided ground for scientists to develop viral particles containing cbVGs that, when introduced to a host infected with the standard virus, can help reduce virus

replication and therefore serve as a therapeutic for treating the infection [46]. These cbVG-containing particles are known as therapeutic interfering particles and are currently being tested for many different viruses as therapeutics [44, 46].

1.3.2 cbVGs and Antiviral Immunity

Another important role cbVGs play during infection is the triggering of antiviral immune responses in the cell that result in inflammation and the development of protective antiviral immunity. it has been demonstrated that during Sendai virus (SeV) and RSV infection cbVGs induce Retinoic acid Inducible Gene-I like receptors (RLRs) that recognize foreign RNA in the cell and activate the Mitochondrial Antiviral Signaling (MAVS) protein [47-50]. MAVS activation leads to a signaling cascade that involves the production of interferons (IFNs) [51]. IFNs are key secreted signaling proteins that bind to IFN receptors in the cell membrane and cause the transcription of IFN stimulated genes (ISGs) in both infected and non-infected neighboring cells [52]. ISGs make a plethora of proteins that will directly combat the virus and/or cause an inflammatory response to recruit innate immune cells that will eventually result in virus clearance from the host [52].

The effects of cbVGs in disease outcome have been demonstrated *in vivo*, where activation of the antiviral immune responses by SeV and RSV cbVGs leads to reduced disease severity and faster recovery from the infection in mice [48, 50]. In humans, timing, and duration of RSV cbVG detection in patients correlate with disease outcome [53]. Early accumulation and fast clearance of cbVGs in human patients correlated with better disease outcomes [53]. In contrast, late accumulation, and longer presence of cbVGs in the patients led to worse

disease outcomes [53]. These correlations show that detection of cbVGs can be used as a tool for prognosis of disease outcomes in patients more accurately than virus titers, which showed to have no correlation with disease outcome [53].

At the molecular level, our laboratory has elucidated the SeV cbVG immunostimulatory motifs necessary for activation of the antiviral immune response. A predicted stem loop structured between nucleotides 70-114 from the most prominent cbVG identified in our SeV virus stocks contained high immunostimulatory capabilities [54]. This motif was necessary and sufficient to induce antiviral immunity. Identification of this motif led to the development of a DVG-derived oligonucleotide (DDO) that works as an effective adjuvant for vaccines against intracellular pathogens [55]. This is important because currently, there are no licensed adjuvants that induce type I immune responses, which include activation of cytotoxic CD8 T cells important for defense against intracellular pathogens like viruses [55]. The use of DDO as an adjuvant demonstrated to be more efficient at mounting immune protection during challenge after vaccination [55]. The use of cbVG detection as a tool to predict disease outcome and the application of DDOs as effective adjuvants demonstrate the power of cbVG research has in advancing the medical field.

1.3.3. cbVGs and Virus Persistence

The counterintuitive role cbVGs have during the virus infection in interfering with replication and activating the immune response can be puzzling, especially because these types of non-standard viral genomes appear to be selected for throughout the virus evolution. In the context of an infection in a host, reducing the virus titers by interfering with replication

and activating the immune response could be beneficial to the virus by reducing the rate of infection within the host that would otherwise kill the host before the virus has a chance to spread to other hosts. Recent studies have shed light into some of the mechanisms by which the antiviral immune response is related to the establishment of persistent infections [56]. These studies follow previous work that for decades have correlated presence of non-standard viral genomes with the establishment of persistent RNA infections [57-60]. In a study form our laboratory it was shown that during SeV infection, activation of MAVS signaling by cbVGs led to the induction of a Tumor Necrosis Factor dependent-survival pathway that allows cells to survive the infection [56]. This survival mechanism led to the generation of persistently infected cells that could be maintained in culture for indefinite amounts of time [56]. The role of cbVGs in establishing persistent infections is important to consider when developing cbVG-based therapies. Therefore, additional to studying how cbVG particles can be used to reduce pathogenesis and virus replication, these studies should also look at the long-term effects these therapies can have in the study subjects.

1.4. Role of the Integrated Cellular Stress Response During Virus Infections

1.4.1 The integrated Cellular Stress Response

It is now clear that cbVGs are an important component of the RNA virus population and key interactors with the host cell. The diverse functions cbVGs have during infection opens the potential to explore other cellular pathways cbVGs could be activating in the cell. One previously unexplored pathway is the activation of the stress responses that have been described to be induced during RNA virus infection. The cellular stress response is activated

when a cell is exposed to specific environmental stresses that threaten cellular homeostasis. Different types of stresses are detected by four cytoplasmic kinases that initiate the stress response: Heme-regulated eIF2α kinase (HRI), which detects reactive oxygen species [61]; General Control Non-depressible 2 (GCN2) detects low amino acid availability due to starvation [62]; Protein kinase R-like ER kinase (PERK) detects unfolded proteins [63] and Protein Kinase R (PKR) detects dsRNA [64]. The activation of any of these kinases leads to the phosphorylation of the eukaryotic initiation factor 2 alpha (eIF2α) which is important for initiating cap-dependent translation [65]. In the unphosphorylated form, eIF2α can recruit the first methionine tRNA to the ribosome allowing ribosome elongation for protein synthesis [65]. Once translation initiates, eIF2α is released to be recycled for recruitment of the first tRNA to other ribosomes [65]. Recycling of eIF2α requires the exchange of GDP to GTP by the eIF2B factor [66]. When the serine 51 residue of eIF2α is phosphorylated, the affinity of eIF2B binding to eIF2α increases, preventing exchange of GDP to GTP [67]. This process inhibits eIF2α recycling and therefore blocks initiation of cap-dependent translation **(Figure 1.3)** [67].

The inability of ribosomes to initiate reading through the mRNAs causes ribosome-mRNA disassembly, leading to an accumulation of free mRNA in the cytoplasm of the cell [68]. To avoid degradation of the host mRNA and activation of RNA detectors in the cytoplasm, the cell induces a process where proteins will bind to the mRNA to form liquid-liquid phase separated non-membranous organelles called stress granules **(Figure 1.3)** [68, 69]. Stress granules form to stabilize the mRNA and many translation initiation factors while the cell recovers from the stress [70]. This way, translation can continue after the cell recovers without the need to replenish the mRNA pool.

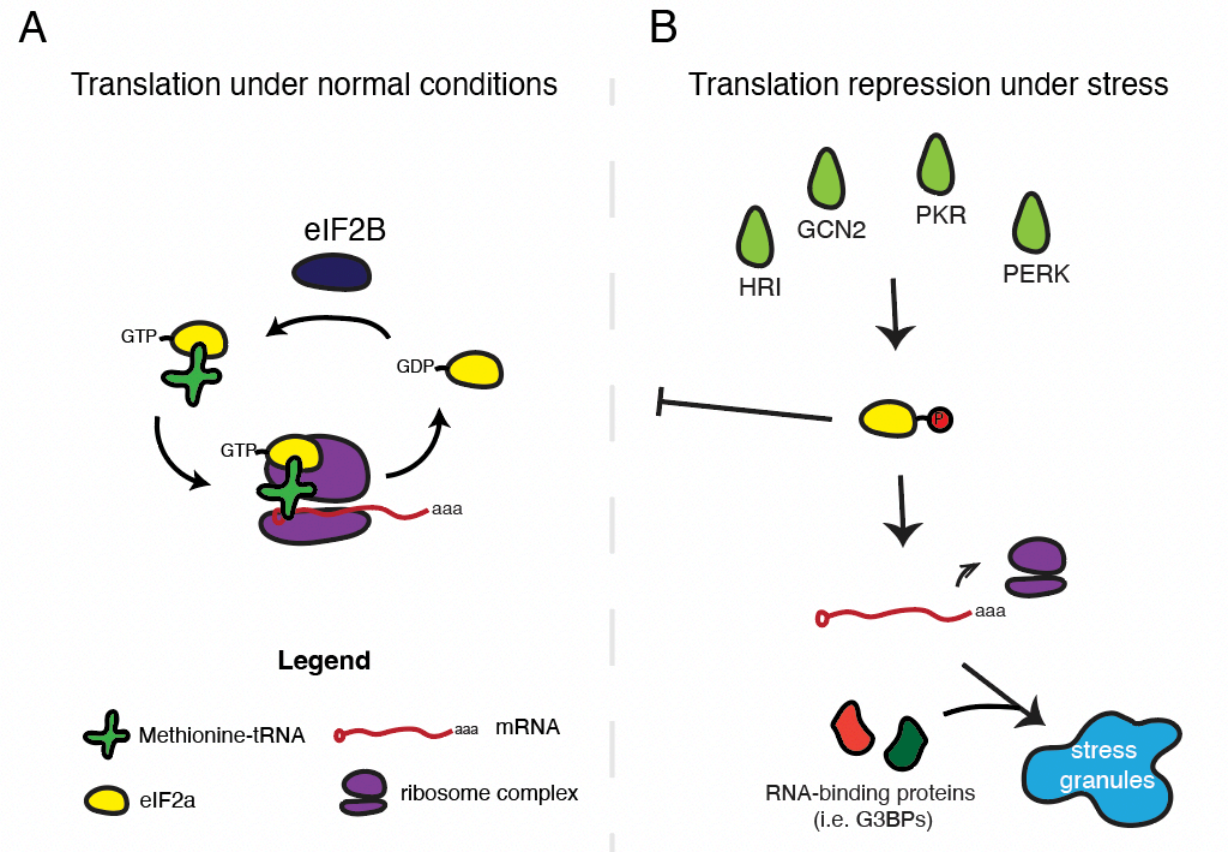

Figure 1.3. Regulation of Cap-dependent Translation. (A) Under normal conditions, eIF2α in its GTP form recruits the first methionine tRNA to the ribosome complex to initiate peptide synthesis. Upon recruitment, GTP is hydrolyzed and eIF2α remains in its GDP form until EIF2B binds GDP-eIF2α and causes GTP exchange. Once this occurs, eIF2α can be reused to continue initiation of translation of other mRNAs. (B) When any of the eIF2α kinases phosphorylates eIF2α, eIF2α cannot be recycled for translation, causing disassembly of mRNA from ribosomes. This disassembly, together with recruitment of RNA binding proteins like Ras GTPase-activating protein-binding (G3BP1), leads to stress granule formation.

Translation inhibition by eIF2α kinases together with stress granule formation are two tied processes that allow the cell to conserve energy in times of stress. By inhibiting cap-dependent translation, the cell reconfigures the translating machinery to stop the production of

unessential proteins and produce proteins that specialize in stress recovery [71]. Many of these stress proteins contain upstream open reading frames that only translate when eIF2α is phosphorylated. Some of these proteins, like GADD34, are also part of a negative feedback loop that reverses eIF2α phosphorylation upon resolution of the stress [72]. While the cell recovers, the untranslated mRNA is stored in stress granules to prevent energy expenditure re-transcribing all the mRNA after the stress resolves. Because viruses require the translation machinery to produce viral proteins, it is not surprising that the stress response has evolved to detect virus components and induce translation inhibition to prevent viral proteins from being made by the cell. On the same line, viruses have also evolved mechanisms to prevent or hijack the stress response to facilitate virus replication.

1.4.2. The Stress Response and Antiviral Immunity

Stress granule formation occurs during infections with many viruses and for the most part, are formed through the induction of PKR signaling, except for Sinbis virus which has shown to activate GCN2 instead [73]. PKR is a double-stranded RNA-binding protein that can detect host and viral double-stranded RNA [74, 75]. Additional to playing a role in activating the stress response, PKR can activate the antiviral immune response and control cell survival [76, 77]. The role PKR has in cell survival is controversial, as conflicting evidence shows that PKR can both induce and inhibit cell apoptosis [76-78]. In context of antiviral immunity, PKR has shown to be important only in the context of some virus infections. Knocking out PKR leads to a reduction of IFN expression during Theiler's murine encephalomyelitis, Semliki Forest, West Nile and encephalomyocarditis virus infection [79, 80]. This effect on IFN expression was not observed, however, during IAV or SeV infection [79, 80]. A role for PKR in inducing nuclear

factor kappa B subunit 1 (NF-KB) signaling has also been demonstrated, although these studies were done using synthetic RNA transfections and may not reflect what occurs during natural infections [81]. Because many viruses, including RSV, IAV and HCV, encode antagonists that block PKR activity it is widely accepted that PKR is an antiviral protein [82-87]. However, whether the antiviral roles PKR has are due to the role in antiviral immunity, apoptosis or translation inhibition needs to be elucidated. Nevertheless, interfering with PKR activity is a well-described mechanism of inhibiting the stress response.

Some viruses can inhibit the stress response by directly affecting eIF2α phosphorylation downstream of PKR. This occurs by upregulating factors like GADD34, which reverse the phosphorylation of eIF2α and allows translation to resume during the infection [88, 89]. Other viruses antagonize the stress response downstream of PKR and eIF2α phosphorylation by antagonizing stress granule nucleating factors like the Ras GTPase-activating protein-binding protein 1 (G3BP1), suggesting that formation of stress granules can also have antiviral roles independent of the translation inhibition [90-93]. Members of the picornaviruses prevent stress granule formation by cleavage of G3BP1 by one of the viral encoded proteins [92, 94, 95]. Other viruses, like the flaviviruses and coronaviruses, sequester stress granule components and recruit them to sites of replication, preventing stress granule assembly [90, 96, 97]. This is also observed during SeV infection, where the trailer sequence of the RNA sequesters the stress granule component TIAR to prevent stress granules from forming [98].

The implications of translation inhibition and stress granule formation during virus infections have been the subject of intensive research. Particularly, accumulating evidence

suggests that the formation of stress granules is important for inducing the antiviral immune response and inhibition of stress granules leads to reduced levels of IFN production [99, 100]. This has been proposed during IAV [101], SeV [102], Encephalomyocarditis virus [103] and Newcastle disease virus [104]. Moreover, stress granules are often described to be signaling hubs where the cell encounters the viral RNA to induce antiviral immunity [101, 102, 105]. This is all based on localization of receptors like RIG-I, MDA-5 and PKR into the stress granules using fluorescence imaging [101, 102, 106]. However, it has also been shown that localization of MDA-5 in stress granules is not necessary for the induction of IFN [106], and these receptors still localize in stress granules when the stress response is induced by drugs that do not lead to activation of the antiviral immune response [106]. In addition, studies using Encephalomyocarditis virus, Mumps and SeV demonstrated that stress granules are not required to induce the antiviral immune response, and, in some instances, they function to tamper the antiviral immune response [106-109].

There are several potential explanations for the contradictory roles stress granules have been shown to play during infection. First, many of these studies are done by using viruses that lack expression of inhibitors of the stress response. IAV lacking NS1 expression is used to study formation of stress granules [101]. Likewise, SeV and Measles viruses lacking expression of the C protein also are used to induce activation of PKR [110, 111]. Using these viruses does not represent the wildtype virus and provide little information about the actual role stress granules play during a natural infection. The absence of these viral proteins could also be causing effects during the infection that are independent of stress granule formation.

The different mechanisms of inhibiting stress granules can also be a contributing factor to the contradictions in the literature. There are inconsistencies in the literature with the cellular systems used to prevent formation of stress granules. This is particularly important because molecules like PKR and G3BP1, which are often knocked out to inhibit stress granule formation, have stress granule-independent roles. As mentioned before, PKR has shown to be involved in NFkB signaling and proper induction of IFN during viral infections [81, 112]. G3BP1 has shown to enhance RIG-I activation [113, 114]. Therefore, knocking out proteins that have stress granule-independent roles can lead to misinterpretations of the function stress granules play during the infection.

Another important source of discrepancy within the field is the characterization of the granules themselves. Simply staining for stress granule markers is not sufficient to demonstrate that the granules formed during the infection are canonical stress granules. This is important to note because often these studies are often done using transfection of dsRNA into cells, which has been shown to induce RNAse L-dependent bodies (RLBs) and not canonical stress granules [115]. While the function is not known, RLBs inhibit the formation of canonical stress granules [116]. Differentiation of both types of granules is complex as both share many protein markers, which has been demonstrated by proteome composition analysis of stress granules compared to RLBs [115]. For this reason, extended characterization, including treatment with drugs that disassemble stress granules and leave RLBs and other granules intact, together with elucidation of the receptors required to induce the formation of the granules is important when defining the roles of stress granules. Unfortunately, most of

these studies mentioned above do not characterize the granules observed during virus infection.

Finally, a major contributor to the conflicting evidence in the virology field is the lack of characterization of the RNA virus population contained in the virus stocks used in research laboratories. Particularly, surveying the levels of non-standard viral genomes found in virus stocks is important as they are key modulators of the infection outcome. For example, although the factors that lead to generation of cbVGs are not fully elucidated, evidence suggest the C protein is a major contributor in controlling accumulation of cbVGs during paramyxovirus infection [117, 118]. It is not surprising then, that only by using SeV and measles viruses lacking the C protein can researchers detect PKR activation and, potentially, stress granule formation during infection [110, 111]. In other studies where wild type SeV is used, formation of stress granules is likely the result of using virus stocks with large quantities of cbVGs [102]. As it will be shown throughout this dissertation, cbVGs are the main activators of the cellular stress response orchestrated by PKR that leads to formation of canonical stress granules during HPIV-related paramyxovirus SeV and pneumovirus RSV infection. The work shown here attempts to clarify many of the contradictory evidence regarding formation of stress granules during RNA virus infection. More importantly, this work broadens our understanding on the interactions cbVGs have with the cell and provide an avenue to continue exploring other potential roles cbVGs may have in shaping the outcome of the infection at the molecular level.

Chapter 2

Role of cbVGs in Stress Granule Formation

2.1. Abstract

Antiviral responses are often accompanied by translation inhibition and formation of stress granules in infected cells. However, the triggers for these processes and their role during infection remain subjects of active investigation. Copy-back viral genomes (cbVGs) are the primary inducers of the Mitochondrial Antiviral Signaling (MAVS) pathway and antiviral immunity during SeV and RSV infections. The relationship between cbVGs and cellular stress during viral infections is unknown. In this chapter, we show that stress granules form during RSV and SeV infections containing high levels of cbVGs, and not during infections with low levels of cbVGs. We also show an increase in PKR phosphorylation, the main kinase involved in inducing the stress response during virus infections. Moreover, using RNA fluorescent *in situ* hybridization to differentiate accumulation of standard viral genomes from cbVGs at a single-cell level during infection, we show that stress granules form exclusively in cells that accumulate high levels of cbVGs. Altogether, these data demonstrate cbVGs are the RNA molecules that induce the stress response during negative-sense single-stranded RNA virus infection.

2.2. Introduction

Stress granules are reported to form in cells during infections with many different viruses, including RNA viruses like RSV, SeV, Rabies virus and Hepatitis C virus [119]. Because viruses require the translation machinery of the cell to make viral proteins, the translation inhibition accompanied by stress granule formation is often considered to be an antiviral mechanism employed by the cell. This is supported by the fact that many viruses encode for antagonists of the stress response or have evolved mechanisms to bypass cap-dependent translation [100, 120]. For other viruses, as it is for the case of RSV and HCV, stress granule formation is beneficial for the infection either by promoting virus replication or extending cell survival to promote virus persistence, respectively [121-123]. Most of the evidence regarding the role stress granules have during infection suggest that stress granules are necessary for the induction of the IFN response in infected cells. This is accompanied by studies demonstrating co-localization of several innate immune sensors in stress granules, along with stress granule inhibition experiments showing impaired IFN production as a response to the infection [101, 102].

For most viruses, stress granule formation is induced through activation of PKR, a double-stranded RNA binding protein that resides in the cytoplasm. The specific viral factors that cause PKR activation and stress granules to form during the infection are not fully elucidated. Evidence shows that the RNA-binding domain of PKR can bind any RNA with A-form helical structure with no specificity in RNA sequence [124]. *In vitro* studies have shown that double-stranded RNA or single-stranded RNA that can form moieties of more than 30 base pairs is required to activate PKR [124]. During viral infection, PKR can be activated by dsRNA

genomes from rotaviruses and dsRNA replication intermediates formed during positive and negative single-stranded RNA viruses [124]. It has also been shown that during Hepatitis D virus and human immunodeficient virus infection, RNA hairpin loop structures form to activate PKR [124]. Additionally, some cellular RNAs, including mitochondrial RNA and dsRNA Alu repeats, can also lead to PKR activation [74, 75]. However, the specific viral double-stranded RNA molecules that activate PKR during negative sense single-stranded RNA virus infection are unknown. The association of stress granule formation in mediating the antiviral response known to be primarily induced by cbVGs suggested that cbVGs lead to stress granule formation.

In this chapter, we identify cbVGs as the RNA molecules that trigger stress granule formation during both RSV and SeV infection. Cells forming stress granules accumulate exclusively during RSV and SeV infections that contain high levels of cbVGs. In contrast, stress granules do not form during RSV infections depleted of cbVGs even in conditions where high concentration of standard viral particles are added. Presence of cbVGs during infection is accompanied by increased levels of phosphorylated PKR compared to cbVG-low or mock infected cells. Furthermore, using purified cbVG-containing particles to control cbVG concentrations during infection we observe a dose-dependent accumulation of stress granule positive cells in response to increased concentration of cbVG-containing particles. This is not observed, however, when cbVG-containing particles are UV-inactivated to prevent their replication ability, demonstrating that active replication of cbVGs is required for stress granule formation. Finally, we demonstrate that the cells that form stress granules are also the cells that accumulate cbVGs during infection, demonstrating that presence of cbVGs inside the cell lead to formation of stress granules.

2.3. Results

2.3.1. Generation and Characterization of RSV cbVG-high and cbVG-low Virus

Our laboratory has previously reported the preparation of RSV virus stocks that either are enriched in cbVG-containing particles (cbVG-high virus) or are low on cbVG-containing particles (cbVG-low virus) [125]. cbVG-high viruses are prepared by infecting cells at high multiplicity of infection (MOI) to promote accumulation of cbVGs. Conversely, cbVG-low viruses are prepared by infecting cells at low MOI to prevent accumulation of cbVGs. To confirm the cbVG contents of the virus stocks used in this study, we performed a cbVG-specific PCR previously validated to visualize the expected DNA bands corresponding to the cbVGs typically found in our RSV stocks. As expected, various bands are observed exclusively during infections with cbVG-high virus at both 12- and 24-hours post infection (hpi), which correspond to the sizes of the expected cbVG amplicons (**Figure 2.1A**).

Because cbVGs potently induce the IFN response, we expect cbVG-high stocks to induce higher expression of IFNs than a cbVG-low stock [50]. To test this, we performed quantitative PCR for IFN lambda (*IL-29)* expression and, as expected, *IL-29* mRNA levels were increased in cells infected with cbVG-high stocks (**Figure 2.1B**). Additionally, presence of cbVGs during infection is expected to correlate with reduced levels of virus replication in infected cells as compared to cbVG-low stocks due to the activity of IFNs [50]. Using *RSV G* mRNA transcripts as a proxy for virus replication, we confirmed that infection with RSV cbVG-high stocks resulted in reduced levels of *RSV G* mRNA as compared to infection with an RSV cbVG-low stocks (**Figure 2.1B**).

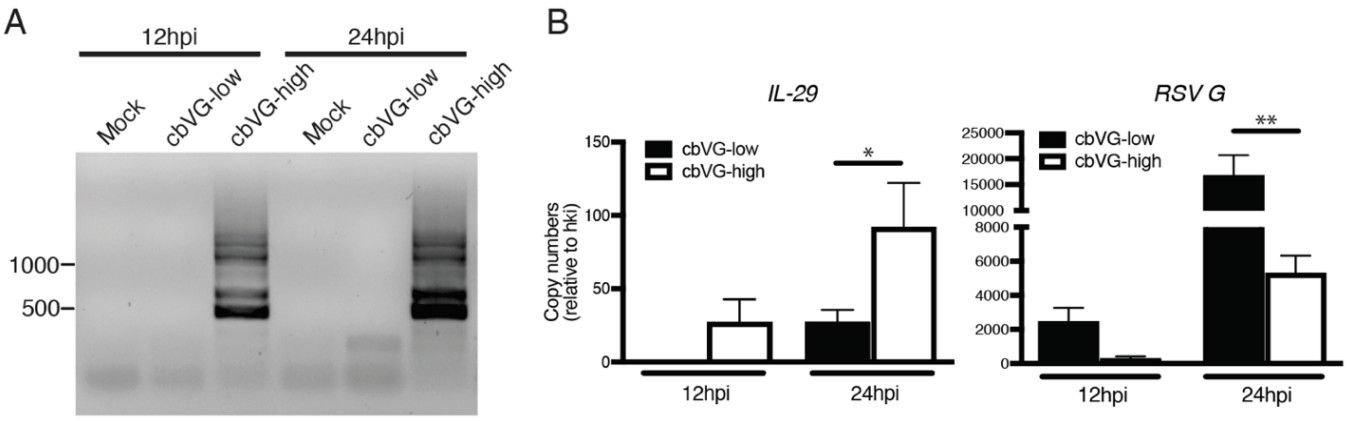

Figure 2.1. (A) Agarose gel of cbVG PCR amplicons from A549 cells 24 hpi with RSV cbVG-high virus at MOI 1.5 $TCID_{50}$/cell. (B) Expression of *RSV G* and *IL-29* mRNAs in A549 cells 24 hpi with RSV cbVG-high or cbVG-low virus at MOI 1.5 $TCID_{50}$/cell. Statistical analysis: one way ANOVA (* $p < 0.05$, ** $p < 0.01$).

2.3.2. Stress Granules Form During RSV Infection Containing High Levels of cbVGs

To assess whether cbVGs induced stress granule formation in cells, we infected lung epithelial A549 cells with cbVG-high and cbVG-low RSV stocks and visualized stress granule formation by immunostaining for the well-characterized stress granule associated protein G3BP1, along with the RSV nucleoprotein (NP) to identify infected cells. Fluorescence imaging analysis showed stress granules in infected cells during RSV cbVG-high infections, while they were rarely detected in RSV cbVG-low infections. Stress granules were observed as early as 12 hours post-infection (hpi) and were still present at 24 hpi (**Figure 2.2A**). The percent of stress granule positive cells during RSV cbVG-high infection increased over time, and approximately 10% of infected cells were stress granule positive at 24 hpi (**Figure 2.2B**).

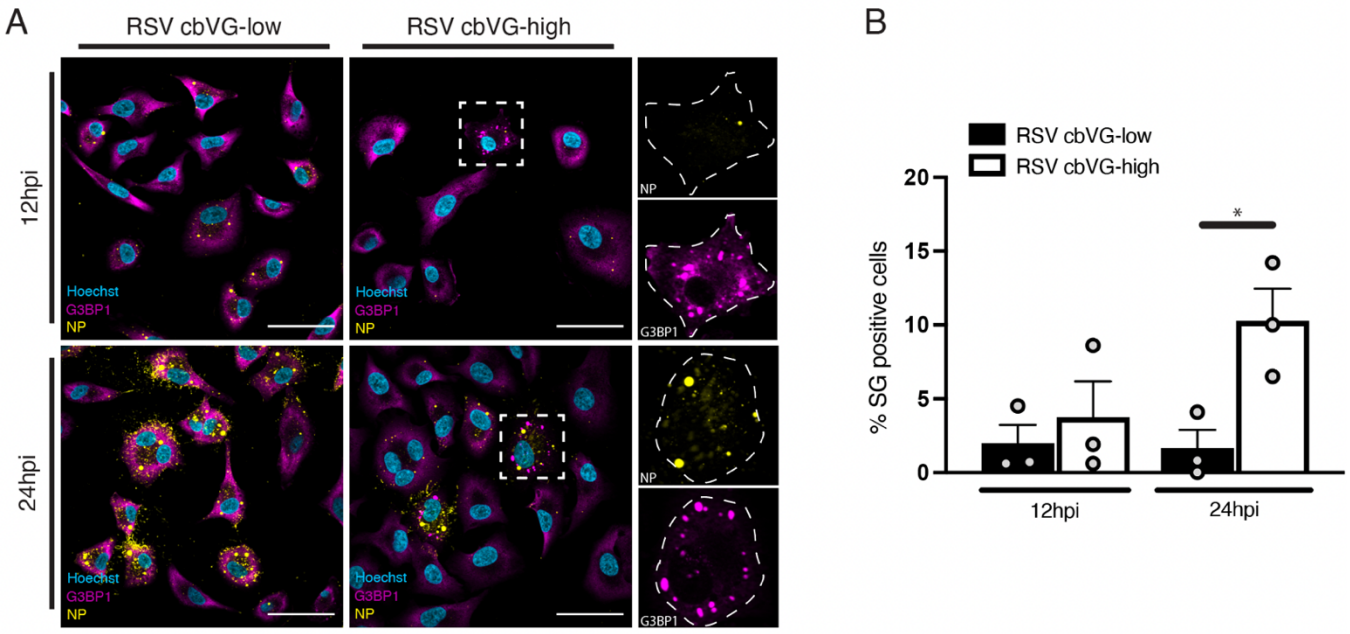

Figure 2.2. (A) Stress granules (G3BP1, magenta) and viral protein (RSV NP, yellow) detection 12 and 24 hpi with RSV cbVG-high or cbVG-low at MOI of 1.5 $TCID_{50}$/cell. (B) Percent of stress granule (SG) positive cells within the infected population 12 and 24 hpi with RSV cbVG-high and cbVG-low infections. Approximately 150 infected cells were counted per condition (average of three independent experiments shown). All widefield images were acquired with the Apotome 2.0 at 63x magnification and are representative of three independent experiments. Scale bar = 50 μm. Statistical analysis: One way ANOVA (*$p < 0.05$).

Although cbVG-containing viral particles can infect cells, they are not considered fully infectious as they can only replicate in cells co-infected with standard virus particles. Thus, infections based on multiplicity of infection (MOI) only account for the number of fully infectious particles in the inoculum. We expect that RSV cbVG-high infections, which contain both infectious standard particles and non-infectious cbVG particles, will contain a higher amount of total viral particles.

To determine if the observed differences in stress granule formation were due to differences in total viral particles added in the inoculum, we infected cells with RSV cbVG-high and RSV cbVG-low at increasing MOIs and compared percent of stress granule positive cells. Increasing the MOI of RSV cbVG-low infection did not increase the percent of stress granule positive cells even when using 10 times more RSV cbVG-low than RSV cbVG-high (**Figures 2.3A and 2.3B)**. We did observe an increase in the percent of stress granule positive cells as we increased the MOI during RSV cbVG-high infection, which correlates with the increased number of cbVG-containing particles in the inoculum. However, no differences in percent of stress granule positive cells were observed between MOI 5 and MOI 10 **(Figure 2.3B)**, suggesting there is a threshold on the amount of stress granule positive cells we can obtain at a given time during the infection. Taken together, these data indicate that presence of cbVGs during RSV infection correlates with stress granule formation.

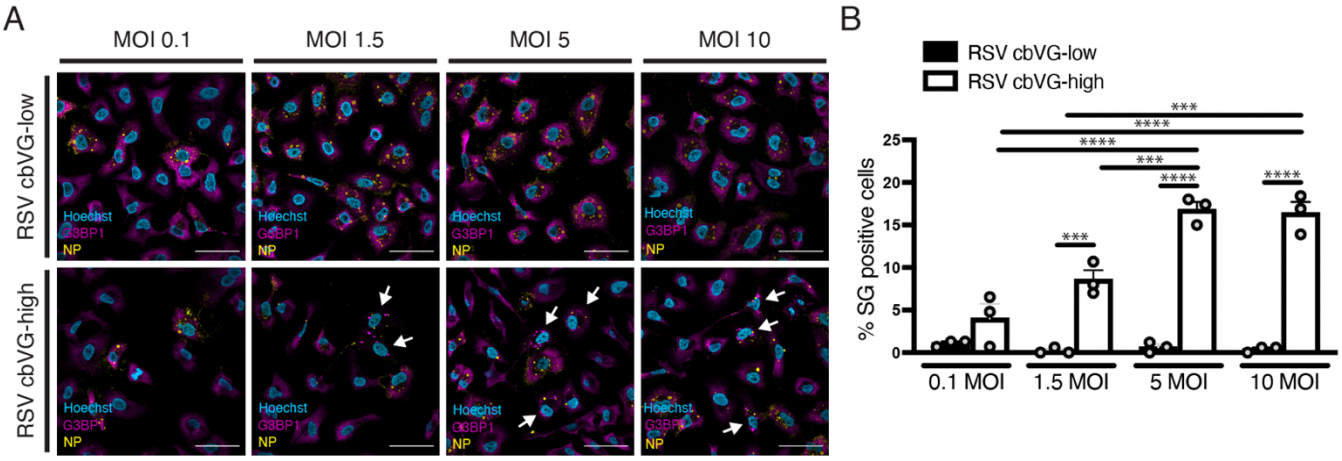

Figure 2.3. (A) Stress granules (G3BP1, magenta) and viral protein (RSV NP, yellow) detection 24hpi with RSV cbVG-high or cbVG-low at MOIs 0.1, 1.5, 5 and 10 $TCID_{50}$/cell. (B) Percent of stress granule (SG) positive cells within the infected population 24 hpi with RSV cbVG-high and cbVG-low infection at MOIs 0.1, 1.5, 5 and 10 $TCID_{50}$/cell. Approximately 150 infected cells were counted per condition (average of three independent experiments shown). All widefield images were acquired with the Apotome

2.0 at 63x magnification and are representative of three independent experiments. Scale bar = 50 μm. Statistical analysis: One way ANOVA (*p < 0.05, **p < 0.01, ***p < 0.001, ****p < 0.00001).

2.3.3. cbVGs Induce Stress Granules During SeV Infection

To determine whether cbVG induction of stress granules occurs during other negative-sense RNA virus infections, we infected cells with cbVG-high or cbVG-low SeV, a member of the paramyxovirus family and close relative to the human parainfluenza virus 1. Like infection with RSV, stress granules formed predominantly during SeV cbVG-high infections (**Figure 2.4A)** where approximately 20% of the infected cells were positive for stress granules at 24 hpi **(Figure 2.4B).** Compared to cells with undetected stress granules or NP (**Figure 2.4A, right panel inset 1)**, some stress granule-positive cells had notably low NP signal (**Figure 2.4A right panel inset 2**) while other stress granule positive cells showed high NP signal (**Figure 2.4A, right panel inset 3).**

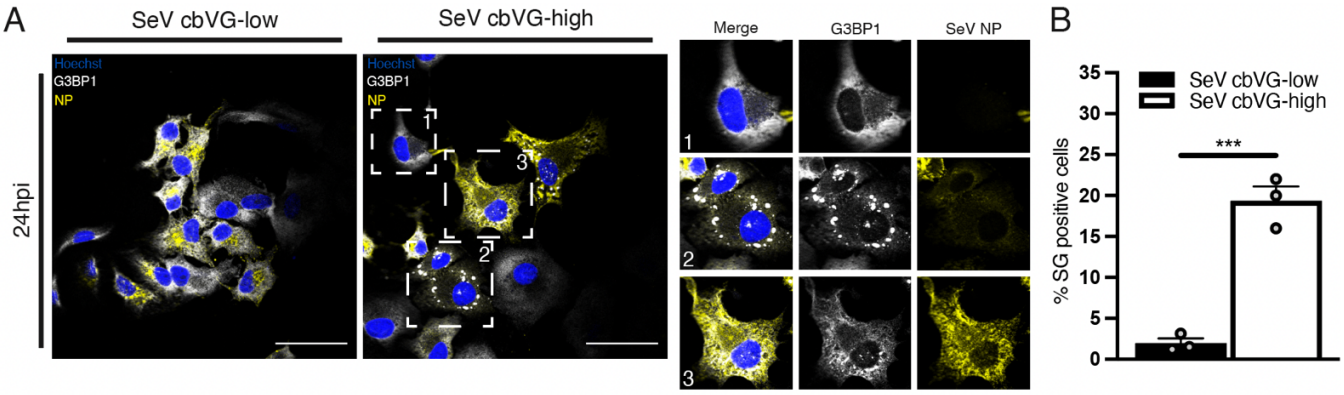

Figure 2.4. (A) Stress granules (G3BP1, white) and viral protein (SeV NP) detection 24 hpi with SeV cbVG-low and cbVG-high (NP, yellow) at MOI 1.5 $TCID_{50}$/cell. Digital zoomed images for each of the marked cells are shown in the panel on the right. (B) Percent of infected stress granule (SG) positive cells 24 hpi with SeV cbVG-low and cbVG-high at MOI 1.5 $TCID_{50}$/cell. Approximately 150 infected cells were counted per condition (average of three independent experiments shown). All widefield images were acquired with the Apotome 2.0 at 63x magnification and are representative of three independent

experiments. Scale bar = 50 μm. Statistical analysis: One way ANOVA (*p < 0.05, **p < 0.01, ***p < 0.001).

To further establish the role of cbVGs in inducing stress granules, we performed a dose-dependent experiment using purified cbVG-containing viral particles. We infected cells with SeV cbVG-low and supplemented the infection with increasing doses of purified cbVG-containing particles. The percent of stress granule positive cells increased in proportion to the amount of purified cbVG-containing particles added **(Figure 2.5A upper panel and 2.5B)**. Stress granules were not observed, however, when we added the same amounts of UV-inactivated purified cbVG particles **(Figures 2.5A lower panel, and 2.5B)**. These data demonstrate that only replication-competent cbVGs induce stress granule formation during RNA virus infection.

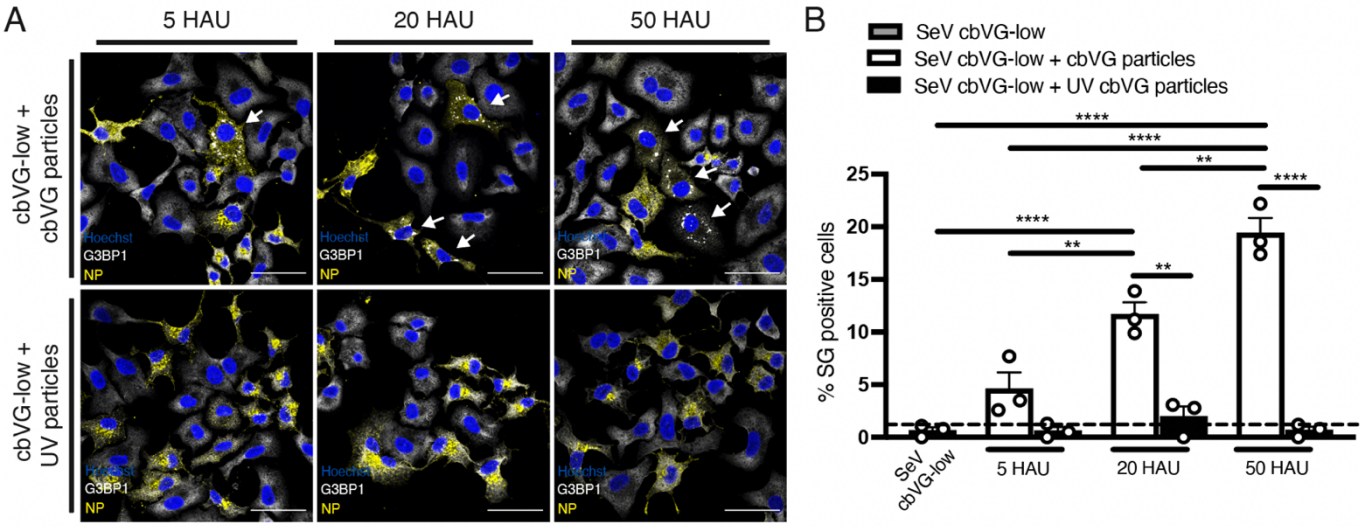

Figure 2.5. (A) Stress granules (G3BP1, white) and viral protein (SeV NP) detection 24 hpi at MOI 1.5 $TCID_{50}$/cell supplemented with either purified cbVG particles or UV-inactivated cbVG particles at increasing hemagglutination units (HAU). (B) Percent of stress granule (SG) positive cells at increasing HAU doses of active/UV inactive cbVG particles. Approximately 200 infected cells were counted per condition (average of three independent experiments shown). All widefield images were acquired with

the Apotome 2.0 at 63x magnification and are representative of three independent experiments. Scale bar = 50 μm. Statistical analysis: One way ANOVA (*p < 0.05, **p < 0.01, ***p < 0.001, ****p < 0.00001).

2.3.4. PKR Phosphorylation is Increased During RSV and SeV cbVG-high Infection

To determine if cbVGs induce stress granules through PKR activation, we probed for PKR phosphorylation during RSV and SeV cbVG-high infection through western blot analysis. As expected, PKR is phosphorylated during RSV and SeV cbVG-high infections compared to RSV and SeV cbVG-low or mock infection **(Figure 2.6A and 2.6B).** Because IFN is induced by cbVGs and PKR is an interferon stimulated gene (ISG), increased total unphosphorylated PKR levels are expected during cbVG-high infections. These data further demonstrate that presence of cbVGs during the infection leads to PKR phosphorylation and, subsequently, stress granule formation.

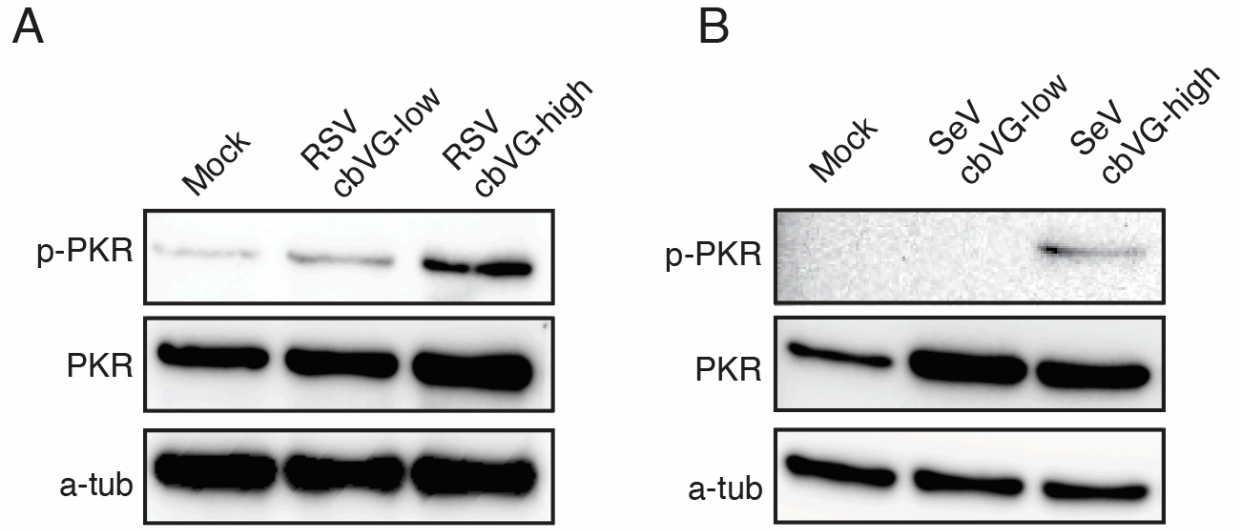

Figure 2.6. (A) Phosphorylation of PKR 24 hpi with RSV cbVG-low and cbVG-high infection at MOI 1.5 $TCID_{50}$/cell. (B) Phosphorylation of PKR 24 hpi with SeV cbVG-low and cbVG-high infection at MOI 1.5 $TCID_{50}$/cell.

2.3.4. Stress Granules Form Exclusively in cbVG-high Cells During RSV cbVG-high Infection

Using a previously described RNA Fluorescence *in situ* hybridization (FISH)-based assay that allows differentiation of full-length genomes from cbVGs at a single-cell level [56], our lab reported that cells infected with RSV or SeV cbVG-high stocks have heterogenous accumulation of viral genomes; some cells accumulate high levels of standard genomes (stVG-high) and others accumulate high levels of cbVGs (cbVG-high) [56, 126, 127]. To determine if stress granules formed differentially within these two populations of cells, we combined RNA FISH with immunofluorescence to detect stress granules using stress granule-associated protein, TIA 1-related protein (TIAR), staining during RSV cbVG-high infection. At 24 hpi, stress granules formed almost exclusively in cbVG-high cells (green) and not stVG-high cells (orange) (**Figure 2.7A)**. Interestingly only around 30% of the cbVG-high cells had stress granules (**Figure 2.7B)**. This could suggest that a threshold of cbVG accumulation in the cells is needed for stress granule formation or that stress granule formation occurs asynchronously during infection which is observed during HCV infection [122]. Nevertheless, these data demonstrate that cbVGs trigger stress granule formation.

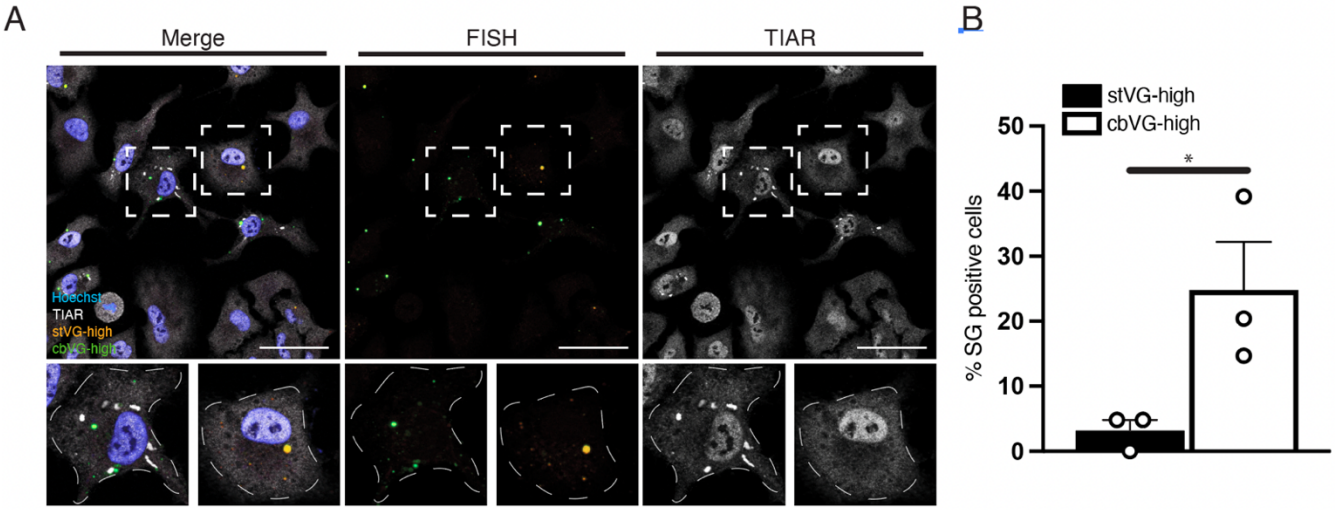

Figure 2.7. (A) Stress granule detection (TIAR, white) in cells staining via FISH for stVG-high (orange) and cbVG (green) cells 24 hpi with RSV cbVG-high at MOI 1.5 $TCID_{50}$/cell. (B) Percent of stress granule positive cells within the stVG-high and cbVG-high cell populations during RSV cbVG-high infection (average of three independent experiments shown). All widefield images were acquired with the Apotome 2.0 at 63x magnification and are representative of three independent experiments. Scale bar = 50 μm. Statistical analysis: One way ANOVA (*$p < 0.05$).

2.4. Discussion

Formation of stress granules during most virus infections occurs through the recognition of viral double-stranded RNA products that are detected by PKR. However, the specific RNAs responsible for activating this response are unknown. In this chapter, we show that stress granules form during RSV and SeV infections that contain high levels of cbVGs. During RSV infection, we could detect stress granules as early as 12 hpi, demonstrating that activation of the response occurs at a relatively late time compared to the induction of the antiviral response after the infection initiated. The presence of cbVGs during the infection also increases phosphorylation of PKR, suggesting cbVGs induce PKR activation.

The formation of stress granules is not dependent on the total amount of standard-virus containing particles added to the inoculum, as increasing the MOI during infections with low-cbVG virus did not increase the percent of stress granule positive cells. We did see an increase of stress granule positive cells as we increased the amount of cbVG particles to the inoculum, further demonstrating that cbVGs induce the stress response. Interestingly, UV-inactivating purified cbVG particles and adding them to the infection did not lead to formation of stress granules in the infected population. UV inactivation can damage the bases of nucleic acids, preventing replication of the cbVG genome [128]. UV inactivation can also crosslink the virus nucleoprotein to the cbVG genome, preventing release of the RNA for the polymerase to replicate. The lack of detection of stress granule positive cells when treating the infected cells with UV-inactivated particles suggest that active replication of the cbVG is needed for the response to be activated. Although we did not successfully demonstrate cbVGs directly bind to

PKR, we hypothesize that exposure of the cbVG to the cell through active virus replication is necessary for PKR activation.

Finally, we demonstrate that stress granules formed exclusively in cells that contained high levels of cbVGs and not those that had low levels of cbVGs. These data demonstrate that activation of the stress response occurs through the accumulation of cbVGs inside the cell and it is not a response led by bystander cells. Because not all cbVG-high cells were positive for stress granules, we predict that a specific threshold of cbVG content in the cell is required to activate the stress response. Alternatively, activation of the stress response could be dependent on other factors, like the state of the cell cycle, metabolism, etc.

2.5. Procedures

Cell lines and viruses

A549 (human type II pneumocytes; ATCC CCL-185) cells were cultured in tissue culture medium (Dubelcco's modified Eagle's medium [DMEM; Invitrogen]) supplemented with 10% fetal bovine serum (FBS), gentamicin 50 ng/ml (Thermofisher), L-glutamine 2 mM (Invitrogen) and sodium pyruvate 1 mM (Invitrogen) at 5% CO_2 37 ^oC. Cells were treated with mycoplasma removal agent (MP Biomedical) and tested monthly for mycoplasma contamination using MycoAlert Plus mycoplasma testing kit (Lonza). SeV Cantell strain was grown in 10-day-old, embryonated chicken eggs (Charles River) for 40 h as previously described [129] . RSV stocks were grown in Hep2 cells as previously described [125] and harvested by collecting the cells supernatant. SeV and RSV cbVG-high and cbVG-low stocks were produced and characterized as described previously [125].

Virus infections

For RSV infections, cells were washed once with PBS and then incubated with virus suspended in tissue culture medium supplemented with 2% FBS at 37 ^{o}C for 2 h. Cells were then supplemented with additional 2% FBS tissue culture medium. For SeV infections, cells were washed twice with PBS and then incubated with virus suspended in infectious medium (DMEM; Invitrogen) supplemented with 35% bovine serum albumin (BSA; Sigma-Aldrich), penicillin-streptomycin (Invitrogen) and 5% $NaHCO_3$ (Sigma-Aldrich) at 37 ^{o}C for 1 h. Cells were then supplemented with additional infectious medium. SeV cbVG particles were purified from the allantoic fluid of SeV infected embryonated eggs by density ultracentrifugation on a 5 to 45% sucrose gradient, as described previously [48].

Immunofluorescence

Cells were seeded at 1 x 10^5 cells/mL confluency in 1.5 glass coverslips (VWR) a day prior infection or drug treatment. The coverslips were transferred to a fresh plate and washed with PBS. Cells were fixed on the coverslips using 4% paraformaldehyde (EMS) for 15 min. Cells were then permeabilized with 0.2% Triton X-100 (Sigma-Aldrich) for 10 min. Primary and secondary antibodies diluted in 3% FBS were added and incubated for 1 h and 45 min, respectively. The nuclei were stained with a 1:10,000 dilution of Hoechst (Invitrogen) in PBS for 5 min prior to mounting. Coverslips were mounted in slides using Prolong Diamond anti-fade mounting media (ThermoFisher) and curated overnight at room temperature. Antibodies used: SeV NP (clone M73/2, a gift from Alan Portner, directly conjugated with DyLight 594 or 647 *N*-hydroxysuccinimide (NHS) ester (ThermoFisher)), RSV NP (Abcam catalog number ab94806), G3BP (Abcam catalog numbers ab181150 and ab56574), TIAR (Santa Cruz catalog number sc-398372).

RNA FISH combined with immunofluorescence

Cells were seeded at 1 x 10^5 cells/mL confluency in 1.5 glass coverslips a day prior infection. The coverslips were transferred to a fresh plate and washed with sterile PBS. Cells were fixed in the coverslips using 4% formaldehyde (ThermoFisher) for 10 min and permeabilized with 70% ethanol for 1 h at room temperature. Cells were incubated with primary and secondary antibodies diluted in 1% BSA [Sigma-Aldrich] containing RNAse OUT (ThermoFisher) for 45 and 40 min, respectively. Cells were post fixed with 4% formaldehyde and washed with 2x SSC (ThermoFisher) followed by wash buffer (2x SSC and 10% formamide in water). Cells were hybridized with 2.5 nM RSV specific LGC Biosearch custom probes (See table 1) conjugated to Quasar 570 or Quasar 670. Slides were incubated overnight at 37 °C in a humidified chamber for hybridization. Cells were washed twice with wash buffer for 30 min each and once with 2x SSC for 5 min. Coverslips were mounted using ProLong Diamond Antifade mounting media and curated overnight. Slides were imaged using Zeiss Axio observer widefield microscope.

Table 1. Probe sequences for RSV negative-sense RNA genome probes

Probe sequence	**Probe name**
gtgctctatcatcacagatc	RSV genome_1
ccctagaaattacatgccat	RSV genome_2
ggactacgtttctatcgtga	RSV genome_3
acttatccttctttgttgga	RSV genome_4
ataagtggagctgcagagtt	RSV genome_5
attgtgtcatgctatggcaa	RSV genome_6
ttcttcccacaagctgaaac	RSV genome_7

cagaggatggtactgtgaca	RSV genome_8
ggcgtaactacacctgtaag	RSV genome_9
tagtgctctgagaactggtt	RSV genome_10
agcttcaacaacaccaggag	RSV genome_11
tattcatagcctcggcaaac	RSV genome_12
ttgagttaccaagagctcga	RSV genome_13
ccacacaccatacagaatca	RSV genome_14
tcttcacttcaccatcacaa	RSV genome_15
ccacacaccatacagaatca	RSV genome_16
tcttcacttcaccatcacaa	RSV genome_17
ttggaagcacacagctacac	RSV genome_18
taccatatgcgctaatgtgt	RSV genome_19
aatcatctatgccagcagat	RSV genome_20
ggacagatctggtcttacag	RSV genome_21
caaccatggctcttagcaaa	RSV genome_22
agacaggccacatttacatt	RSV genome_23
attgctctcaacctaatggt	RSV genome_24
tggctaaggcagtgatacat	RSV genome_25
agagatgggcagcaattcat	RSV genome_26
tctaattggtttatatgtgt	RSV DVG_1
gttaaacagcttgacaacca	RSV DVG_2
ctacatatccttacctaagt	RSV DVG_3
aaccatttatatatggtaga	RSV DVG_4

gaagttttcagcaataaact	RSV DVG_5
gtgttgttagtggagatata	RSV DVG_6
actgcattgtcaaaactaaa	RSV DVG_7
ataaagagtctattgatgca	RSV DVG_8
atgctaaattgatactatca	RSV DVG_9
ttcccagtatttaatgtagt	RSV DVG_10
attacaataggtcctgcgaa	RSV DVG_11
gggatcggaggtttacttag	RSV DVG_12

RNA extraction and PCR/qPCR

RNA was extracted using TriZol reagent (Life Technologies] For qPCR, mRNA was reverse transcribed using high-capacity RNA to cDNA kit (ThermoFisher). qPCR was performed using SYBR green (ThermoFisher) and 5 μM of reverse and forward primers for genes *IL-29* (CGCCTTGGAAGAGTCACTCA and GAAGCCTCAGGTCCCAATTC); and *RSV G* (AACATACCTGACCCAGAATC and GGTCTTGACTGTTGTAGATTGCA) on an Applied Biosystems QuantStudio 5 machine. Relative mRNA copy numbers were calculated using relative delta CT values and normalized using a housekeeping index with GAPDH and β-actin. For PCR detection of cbVGs, viral RNA was reverse transcribed using a SuperScript III first-strand synthesis (Invitrogen) with Primer GGTGAGGAATCTATACGTTATAC for SeV and primer CTTAGGTAAGGATATGTAGATTCTACC for RSV. PCR was then performed with Platinum Taq DNA polymerase (Invitrogen) with the reverse transcription primers and primer ACCAGACAAGAGTTTAAGAGATATGTATT for SeV and primer CCTCCAAGATTAAAATGATAACTTTAGG for RSV. Bands were analyzed using gel electrophoresis.

Imaging analysis

Stress granules quantification was performed using Aggrecount automated image analysis as previously described [130].

Western blots

Cells were seeded at 2 x 10^5 cells/mL confluency in a day prior infection or drug treatment. Protein was extracted using 1% NP 40 (Thermo) with 2 mM EDTA, 150 mM NaCL (Thermo), 5 mM Tris-HCL, 10% glycerol (Sigma-Aldrich), Halt™ Protease Inhibitor Cocktail (Thermo) and PhosSTOP (Sigma-Aldrich). After samples were incubated on ice for 20 mins and centrifuged for 20 min at 4 °C, supernatant was transferred to new tubes and protein concentration was quantified using the Pierce BCA Protein Assay Kit (Thermo). Protein (10-25 μg) was denatured for 5 min at 95 °C, loaded in a 4%-12% Bis Tris gel (Bio-Rad) and transferred to a PVDF membrane (Millipore Sigma). Membranes were incubated overnight with primary antibodies diluted in 5% BSA in TBS (Fisher) with 0.1 % Tween20 (Sigma-Aldrich). Membranes were incubated with secondary antibodies (anti-mouse or anti-rabbit) conjugated with HRP for 1 h in 5% BSA in TBST. Membranes were developed using Lumi-light Western blot substrate (Roche) to detect HRP and a ChemiDoc (Bio-Rad). Antibodies used for western blot: PKR (Cell Signaling catalog number 12297), p-PKR (Abcam catalog number ab32036), α-tubulin (Abcam catalog number ab52866).

Statistics

Statistics were calculated using GraphPad Prism. Version 9

Chapter 3

Characterization of cbVG-dependent Stress Granules

3.1. Abstract

Canonical stress granules are distinct cytoplasmic condensates that differentiate from other RNA containing granules by requiring phosphorylation of one of the four main stress-related kinases and forming following polysome disassembly. Canonical stress granules also contain a specific protein profile. RSV-induced stress granules have been previously shown to require PKR, suggesting RSV induces canonical stress granules. Here, we performed several experiments to show that cbVG-dependent stress granules meet with the criteria of canonical stress granules and fully elucidate the molecules required to inhibit their formation. We show that cbVG-dependent stress granule formation depends on polysome disassembly, they are not RNAseL-dependent bodies and, contrary to what has been previously proposed, require both G3BP1 and G3BP2 knockout to be inhibited. We also show that formation of stress granules is not dependent on MAVS signaling, demonstrating the versatility of cbVGs in activating signaling pathways beyond the antiviral immune response.

3.2. Introduction

A cell can induce many types of RNA-containing granules that vary in composition and function [131]. Within these granules, canonical stress granules form as a consequence of translation inhibition, and several physical processes need to occur for mRNA and RNA binding proteins to engage in the liquid-liquid phase separation that forms stress granules. An essential step that occurs after phosphorylation of eIF2α is the disassembly of polysomes from the mRNA [69]. This disassembly is essential for proteins to access and bind free mRNA. Additionally, many RNA binding proteins have intrinsically disordered domains that make them “sticky” and causes the phase separation through protein-protein or protein-RNA interactions [132]. Some of these RNA binding proteins are considered stress granule nucleating proteins as they are the proteins that initiate the formation of the granules [132]. Many of these proteins are also essential for stress granule assembly and knocking them out inhibits protein and mRNA aggregation into granules.

During virus infections, canonical stress granules often form by detection of dsRNA through PKR. However, some viruses can also induce activation of RNAse L, which has shown to induce formation of functionally distinct RNA-containing granules named RNAse L-dependent bodies (RLBs) [115, 133]. Activation of RNAse L causes degradation and turnover of select mRNAs in the cell, while keeping others intact [116]. Because mRNA is required for stress granules to form, formation of RLBs inhibits formation of stress granules [115]. Because they are functionally different, proper characterization of the RNA aggregates that form during a particular condition is pivotal in interpreting the role they play. More importantly, RLBs and stress granules contain overlapping markers, such as G3BP1, making their differentiation by

imaging complex [115]. Thankfully, various methods are described in the literature to properly differentiate cytoplasmic aggregates, including knocking out the receptors that lead to their formation and treatment with drugs that selectively disassemble ones while keeping the others intact.

Inhibiting formation of stress granules is another way to understand the function they play during infection. This can be done through knocking out the main kinase that phosphorylates eIF2α, inhibiting both translation inhibition and stress granule formation. Alternatively, knocking out stress granule nucleating factors inhibit stress granule formation without affecting translation inhibition. During RSV infection, it has been shown that stress granule formation is both PKR and G3BP1 dependent [109, 121]. The same has been shown for other members of the Mononegavirales [108, 110, 134]. Moreover, the relationship between stress granules and the antiviral immune response suggested to us that stress granule formation could be coupled with IFN signaling. Understanding the nature of the cytoplasmic granules being studied, together with the cellular factors required to induce them is essential for defining the role these granules play. This also provides appropriate systems to study their function.

In this chapter, we characterize the cbVG-dependent RNA granules formed during RSV infection as PKR-dependent canonical stress granules. This contrasts with the RLBs induced upon transfection of cbVG-derived oligonucleotides (DDOs) highlighting the differences between natural infections and transfection of virus-derived naked RNA. We show that cbVG-induced stress granules are MAVS independent, demonstrating that cbVGs induce antiviral

immunity and stress granule formation through two independent mechanisms. Finally, we show that to inhibit stress granule formation, knock out of both G3BP1 and G3BP2 is required as G3BP1 or G3BP2 single knockouts are not sufficient to inhibit stress granule formation.

3.3. Results

3.3.1. RSV cbVG-dependent Stress Granules are Canonical

In addition to stress granules and RLBs, viruses can induce the formation of cytoplasmic granules that differ compositionally from canonical stress granules. Viruses can also re-localize stress granule components to viral replication centers increasing the complexity of RNA-containing granules found in infected cells [96, 135-137]. To better characterize the granules observed during RSV cbVG-high infection, we treated RSV cbVG-high infected cells with cycloheximide (CHX). CHX inhibits the formation of canonical stress granules by preventing mRNA disassembly from the ribosomes [70, 138]. Sodium arsenite, a chemical known to induce formation of canonical stress granules, was used as a positive control [61]. Treatment with CHX during RSV cbVG-high infection led to a decrease in stress granule positive cells compared to treatment with the drug's vehicle alone (DMSO) (**Figure 3.1a, 3b**). To rule out any effect the drugs could have on G3BP1 localization, we co-stained with another stress granule marker, TIA-1 related (TIAR) protein. Co-staining with TIAR showed co-localization with G3BP1 in stress granules in the DMSO treated cells and disassembly from granules in the drug-treated conditions (**Figure 3.1a**), demonstrating that cbVG-dependent stress granules are canonical.

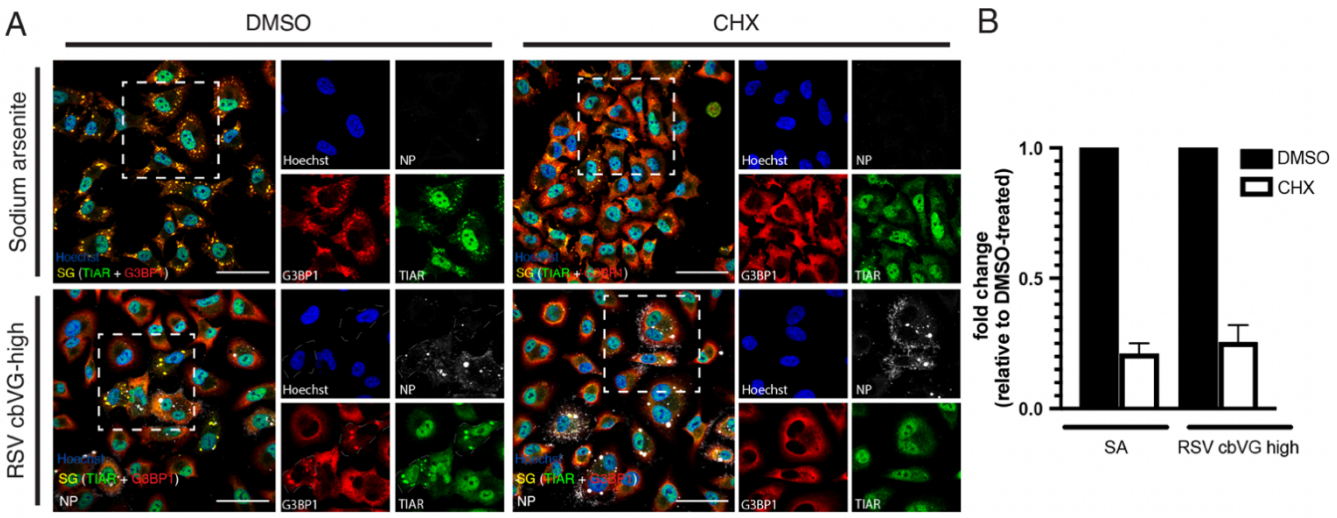

Figure 3.1. (A) G3BP1 (red) and TIAR (green) staining for stress granules in cells treated with sodium arsenite (SA, 0.5mM) for 1 h or infected with RSV cbVG-high (RSV NP, white) at MOI 1.5 $TCID_{50}$/cell 23 hpi and treated with DMSO, CHX (10 μg/mL) 1 h. (B) Quantification of stress granule (SG) positive cells after drug treatment in sodium arsenite or RSV cbVG-high infected cells. Approximately 150 cells were counted for each condition. Fold change relative to DMSO-treated cells is shown. All widefield images were acquired with the Apotome 2.0 at 63x magnification and are representative of three independent experiments. Scale bar = 50 μm.

We next tested whether RSV-induced granules were RLBs [115]. To do this, we infected RNAse L knockout cells with RSV cbVG-high virus and looked at differences in stress granule formation comparing to poly I:C transfection which is known to induce RLB formation [115]. Structurally, RLBs are smaller, more punctate, and contain less TIAR than canonical SG (**Figure 3.2, left panel)**. RNAse L activation prevents canonical stress granules from forming by degrading free mRNA necessary for stress granules to form and only when knocking out RNAse L, can canonical stress granules form upon stimulation [115, 116]. Stress granules are structurally bigger and less uniform than RLBs. Stress granules formed during RSV cbVG-high infection even in RNAse L knockout (KO) cells, and the structure of these granules was

unchanged between cell lines, demonstrating that RSV-dependent stress granules are not RLBs (**Figure 3.2**).

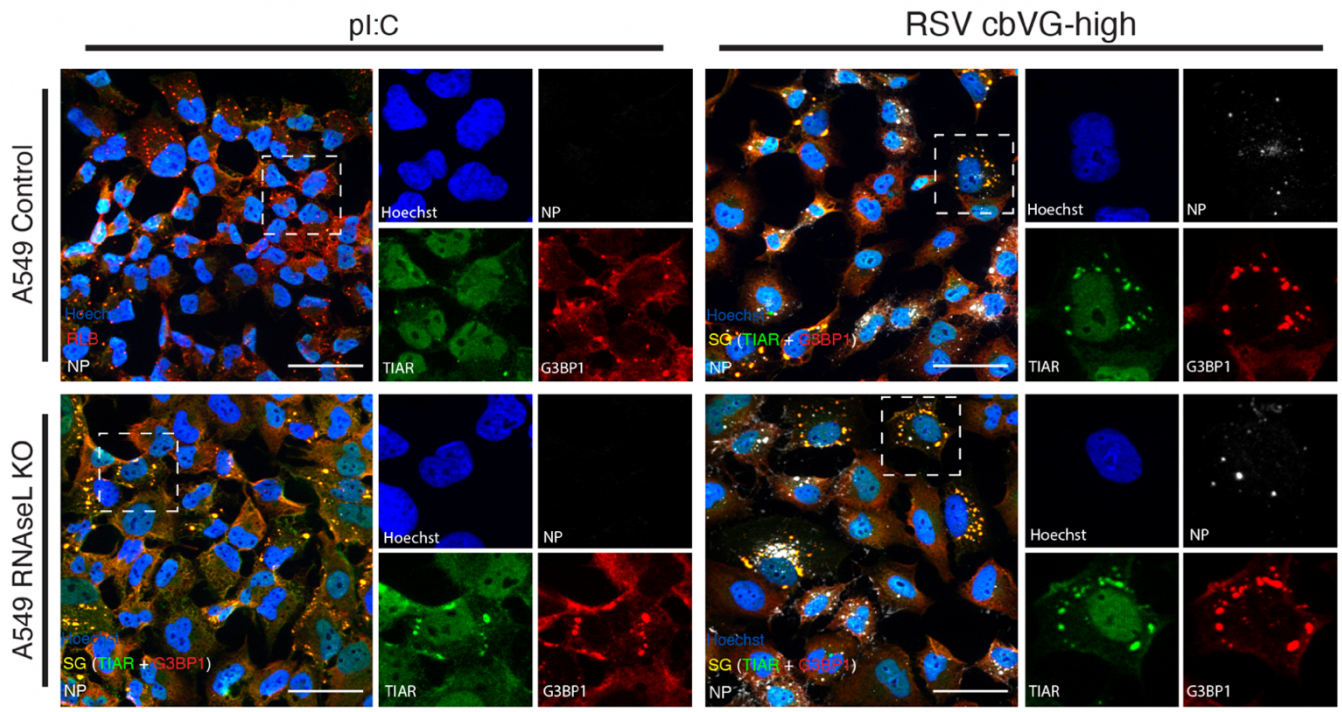

Figure 3.2. RNA granule detection (G3BP1, red; TIAR, green) in control and RNAseL KO cells transfected with poly I:C 10 μg/mL or infected with RSV cbVG-high (RSV NP, white) 24hpi at MOI 1.5 $TCID_{50}$/cell. All widefield images were acquired with the Apotome 2.0 at 63x magnification. Scale bar = 50 μm.

We then investigated if, out of the context of an infection, cbVG RNA would still induce formation of canonical stress granules, or would induce RLBs similar to poly I:C. We transfected *in vitro* transcribed RSV and SeV cbVG-derived oligonucleotides that maintain the key stimulatory domains of cbVGs (RSV 238 and SeV 268 [54]) into A549 cells and compared to poly I:C-induced RLBs. We saw no differences in RNA granule formation and G3BP1 and TIAR contents between poly I:C RLBs and the granules observed with transfected cbVG-derived oligonucleotides (**Figure 3.3**) indicating that cbVG induce canonical stress granules

only in the context of SeV or RSV infection while RLBs are produced in response to naked cbVG RNA.

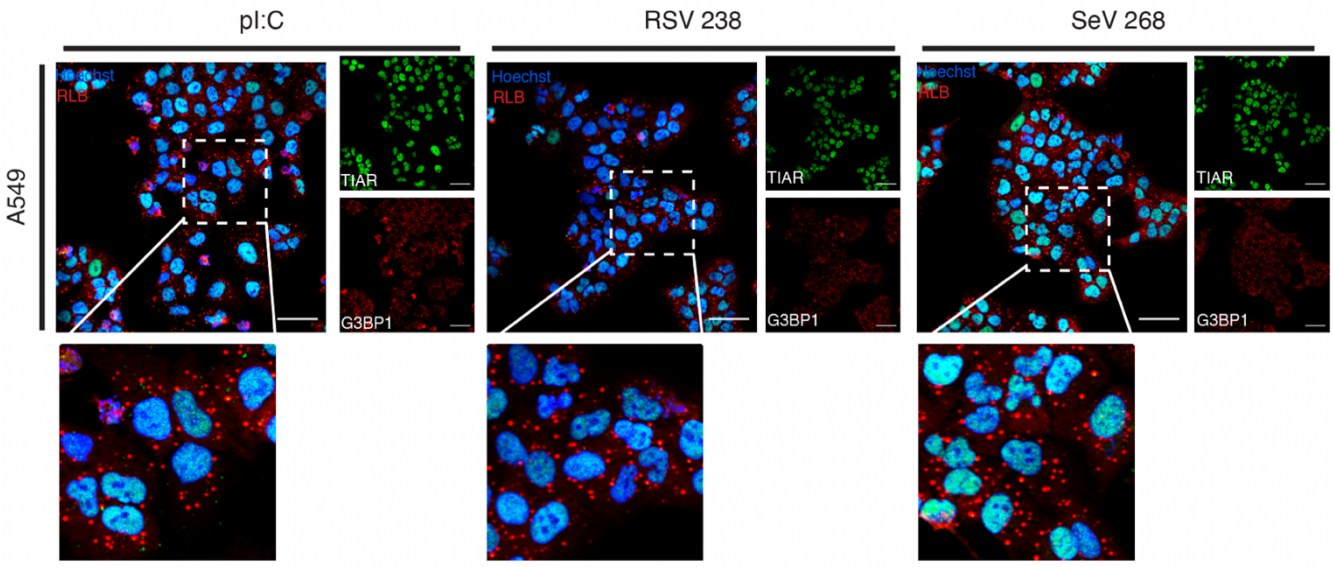

Figure 3.3. RNA granule detection (G3BP1, red; and TIAR, green) A549 cells transfected with poly I:C or RSV and SeV cbVG derived oligonucleotides RSV 238 and SeV 268. All widefield images were acquired with the Apotome 2.0 at 40x magnification are representative of three independent experiments. Scale bar = 50 μm. This experiment was performed by Matthew Hackbart.

3.3.2. cbVG-dependent Stress Granules are PKR-dependent and MAVS-independent

To better understand the molecular mechanisms leading to stress granule formation in response to cbVGs during infection, we investigated the role of major dsRNA sensors in stress granule induction. Stress granule formation during infection with many viruses, including RSV, depends on PKR activation [109]. To determine if cbVG-induced stress granules were PKR dependent, we infected A549 PKR KO cells (**Figure 3.4A, middle lane**) and visualized stress granule formation. Consistent with the literature, PKR KO cells infected with RSV cbVG-high virus did not show stress granule positive cells (**Figures 3.5A and B middle panel and bar**).

RSV G mRNA levels were similar between cell types, confirming that inhibition of stress granules in PKR KO cells was not due to lower replication of the virus (**Figure 3.4B, middle bar**). Together, these data suggest that the stress granules observed during RSV cbVG-high infection are PKR-dependent and that cbVG induction of stress granules is mediated by PKR activation.

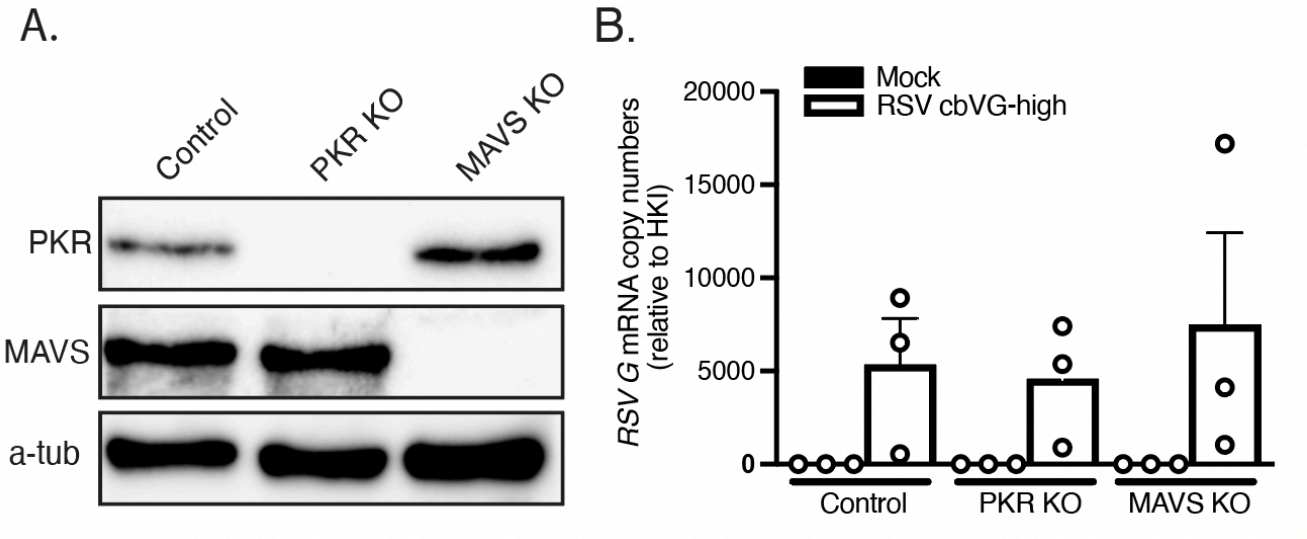

Figure 3.4. (A) Western blot analysis showing efficient KO of PKR and MAVS in A549 cells. (B) Expression of *RSV G* gene mRNA 24 hpi with RSV cbVG-high infection at MOI 1.5 TCID50/cell in control, MAVS or PKR KO A549 cells (average of three independent experiments are shown). No statistical significance was found.

Because cbVGs exert most of their functions through RLR stimulation which leads to MAVS activation and enhanced production of IFN, we sought to investigate whether cbVGs also induced stress granules through MAVS signaling. To our surprise, MAVS KO cells (**Figure 3.4A, right lane**) infected with RSV cbVG-high virus showed stress granule positive cells (**Figure 3.5A, 3.5B right panel and bar**). The percent of stress granule positive cells trended slightly lower than control but was not statistically significant (**Figure 3.5B).** This is most likely

due to a reduced expression of PKR, a well-known ISG. These data indicate that cbVGs induce stress granules independent of cbVGs immunostimulatory activity. To our knowledge, this is the first time cbVGs have shown to modulate cell processes that are independent of MAVS signaling.

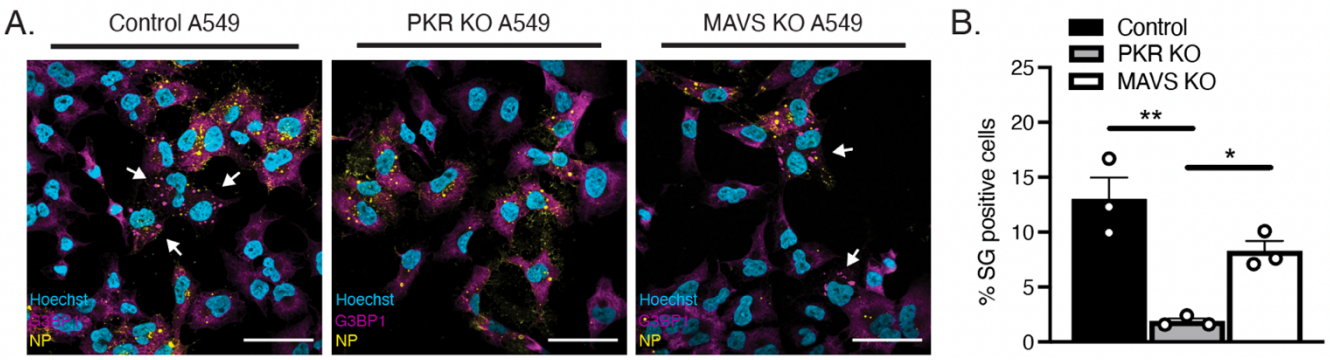

Figure 3.5 (A) Stress granules (G3BP1, magenta) and viral protein (RSV NP) detection in PKR KO and MAVS KO A549 cells 24 hpi with RSV cbVG-high virus at MOI 1.5 $TCID_{50}$/cell. (B) Quantification of stress granule (SG) positive cells 24 hpi with RSV cbVG-high at MOI 1.5 $TCID_{50}$/cell in PKR or MAVS KO A549 cells. Approximately 300 cells were counted per condition. All widefield images were acquired with the Apotome 2.0 at 63x magnification and are representative of three independent experiments. Scale bar = 50 μm. Statistical analysis: One way ANOVA (*$p < 0.05$, **$p < 0.01$).

3.3.3. cbVG-dependent Stress Granule Inhibition is Both G3BP1 and G3BP2-dependent

Following translation inhibition, nucleating factors initiate RNA protein aggregation and liquid phase-separation to form stress granules [139]. Studies suggest that G3BP1 is necessary and sufficient for stress granules to form during viral infections [102, 121, 134]. To determine if G3BP1 is sufficient for cbVG-dependent stress granules, we infected G3BP1 KO cells (**Figure 3.6A, second lane**) with RSV cbVG-high virus and looked at stress granules using TIAR staining as proxy for stress granule formation. *RSV G* mRNA levels confirmed that there were not significant differences in viral replication between cell types (**Figure 3.6B**).

Unexpectedly, we observed TIAR-containing SG in G3BP1 KO cells (**Figure 3.7, upper panel**). To confirm that these were canonical stress granules and not aggregation of TIAR as an artifact of knocking out G3BP1, we treated the cells with CHX. Indeed, TIAR-containing SG in G3BP1 KO cells are sensitive to CHX, suggesting these are canonical stress granules (**Figure 3.7, lower panel**). These data indicate that knocking out G3BP1 is not sufficient to inhibit RSV-dependent stress granules, contradicting what has previously been suggested in the literature [121].

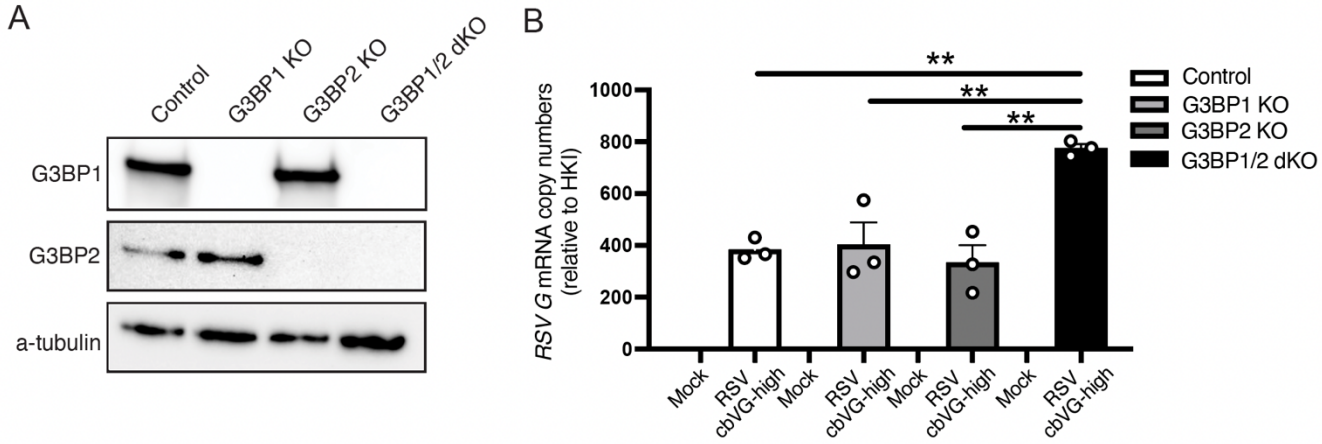

Figure 3.6. (A) Western blot analysis validating A549 G3BP1 KO, G3BP2 KO and G3BP1/2 dKO (B) Expression of *RSV G* gene mRNA 24 hpi with RSV cbVG high infection at MOI 1.5 TCID50/cell in control, G3BP1 KO, G3BP2 KO and G3BP1/2 dKO. Statistical analysis: One way ANOVA (**p < 0.01).

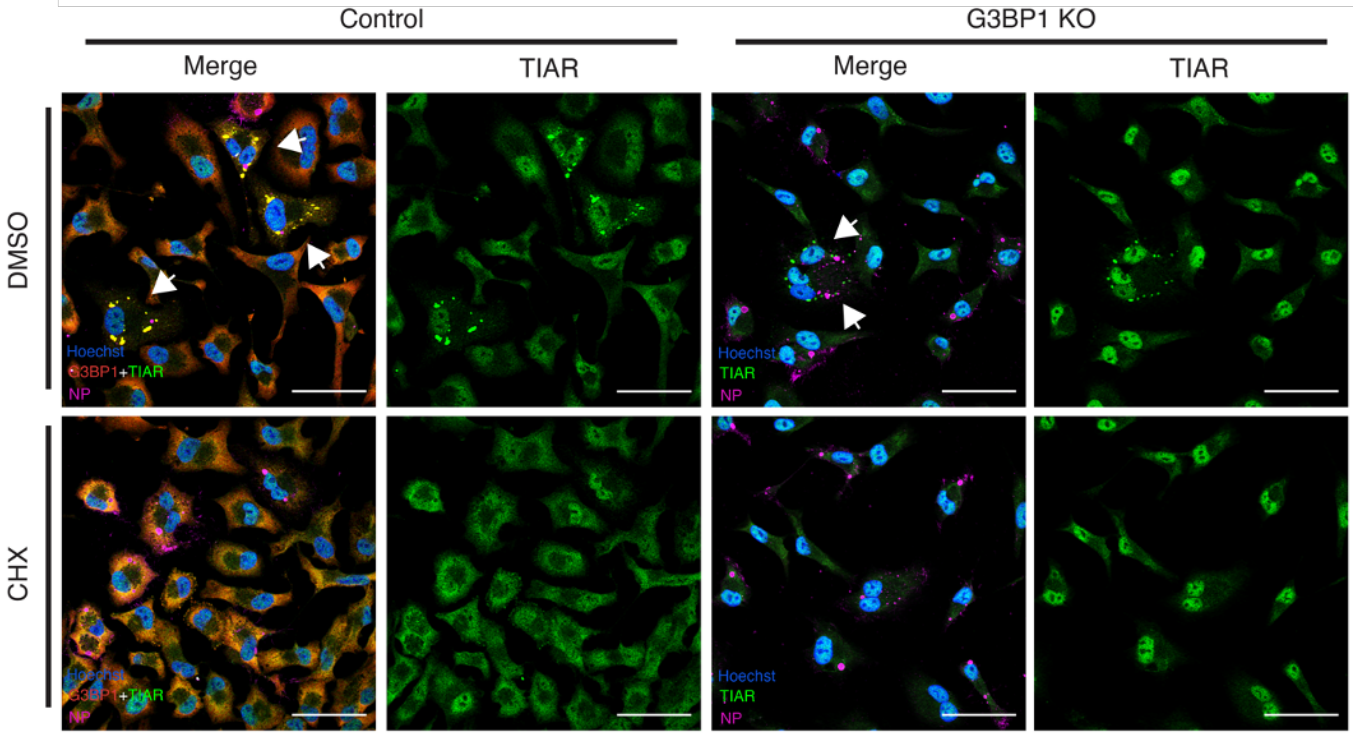

Figure 3.7. G3BP1 (red) and TIAR (green) staining for stess granules and viral protein (RSV NP) detection in control and G3BP1 KO cells 24 hpi with RSV cbVG-high at MOI 1.5 $TCID_{50}$/cell and treated with DMSO (upper panel) or CHX (10μg/mL) (lower panel). All widefield images were acquired with the Apotome 2.0 at 63x magnification and are representative of three independent experiments. Scale bar = 50 μm.

In the context of some non-virus induced stresses, knocking out both G3BP1 and G3BP2 have been shown to be necessary for stress granule inhibition [140]. To test if cbVG-dependent stress granule inhibition requires KO of both G3BP1 and G3BP2, we next generated a G3BP2 KO cell line as well as a G3BP1/2 double KO (dKO) cell line (**Figure 3.6A**). *RSV G* mRNA levels showed only significant differences in viral replication between control and G3BP1/2 dKO cells **(Figure 3.6B**). When we infected G3BP1/2 dKO cells with RSV cbVG-high virus stocks, we no longer observed stress granules upon staining for TIAR,

but stress granules were still formed in G3BP1 and G3BP2 single KO cells (**Figure 3.8**). These data demonstrate that cbVG-dependent stress granule inhibition requires KO of both G3BP1 and G3BP2.

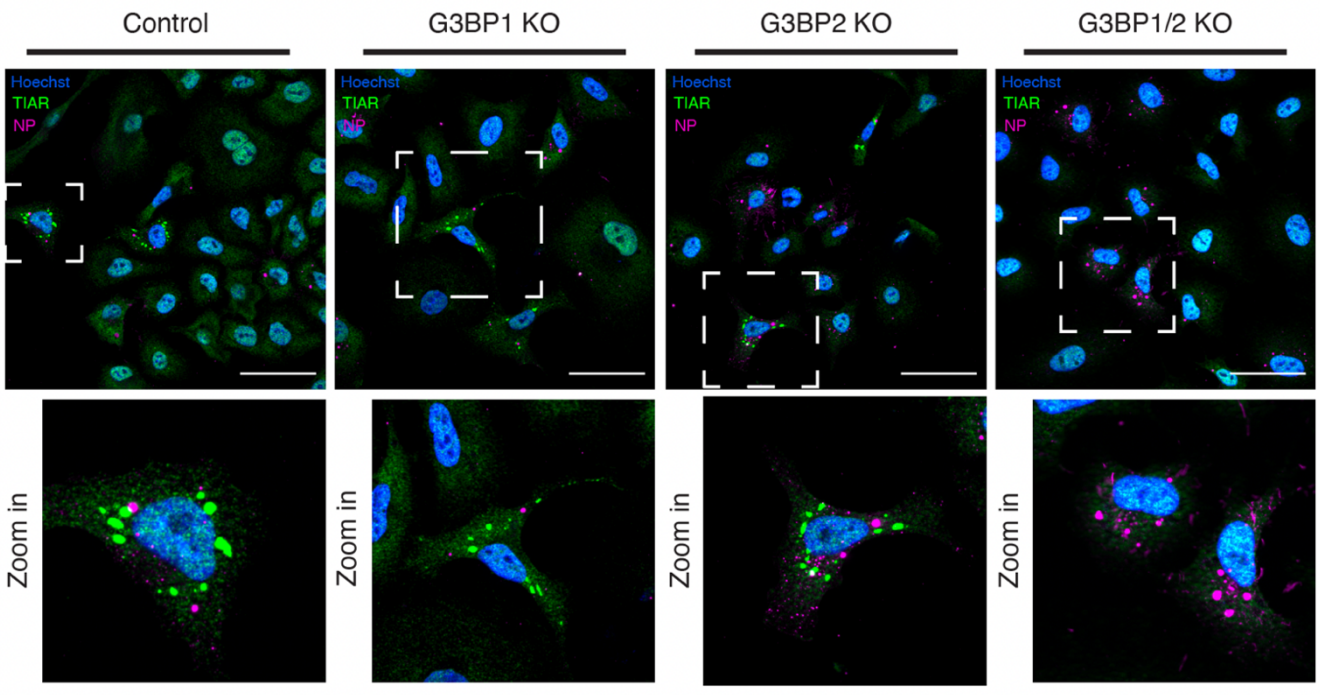

Figure 3.8. G3BP1 (red) and TIAR (green) staining for stress granules and viral protein (RSV NP) detection in control, G3BP1 KO, G3BP2 KO and G3BP1/2 dKO cells infected 24 hpi with RSV cbVG-high at MOI 1.5 $TCID_{50}$/cell. All widefield images were acquired with the Apotome 2.0 at 63x magnification and are representative of three independent experiments. Scale bar = 50 μm.

3.4. Discussion

Characterizing the cytoplasmic granules under study provides insight into the potential role they play during infections. Here, we confirmed that cbVG-dependent stress granules are canonical and are not RNAse L-dependent. This is demonstrated by the fact that cbVG-dependent stress granules are dependent on polysome disassembly and do not require RNAse L to form (**Figure 3.1 and Figure 3.2**). These data also demonstrate that RNAse L is not activated during negative-sense RNA virus infection, which has been previously shown [141]. Out of the context of an infection, transfection of cbVG-derived RNAs induce RLBs, highlighting the differences in responses between virus infection and virus RNA transfections. These data demonstrate that, although utilizing RNA transfections to study biological processes can be very powerful, it often does not reflect what occurs during virus infections.

As expected, cbVG-dependent stress granules are PKR-dependent **(Figure 3.5)**. However, MAVS signaling was dispensable for inducing stress granule formation during cbVG-high infections **(Figure 3.5)**. These data demonstrate that cbVGs activate both the stress response and the antiviral immune response independently. To our knowledge, this is the first description of cbVGs activating cellular responses independent on their immunostimulatory activity, diversifying the role of cbVGs as key interactors with the host. The uncoupling of both signaling pathways also suggest that the role the stress response has during infection is independent on the antiviral immune response.

During virus infection, stress granules can be inhibited by knocking out PKR, inhibiting both translation inhibition and stress granule formation, or by knocking out nucleating factors

like G3BP1, which only inhibits the physical formation of stress granules and not translation inhibition [109, 142-144]. To test the requirement of stress granule nucleating factors during infection, we generated a G3BP1 KO model which was previously shown to be required for stress granule formation during RSV infection [121]. To our surprise, knocking out G3BP1 was not sufficient to inhibit the formation of canonical stress granules containing TIAR (**Figure 3.7**). After demonstrating that knocking out G3BP2 was also insufficient to inhibit stress granule formation, we developed a G3BP1 and G3BP2 dKO cell line, which successfully stopped stress granules from forming during RSV cbVG-high infection (**Figure 3.8**). Our data agrees with a recent report showing that knocking out both G3BP1 and G3BP2 is required for stress granule inhibition during viral infections [107]. We attribute the contradiction regarding the requirement of G3BP1 for stress granule formation during infection with mononegaviruses to differences in the approaches used to validate the absence of stress granules, and staining for TIAR represents a good alternative stress granule marker for this purpose.

3.5. Procedures

Drug treatments

For sodium arsenite treatment, cells were washed once with PBS and replaced with fresh media. 0.5 mM of sodium arsenite (Sigma-Aldrich) was added to the media and cells were incubated for 1 h at 37 °C. For ISRIB or CHX treatment, infected cells or cells treated with sodium arsenite were treated with 200 nM of ISRIB (Sigma-Aldrich) or 10 μg/mL of CHX for 1 h at 37 °C.

In Vitro Transcription of cbVGs

The pSL1180 plasmid was cloned to encode the SeV or RSV cbVGs as previously described [54]. The cbVG plasmid was linearized, and in vitro transcribed using the MEGAscript T7 kit (Thermofisher). The resulting product was DNAse-treated and purified by LiCl precipitation according to the manufacturer's protocol. All IVT RNA was quantified by Qubit (Thermofisher) and quality checked through Bioanalyzer (Agilent) to ensure a single band of the correct RNA length was obtained. For transfections, 5 pmol of the IVT cbVG or Low Molecular Weight polyinosine-polycytidylic acid (poly I:C, InvivoGen) were transfected into control A549 or RNAseL-KO A549 cells. At 6 hours post transfection, cells were fixed, permeabilized, and immunostained as described below for Immunofluorescence.

Immunofluorescence

Immunofluorescence was performed as described in Chapter 2.

RNA extraction and PCR/qPCR

RNA extraction and qPCR were performed as described in Chapter 2.

Imaging analysis

SG quantification was performed using Aggrecount automated image analysis as previously described [130].

Western blots

Western blots were performed as described in Chapter 2. Antibodies used for western blot: PKR (Cell Signaling catalog number 12297), MAVS (Cell Signaling catalog number 3993),

G3BP (Abcam catalog numbers ab181150 and ab56574), G3BP2 (Cell Signaling catalog number CS 31799) , α-tubulin (Abcam catalog number ab52866).

Statistics

Statistics were calculated using GraphPad Prism. Version 9

Chapter 4

Role of Translation Inhibition and Stress Granule Formation During SeV and RSV cbVG-high Infection

4.1. Abstract

The role stress granules play during virus infection remains controversial. While some work in the literature suggests an important role for stress granule formation in proper expression of IFN and ISGs, others demonstrate otherwise. Conflicting evidence also demonstrates inconsistent roles for activation of the stress response in reducing or enhancing virus replication. Here we show that key immune signaling proteins do not co-localize in stress granules, contradicting the current model suggesting stress granules serve as signaling hubs of the antiviral immune response. Translation inhibition and SG formation do not affect the overall expression of IFN and ISGs during infection, making the stress response dispensable for antiviral immunity. Using live-cell imaging, we show that SG formation is highly dynamic and correlates with a drastic reduction of viral protein expression even in cells infected for several days. Through analysis of active protein translation at a single cell level, we show that infected cells that form SG show inhibition of protein translation. Our work contradicts current literature suggesting a role of stress granules in inducing the global antiviral immune response and instead shows activation of the stress response leads to translation inhibition and reduction of viral protein expression in stress granule positive cells.

4.2. Introduction

The localization of immune signaling proteins in stress granules together with the reduced levels of IFN observed in cells that cannot form stress granules has led to the hypothesis that stress granules are necessary to induce the antiviral immune response [100]. This has been challenged by contradictory evidence regarding the ability of viruses to induce the stress response and the effect this response has in the outcome of the infection [121, 145, 146]. To study the role of the stress response, knockout cell systems are often used to inhibit the response. G3BP1 or PKR knockout cell lines are common systems used to understand the role stress granules play during infection. Although both systems can be informative, it is important to understand the differences when interpreting the data. Knocking out PKR leads to inhibition of both translation inhibition and stress granule formation. Knocking out G3BP1/2 only inhibits stress granule formation while leaving the translation inhibition intact. More importantly, both proteins have stress-independent roles in the cell, and it is worth keeping this in mind when interpreting the data [147, 148].

Additional to the roles in the antiviral immune responses, the stress response is also a mechanism to prevent synthesis of viral proteins necessary for the virus life cycle [100]. Interestingly, the translation arrest that accompanies stress granule formation does not affect the global expression of IFN and ISGs, suggesting that mRNAs for these proteins are protected from cap-dependent translation inhibition. This observation is puzzling because ISG mRNAs do not contain elements that would allow for cap-independent translation [100]. A heterogeneity in the timing of the stress response activation could reconcile both virus protein interference and IFN production occurring during the infection. Additionally, a heterogeneity in

the cells that activate the response during infection could also account for both seemingly contradictory processes.

In this chapter we show that the stress response is dispensable for induction of global antiviral immunity during RSV and SeV cbVG-high infections. This is demonstrated by the lack of co-localization of immune signaling molecules in stress granules and by the lack of differences in global IFN and ISG expression between control, G3BP1/2 KOs and PKR KO cells during cbVG-high infection. We show that stress granule formation during SeV cbVG-high infection is asynchronous and correlates with reduced levels of virus protein levels. We show that the translation inhibition in stress granule positive cells leads to reduced levels of virus protein expression. The reduction in virus protein expression is not dependent on MAVS signaling, demonstrating that the interference at the virus protein level is not due to IFN signaling. These data demonstrate a novel cbVG-driven mechanism of virus interference where activation of the stress response leads to a reduction of virus protein at the translational level.

4.3. Results

4.3.1. Antiviral Signaling Molecules Do Not Localize in cbVG-dependent Stress Granules

As stress granules formation is often associated with induction of the antiviral response [100, 101, 108, 149], we began the involvement of stress granules in the antiviral response induced by cbVGs. Evidence in the literature have suggested that stress granules are signaling hubs where RNA sensors and antiviral molecules localize to facilitate RNA detection and activation of the signaling pathway [101]. To test this, we determined if signaling molecules such as MAVS and RIG-I localize in stress granules. Contrary to reports in the literature, we did not observe localization of MAVS in stress granules (**Figure 4.1A)**, nor recruitment of RIG-I to SG during SeV cbVG-high infection (Figure **4.1B).** Additionally, we performed Immunostaining of PKR during RSV cbVG-high infections, and, like RIG-I and MAVS, PKR did not show co-localization in stress granules (**Figure 4.2**). These data argue against the function of stress granules in recruiting signaling molecules and enhancing the antiviral immune signaling pathway activated during virus infections [101, 107].

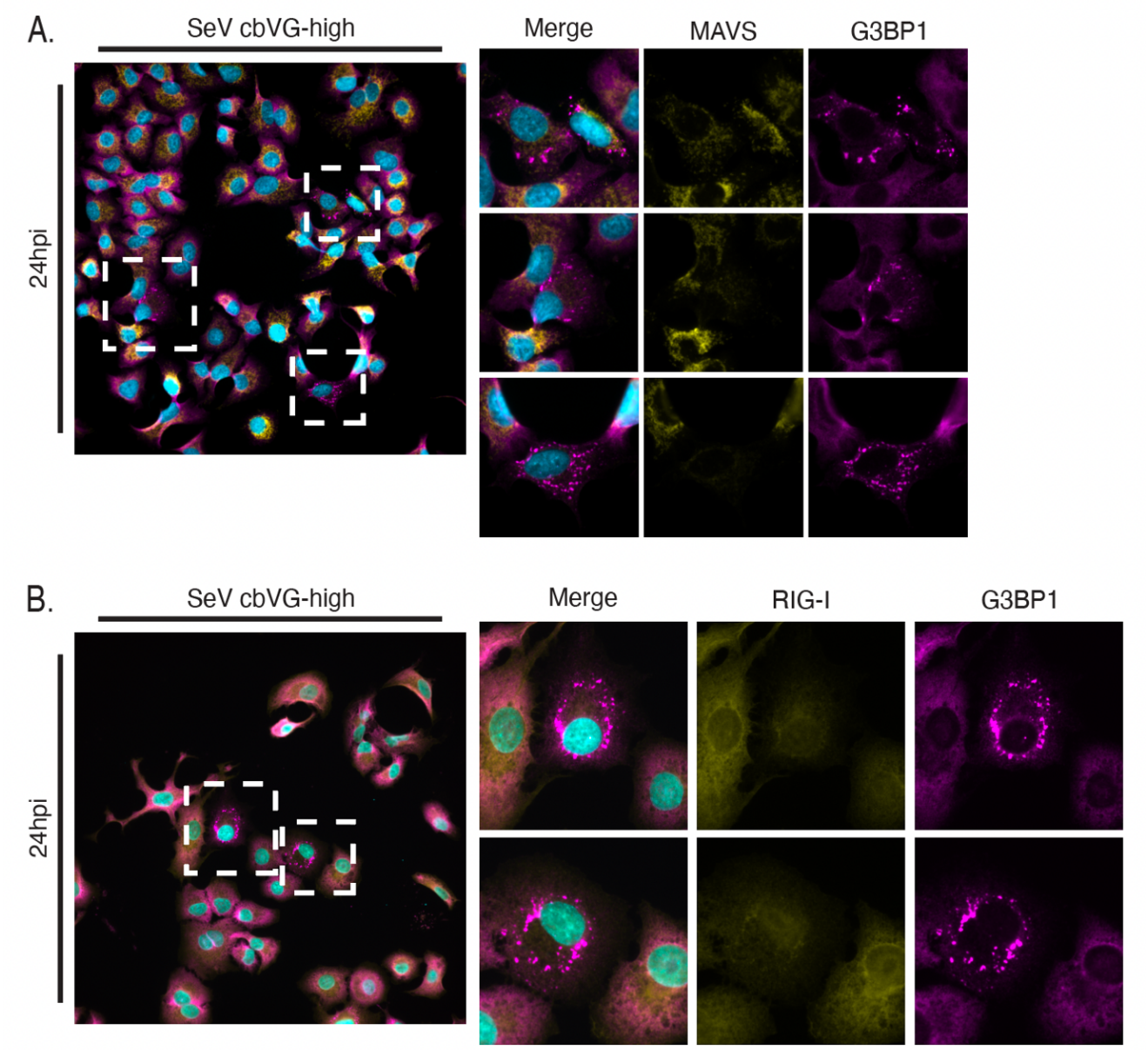

Figure 4.1. (A) Stress granules (G3BP1, magenta) and MAVS (yellow) staining in A549 cells 24 hpi with SeV cbVG-high virus MOI 1.5 $TCID_{50}$/cell. Zoomed in images of stress granule positive cells are shown on the right with merge and MAVS and G3BP1 single channel. (B) Stress granules (G3BP1, magenta) and RIG-I (yellow) staining in A549 cells 24 hpi with SeV cbVG-high virus MOI 1.5 $TCID_{50}$/cell. Zoomed in images of stress granule positive cells are shown on the right with merge and RIG-I and G3BP1 single channel. Widefield images at 40x magnification.

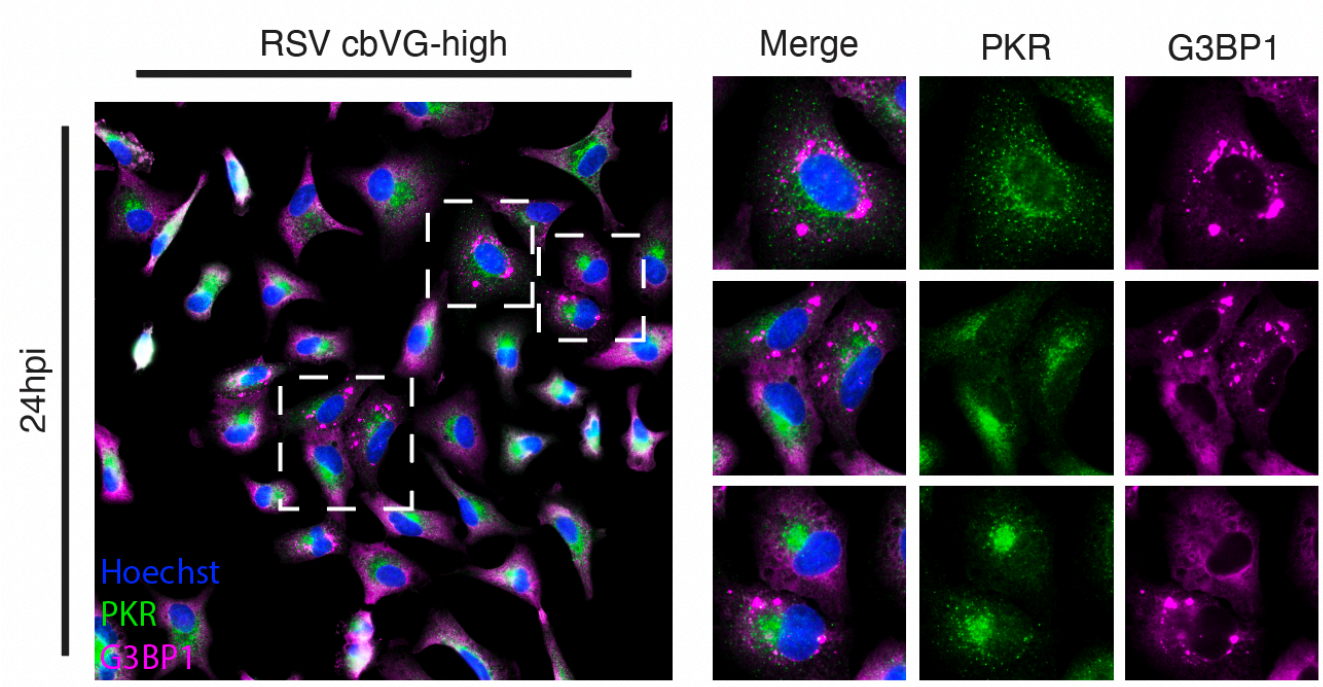

Figure 4.2. Stress granule (G3BP1, magenta) and PKR (yellow) staining in A549 cells 24 hpi with RSV cbVG-high virus MOI 1.5 $TCID_{50}$/cell. Zoomed in images of stress granule positive cells are shown on the right with merge and PKR and G3BP1 single channel. Widefield images at 40x magnification. This experiment was performed by Sydney Briner.

4.3.2. The Stress Response Induced by cbVGs are Dispensable for Global Antiviral Immunity

We then determined if stress granules are necessary for the expression of antiviral genes in response to cbVGs. To do this, we infected control, G3BP1 KO, G3BP2 KO and G3BP1/2 dKO cells with RSV cbVG-high and looked for differences in expression of genes involved in antiviral immunity, including IFN and ISGs, at 24 hpi by qPCR. Expression of *IL-29*, *ISG56* and *IRF7* mRNAs was not impaired when comparing control and G3BP1/2 dKO cells, and only statistically significance differences were observed in *IL-29* expression between G3BP1 KO and dKO (**Figure 4.3 A-C)**. To assess the impact of stress granules on the host

antiviral response more broadly, we looked at the whole transcriptome in control and KO cells at 24 hpi. Most ISGs were expressed at similar levels in control and dKO cells (difference in expression were less than 2 folds; **Figure 4.4**). In the few cases when there were differences of 2-fold decrease or more in expression, the difference was also observed in the G3BP1 or G3BP2 single KO conditions, suggesting the difference is driven by processes independent of stress granule formation (**Figure 4.4, right panel)**.

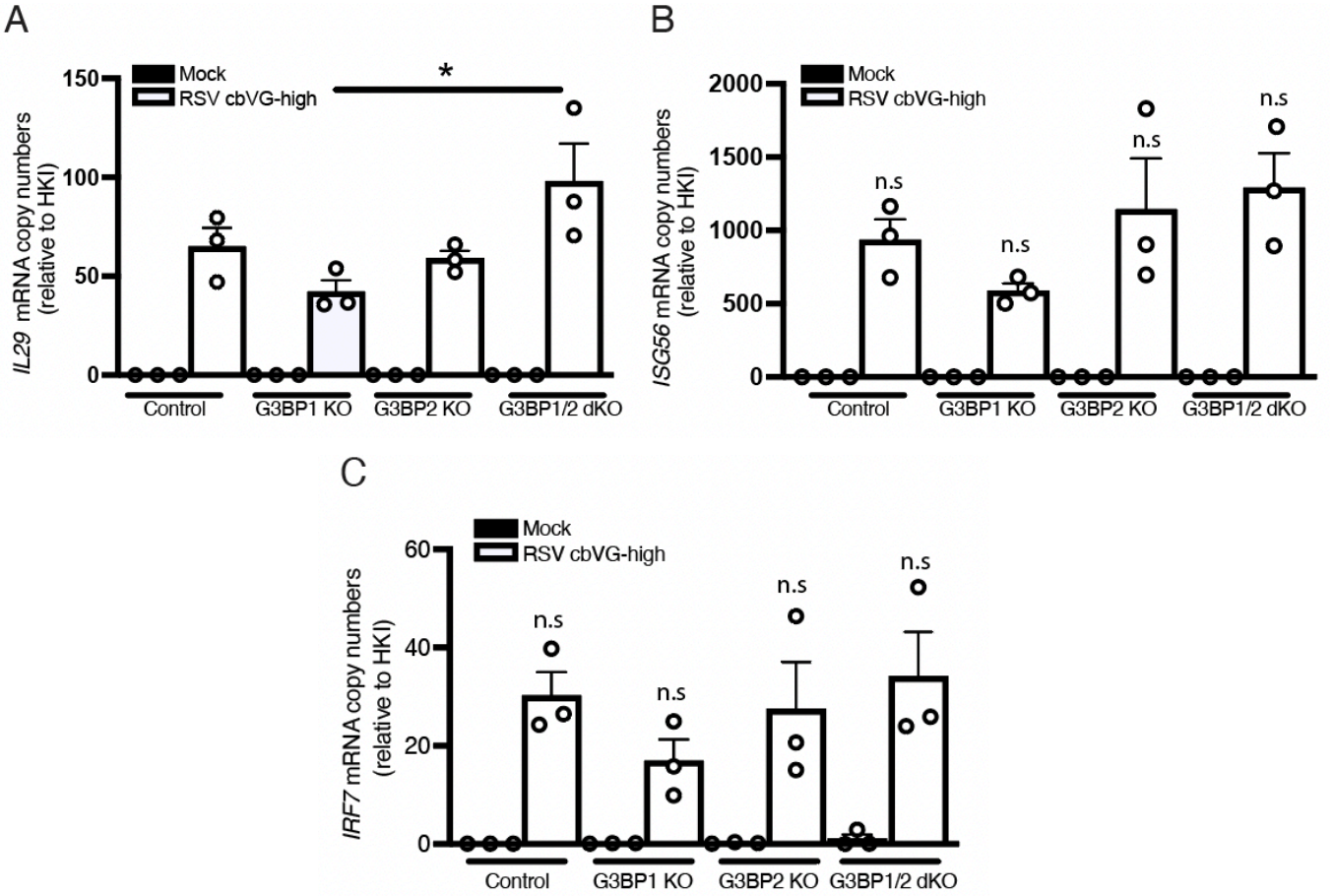

Figure 4.3. mRNA copy numbers of (A) *IL29*, (B) *ISG56* and (C) *IRF7* in control, G3BP1 KO, G3BP2 KO and G3BP1/2 dKO cells 24 hpi with RSV cbVG-high at MOI 1.5 $TCID_{50}$/cell. Statistical analysis: One way ANOVA (*$p < 0.05$).

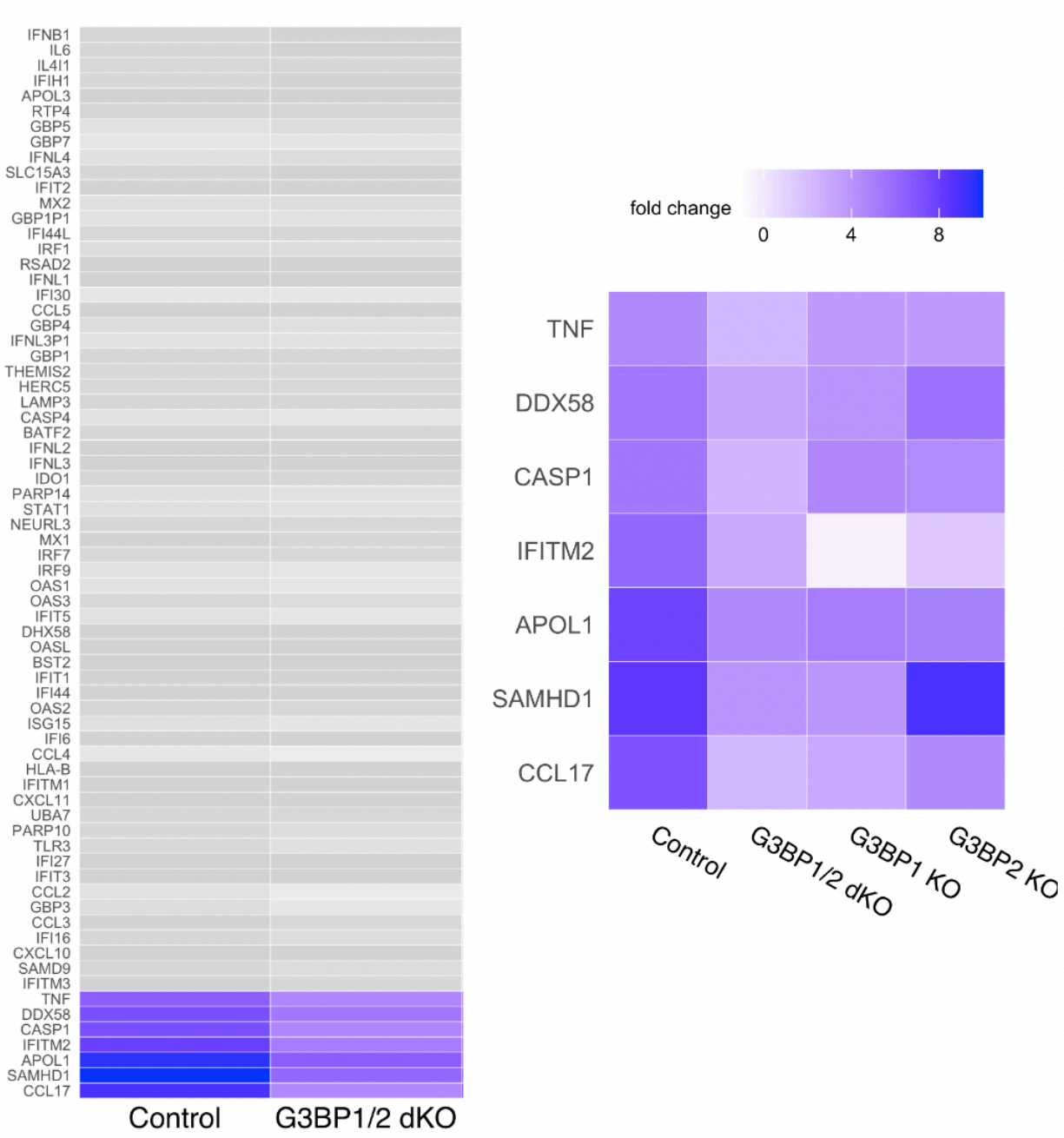

Figure 4.4. Log 2-fold change analysis of genes related to the antiviral response in control, G3BP1 KO, G3BP2 KO and G3BP1/2 dKO cells 24 hpi with RSV cbVG-high at MOI 1.5 $TCID_{50}$/cell relative to mock infected cells. Genes that had less than a 2-fold decrease difference between control and G3BP1/2 dKO are represented in grey color. Genes that had more than a 2-fold decrease difference are highlighted in color. Genes with 2-fold decrease or more difference between control and G3BP1/2 dKO are shown in the right panel and compared to the log 2-fold change of G3BP1 and G3BP2 single KOs.

Additionally, we tested whether absence of stress granules leads to reduced protein expression of ISGs. Expression of the ISGs IFIT1, IRF7 and RIG-I was not different between the cell lines, demonstrating that the antiviral response is not dependent on stress granules (**Figure 4.5A, 4.5B**).

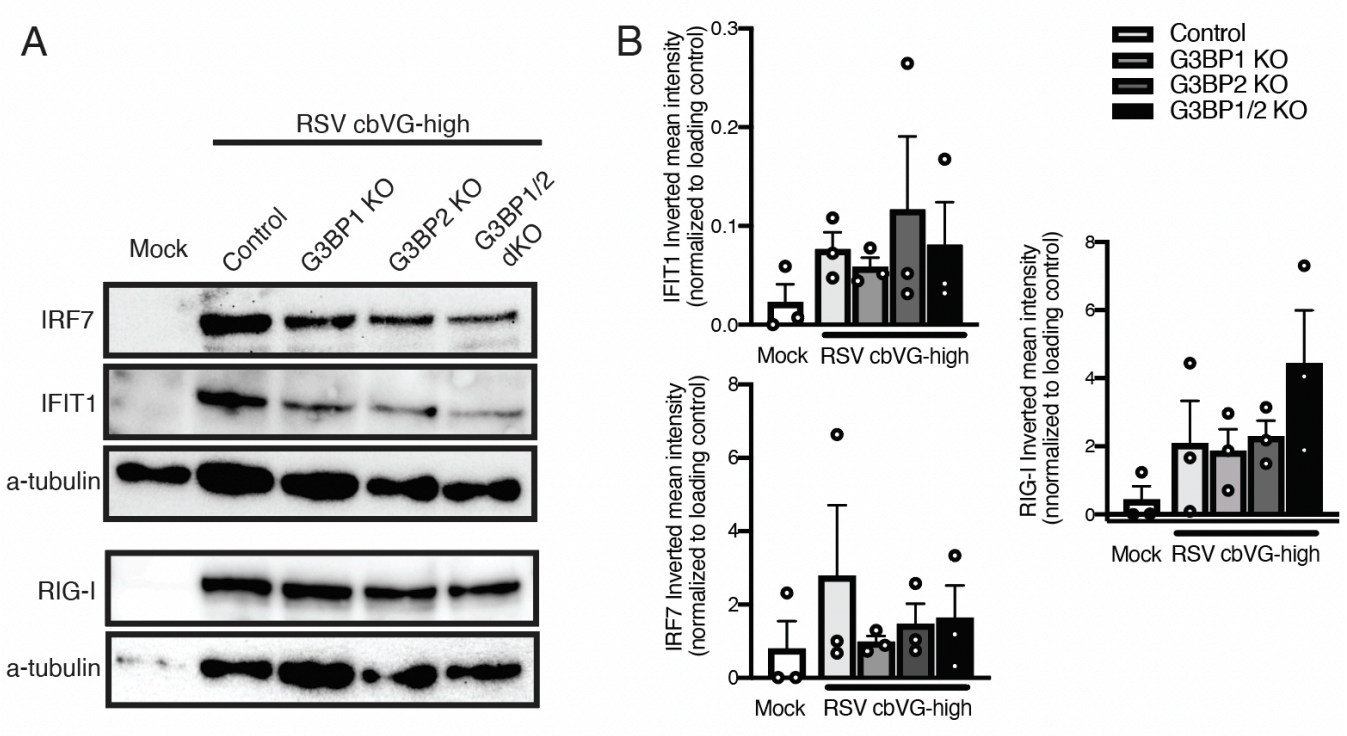

Figure 4.5. (A) Western blot analysis of RIG-I, IFIT1 and IRF7 in control, G3BP1 KO, G3BP2 KO and G3BP1/2 dKO cells 24 hpi with RSV cbVG-high at MOI 1.5 $TCID_{50}$/cell. Blots shown are representative of three independent experiments. (B) Inverted mean intensity quantification of IRF7, IFIT1 and RIG-I western blot bands relative to α-tubulin loading control. Statistical analysis: One way ANOVA. No statistical significance was found.

Because the role G3BPs have in the stress response is directly in stress granule formation and not the translation inhibition that occurs upstream of the pathway, we looked at the direct role of PKR signaling in antiviral immunity. For this, we infected PKR KO cells with RSV cbVG-high virus and compared *IL-29* transcript levels and IFIT1 protein levels to control infected cells and saw no significant differences (**Figure 4.6A, 4.6B**). Similarly, cells infected with SeV cbVG-high virus had no differences in phosphorylation of IRF-3, the primary transcription factor leading to type I IFN expression, nor differences in protein expression of the antiviral gene IFIT1 (**Figure 4.7A, 4.7B**). Altogether, these data suggest that PKR activation and stress granule formation are dispensable for global induction of antiviral immunity.

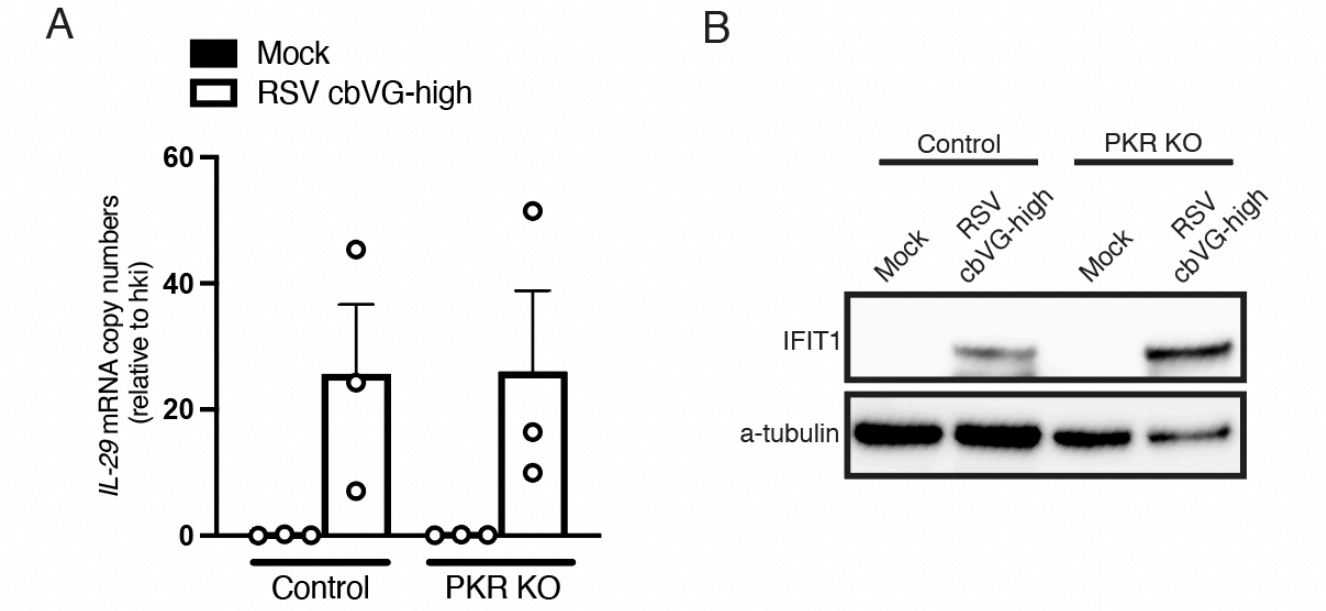

Figure 4.6. (A) *IL29* mRNA levels relative to the house keeping index (hki) in control and PKR KO cells cells 24 hpi with RSV cbVG-high at MOI 1.5 $TCID_{50}$/cell. Statistical analysis: One way ANOVA. No statistical significance was found. (B) Western blot analysis of IFIT1 and IRF7 in control and PKR KO cells 24 hpi with RSV cbVG-high at MOI 1.5 $TCID_{50}$/cell. Blots shown are representative of two independent experiments.

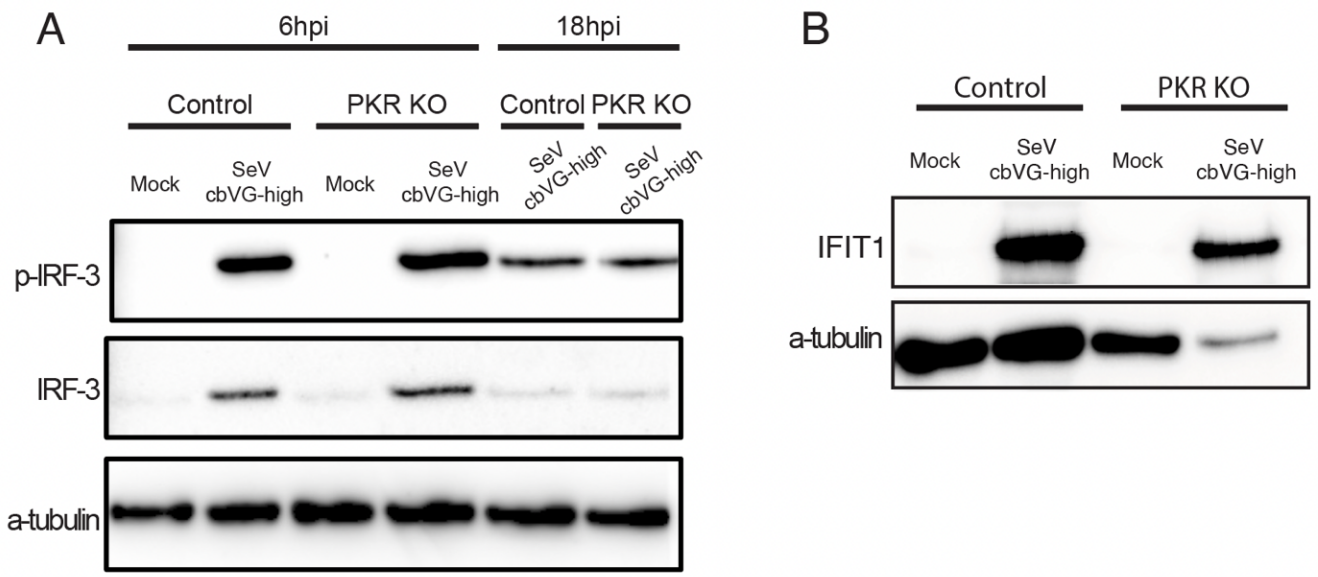

Figure 4.7 (A) Western blot analysis of phosphorylated IRF-3 in control and PKR KO cells 6 and 18 hpi with SeV cbVG-high at MOI 1.5 $TCID_{50}$/cell. (B) Western blot analysis of IFIT1 in control and PKR KO cells 24 hpi with SeV cbVG-high at MOI 1.5 $TCID_{50}$/cell.

4.3.3. SeV cbVG-dependent Stress Granules Form Dynamically During Infection and Persist After Several Days Post-infection

To study the dynamics of stress granule assembly and disassembly as well as assess the impact of stress granules during infection, we generated G3BP1-GFP expressing A549 cells to visualize stress granule formation in real time. Using live-cell imaging of cells infected with a recombinant SeV expressing miRFP670 and supplemented with purified cbVG particles, we show dynamic formation and disassembly of stress granules throughout the course of the infection. During the period of 6 – 72 hpi we identified several subpopulations of cells (**Figure 4.8, Figure 4.9**). Some cells formed stress granules after infection and eventually disassembled them (**Figure 4.9, series 1).** These cells showed faint levels of miRFP670 signal early in infection. Once stress granules disassembled, the miRFP670 signal increased. Other

cells formed stress granules and eventually died (**Figure 4.9, series 2**). A few cells assembled and disassembled stress granules and remained very low in miRFP670 signal throughout the infection (**Figure 4.9, series 3**). Moreover, formation of stress granules persisted in the population even 13 dpi **(Figure 4.10).** These data demonstrate that SeV cbVG-dependent stress granules form asynchronously, and that formation of stress granule continues throughout the infection.

Figure 4.8. Video of G3BP1-GFP expressing A549 cells infected with rCantell-miRF670 reporter virus at MOI 3 $TCID_{50}$/cell with 20 HAU of supplemented cbVG purified particles, timelapse microscopy 6 – 72 hpi, images every 6 h at a 20x magnification.

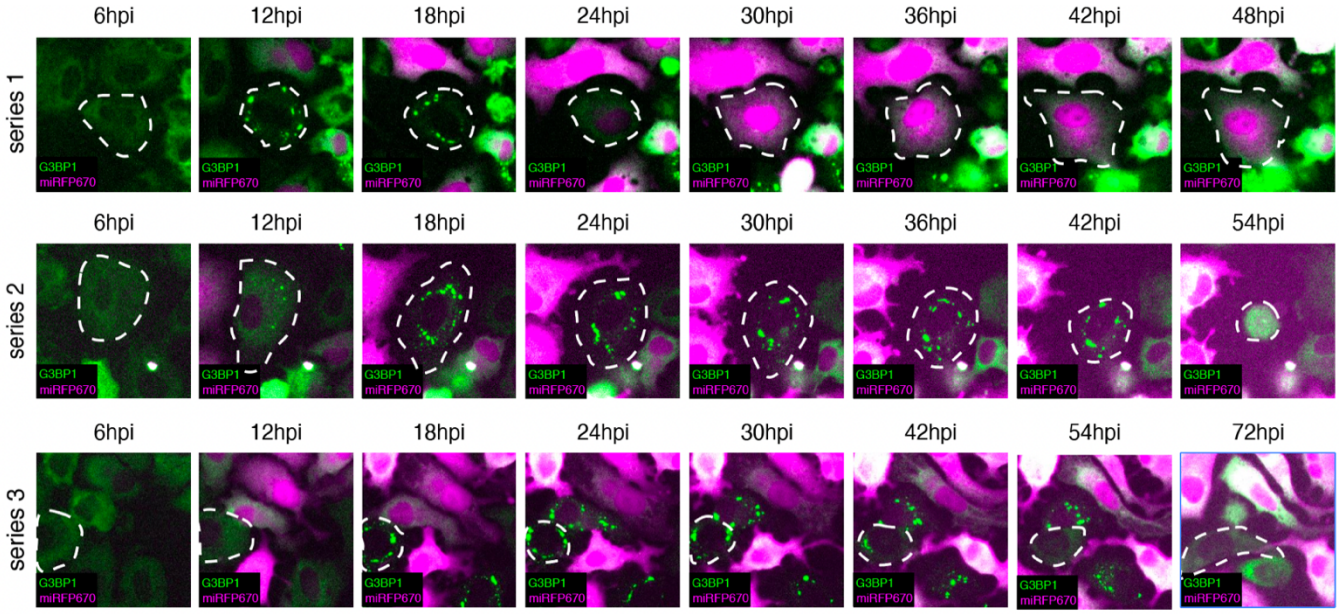

Figure 4.9. G3BP1-GFP (green) expressing A549 cells infected with rCantell-miRF670 (magenta) reporter virus at MOI 3 $TCID_{50}$/cell with 20 HAU of supplemented cbVG purified particles, timelapse microscopy 6 - 72hpi, images every 6 h at a 20x magnification. Series show focus of different cells in the population.

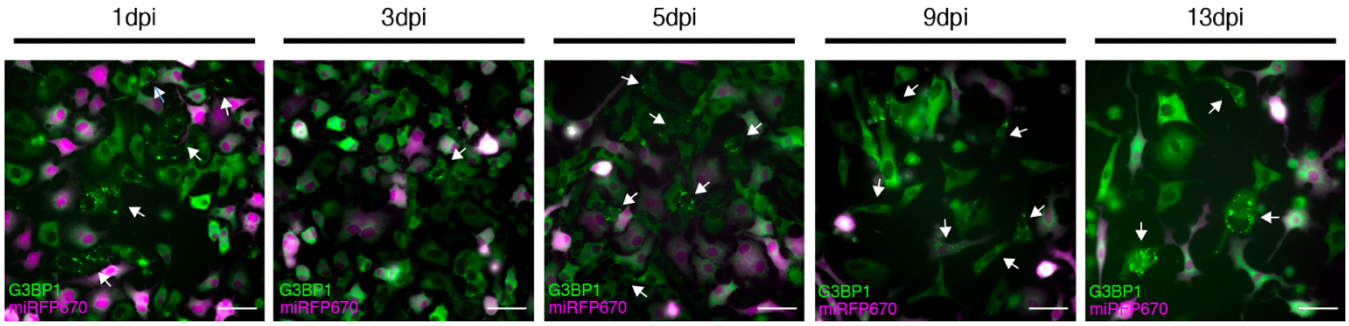

Figure 4.10. timelapse microscopy images of G3BP1-GFP (green) expressing A549 cells infected with rCantell-miRF670 (magenta) reporter virus at MOI 3 $TCID_{50}$/cell with 20 HAU of supplemented cbVG purified particles from day 1 to day 13. Arrows point at stress granule positive cells.

4.3.4. cbVG-dependent Stress Granules Correlate With Reduced Levels of Viral Protein Expression

In these experiments, we observed that the signal for the viral reporter gene miRFP670 was low in stress granule positive cells, to the point where some cells appeared uninfected. This is similar, but more extreme, than our observation via immunofluorescence that SeV NP positive stress granule positive cells often showed lower signal for SeV NP compared to those that were stress granule negative cells (**Figure 2.4A**). We observed similar findings in RSV cbVG-high infection when staining for the RSV F protein (**Figure 4.11**). We hypothesized that a single cell could gain and lose miRFP670 signal within a 6h window, resulting in stress granule positive cells that appeared uninfected at the time of imaging. To confirm that stress granule positive cells during live imaging were infected, we performed timelapse imaging starting at 6 hpi before we begin to see stress granule positive cells during the infection and tracked stress granule positive cells every 30 min from 6 to 24 hpi to assess changes in the miRFP670 signal with a higher temporal resolution. stress granule positive cells showed miRFP670 before forming stress granules and lost the signal as time went by, demonstrating that stress granule formation is correlated with a reduction in viral protein expression (**Figure 4.12, 4.13)**.

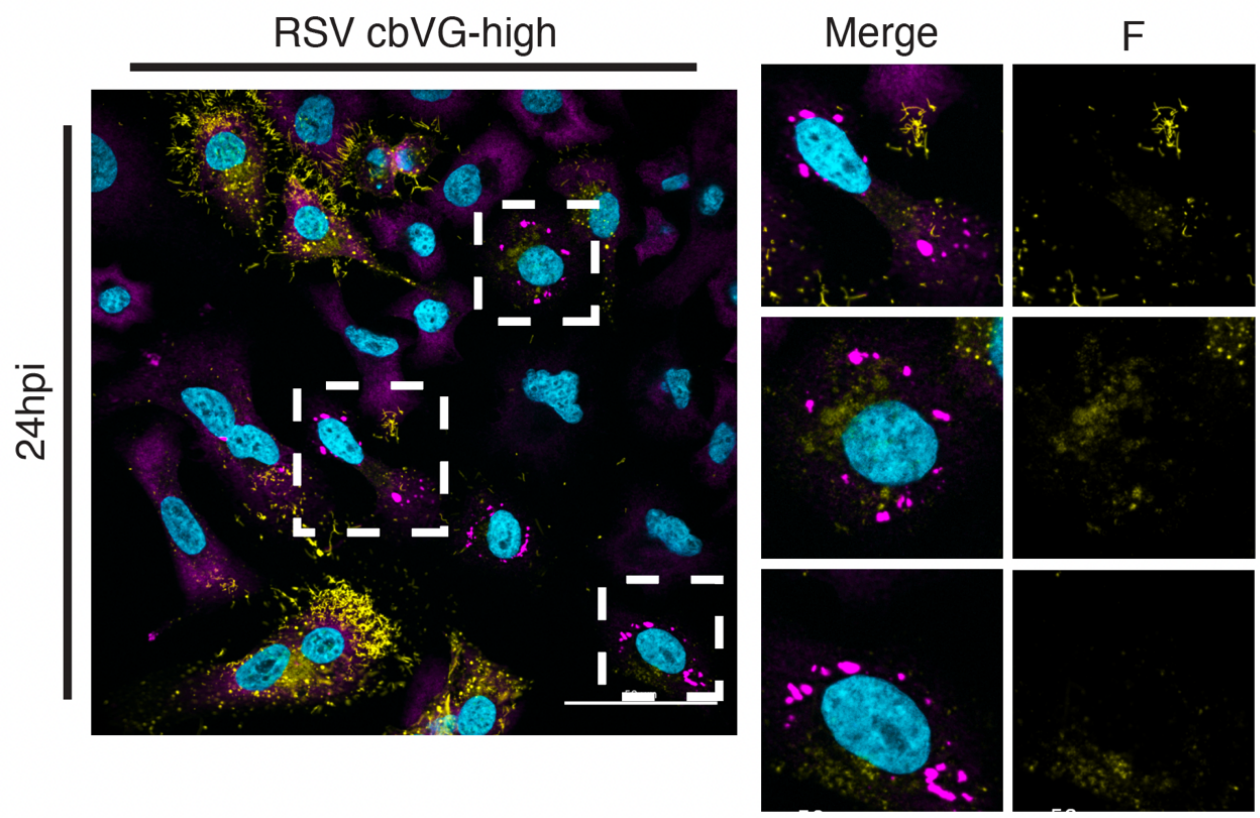

Figure 4.11. Stress granule (G3BP1, magenta) and viral protein (RSV F, yellow) detection in A549 cells 24 hpi with RSV cbVG-high virus at MOI 1.5 $TCID_{50}$/cell. Zoomed in images of stress granule positive cells are shown on the right with merge and RSV F single channel. Widefield image was acquired with the Apotome 2.0 at 63x magnification, scale bar = 50 μm. This experiment was performed by Nicole Rivera-Espinal.

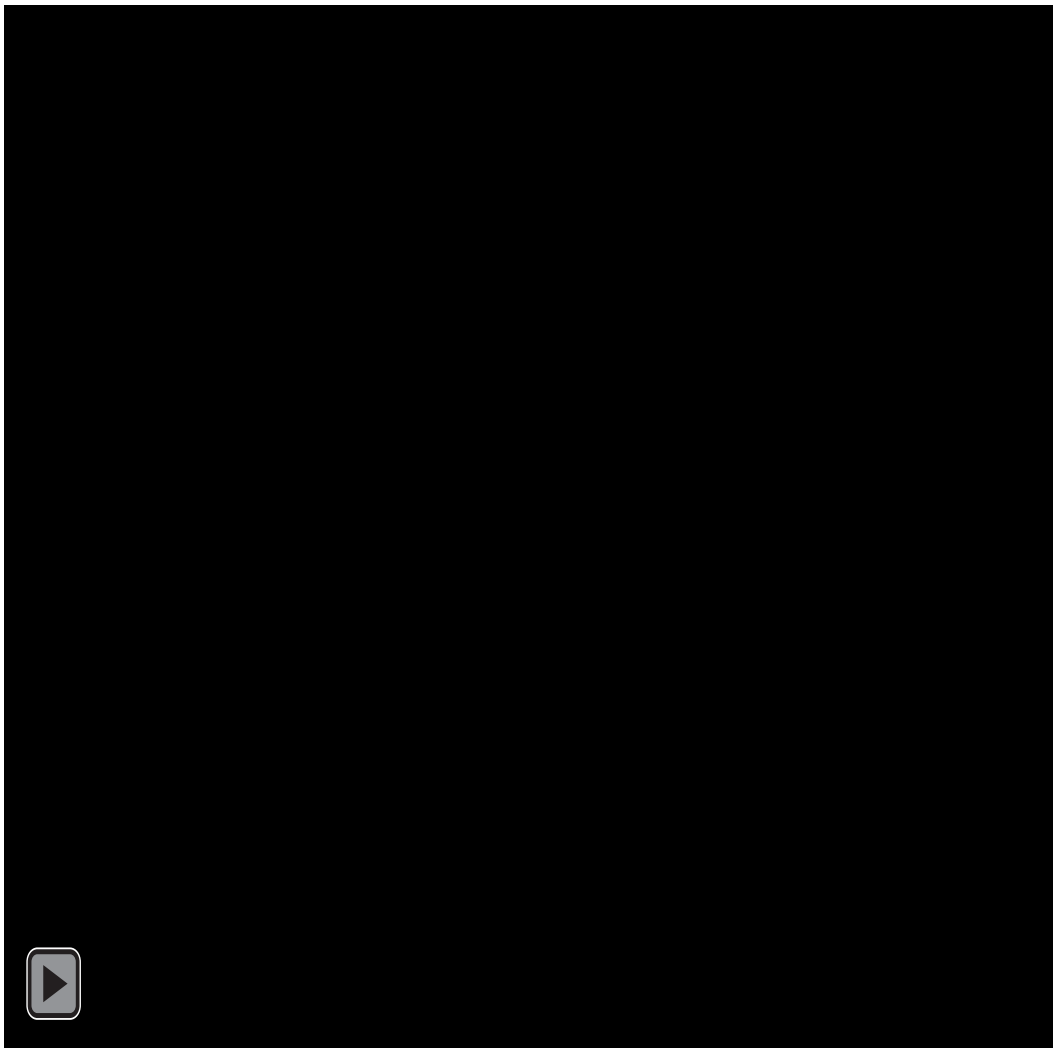

Figure 4.12. Video of G3BP1-GFP expressing A549 cells infected with rCantell-miRF670 reporter virus at MOI 3 $TCID_{50}$/cell with 20 HAU of supplemented cbVG purified particles, timelapse microscopy 12 – 24 hpi, images taken every 30 min at a 40x magnification using a widefield microscope.

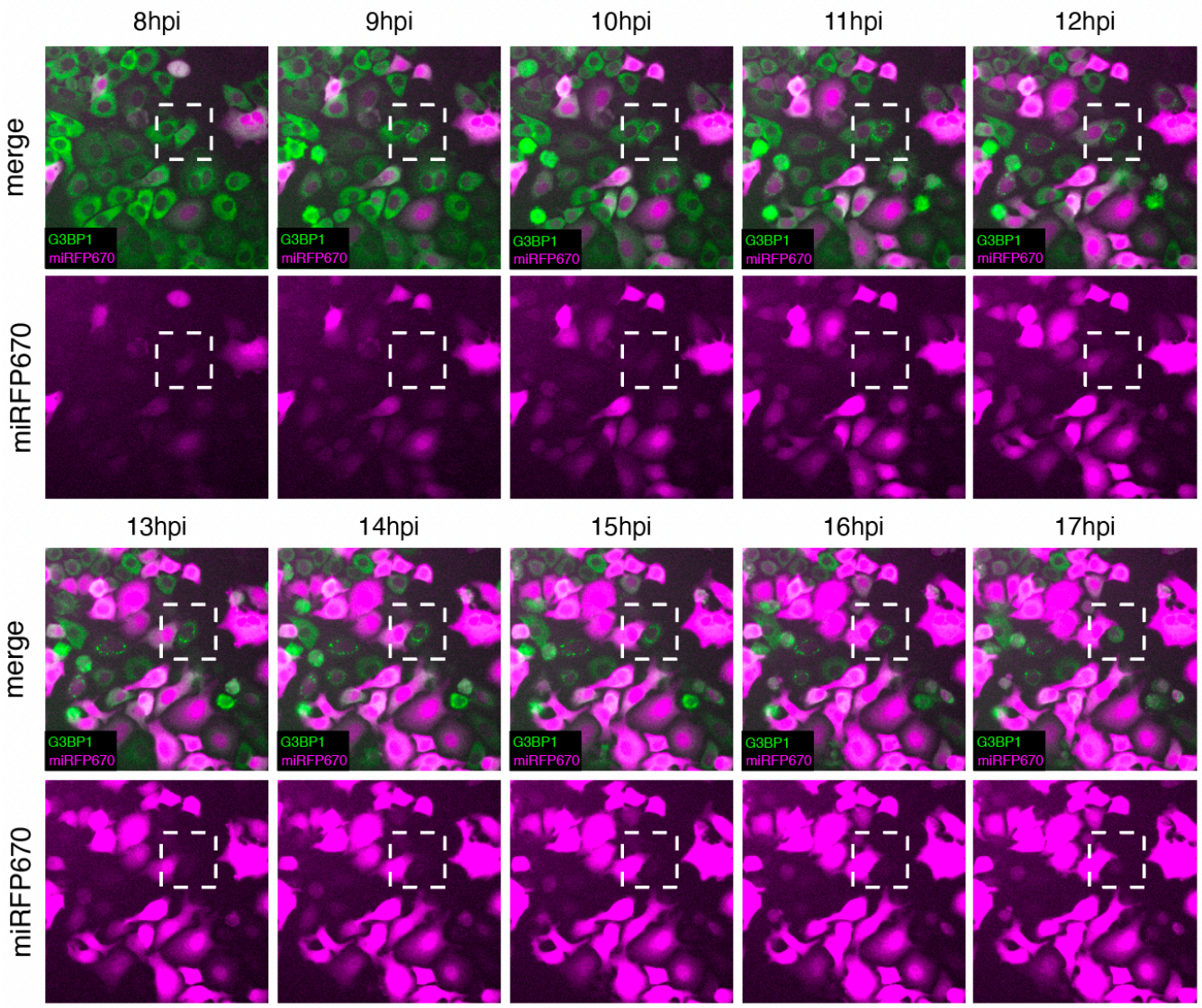

Figure 4.13. G3BP1-GFP (green) expressing A549 cells infected with rCantell-miRF670 (magenta) reporter virus at MOI 3 $TCID_{50}$/cell with 20 HAU of supplemented cbVG purified particles, timelapse microscopy 8 - 18hpi, images taken every 1 h. All timelapse images were acquired with a widefield microscope at 20x magnification.

4.3.5. cbVG-mediated Interference with Viral Protein Expression is Independent on MAVS Signaling in Stress Granule Positive Cells

The reduction on virus protein levels in stress granule positive cells led us to hypothesize that the well-established virus interference function of cbVGs is at least in part mediated by the induction of the cellular stress response. Because cbVGs are known to interfere with virus replication through the induction of MAVS signaling and IFN production which consequently leads to a reduction of viral protein levels, we determined if this viral protein reduction observed in stress granule positive cells was a due to the IFN response and independent on stress granule formation. To test this, we infected MAVS KO cells with SeV cbVG-high and compared viral protein SeV NP expression to control infected cells. Stress granule positive cells showed similar SeV NP fluorescence in control and MAVS KO cells (**Figure 4.14**). These data suggest that the interference in viral protein expression observed in cbVG and stress granule positive cells is not due to the IFN response, and instead suggest a direct role for the cellular stress response in reducing viral protein expression.

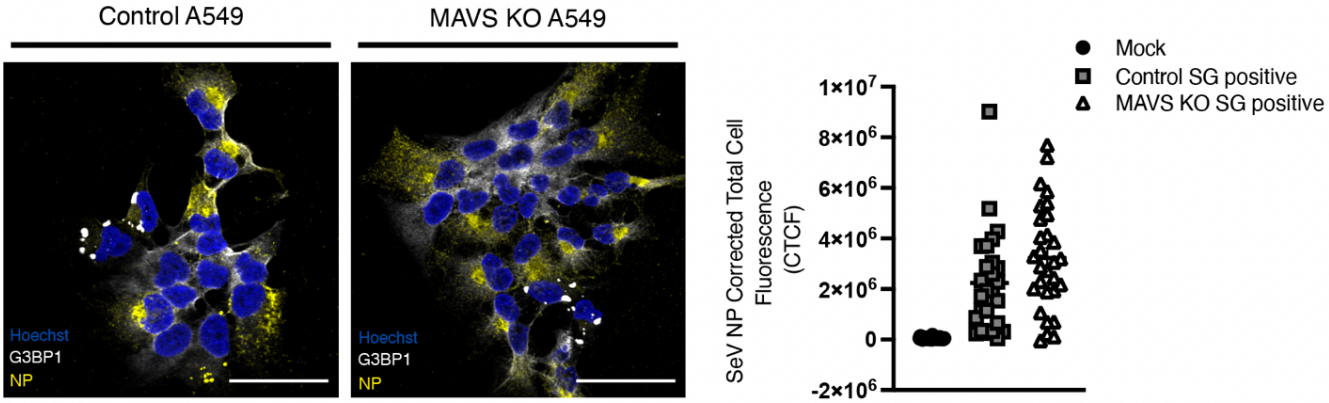

Figure 4.14. Stress granules (G3BP1 white) and viral protein (SeV NP) detection in control and MAVS KO A549 cells 24 hpi with SeV cbVG-high virus at MOI 1.5 $TCID_{50}$/cell 24 hpi. All widefield images were acquired with the Apotome 2.0 at 63x magnification and are representative of three independent

experiments. Corrected total cell fluorescence (CTCF) quantification of SeV viral protein NP in control and MAVS KO A549 stress granule positive cells.

4.3.6. cbVGs Induce Translation Arrest in Stress Granule Positive Cells Leading to Reduced Viral Protein Expression

Stress granules form because of translation inhibition, which could affect virus protein levels in stress granule positive cells. To determine if translation is inhibited specifically in cbVG-induced stress granule positive cells, we performed a ribopuromycylation assay to detect active translation at a single cell level using puromycin (PMY) immunostaining. PMY mimics the tyrosine-modified tRNA and upon exposure to cells, is added to nascent peptides. By combining with a translation elongation inhibitor to trap peptides into ribosomes and upon fixing and immunostaining with a PMY-specific antibody, we can detect translation at a single cell level. We performed ribopuromycylation in SeV cbVG-high infected cells and compared PMY staining in stress granule positive cells to stress granule negative cells. A reduction of PMY signal was observed almost exclusively in stress granule positive cells during SeV cbVG-high infection (**Figure 4.15, lower panel, and Figure 4.16**). This reduction in signal was comparable to sodium arsenite treated cells (**Figure 4.15, middle panel and 4.16**).

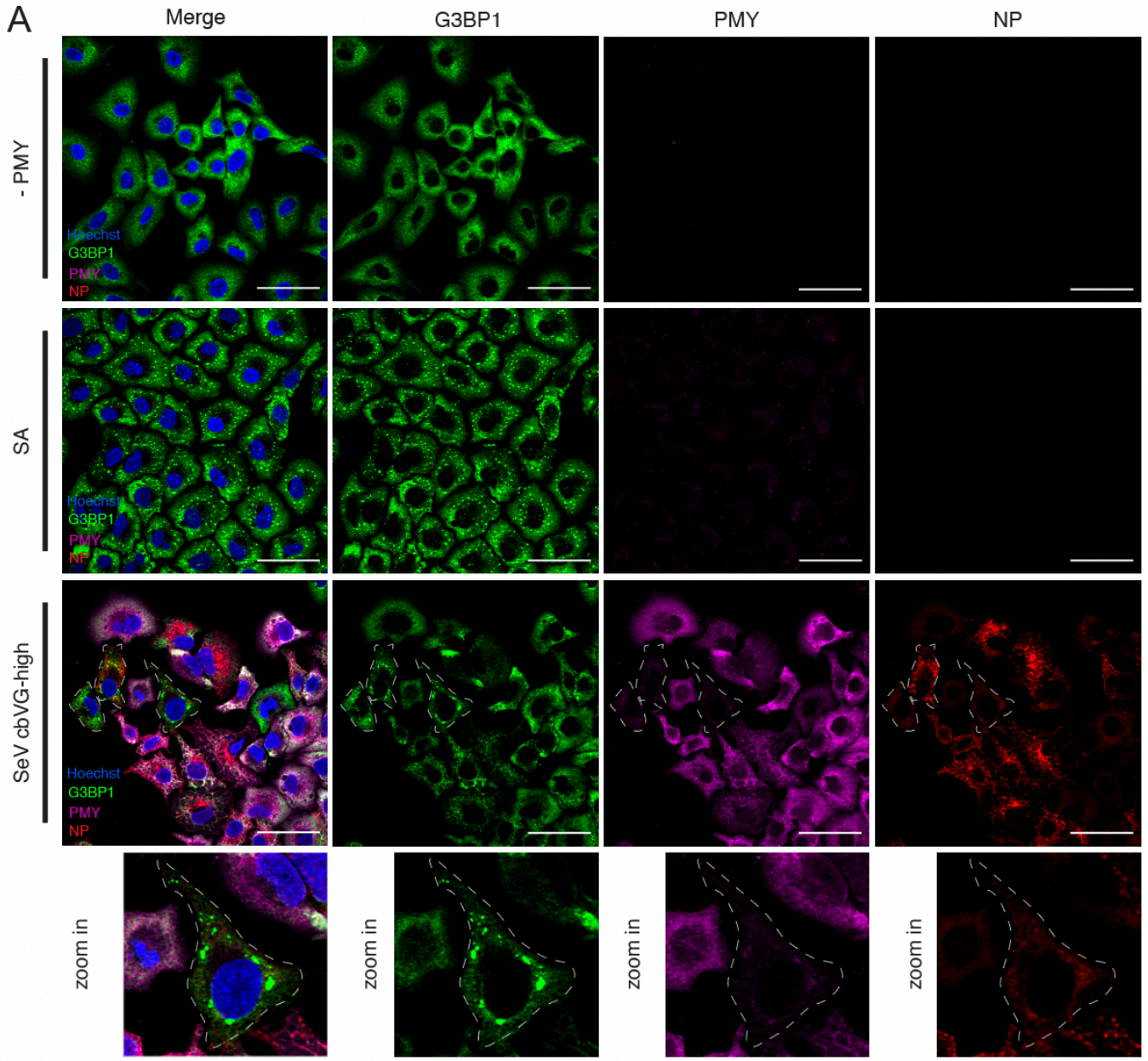

Figure 4.15. G3BP1 (green) for stress granule detection and PMY (magenta) for translation in cells infected with SeV cbVG-high (SeV NP, red) at MOI 3 $TCID_{50}$/cell 24 hpi or treated with sodium arsenite, with and without treatment with PMY for 5 min. Widefield images were acquired with the Apotome 2.0 at 63x magnification All widefield images were acquired with the Apotome 2.0 at 63x magnification and are representative of three independent experiments, scale bar = 50 μm.

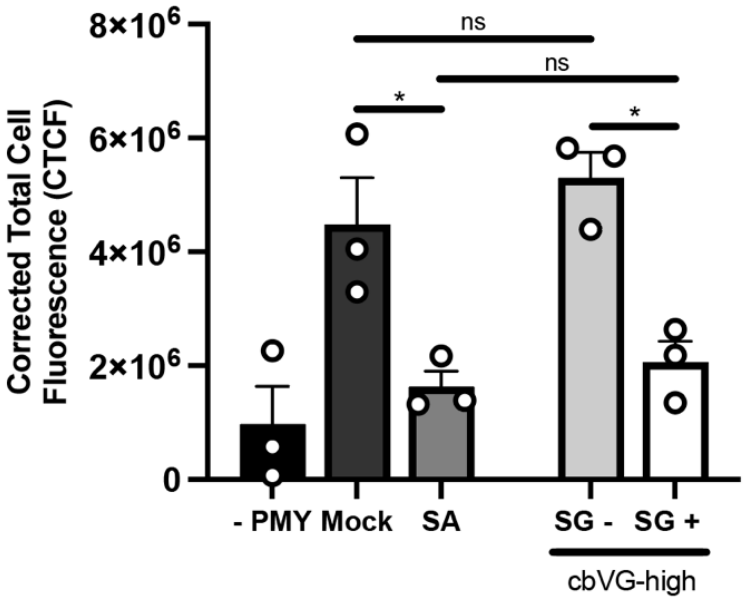

Figure 4.16. PMY intensity (Corrected Total Cell Fluorescence) in cells after drug treatment with sodium arsenite (SA) or stress granule positive (SG +) and stress granule negative (SG -) SeV cbVG-high infected cells. Each dot represents the CTCF average of approximately 100 cells for each condition. Statistical analysis: One Way ANOVA (* $p < 0.05$).

4.3.7. Stress Granule Formation is Not Required to Induce Translation Inhibition During cbVG-high Infections

To determine if stress granule formation is necessary for translation inhibition and reduced viral protein expression, we performed ribopuromycylation in G3BP1/2 dKO and compared PMY staining with control infected cells. As expected, we observe low PMY in G3BP1/2 dKO single cells (**Figure 4.17**), demonstrating that stress granules form because of translation inhibition and are not the drivers of translational arrest. Overall, these data highlight a new function of cbVGs in triggering translation inhibition and stress granule formation independent of their role in inducing the antiviral response.

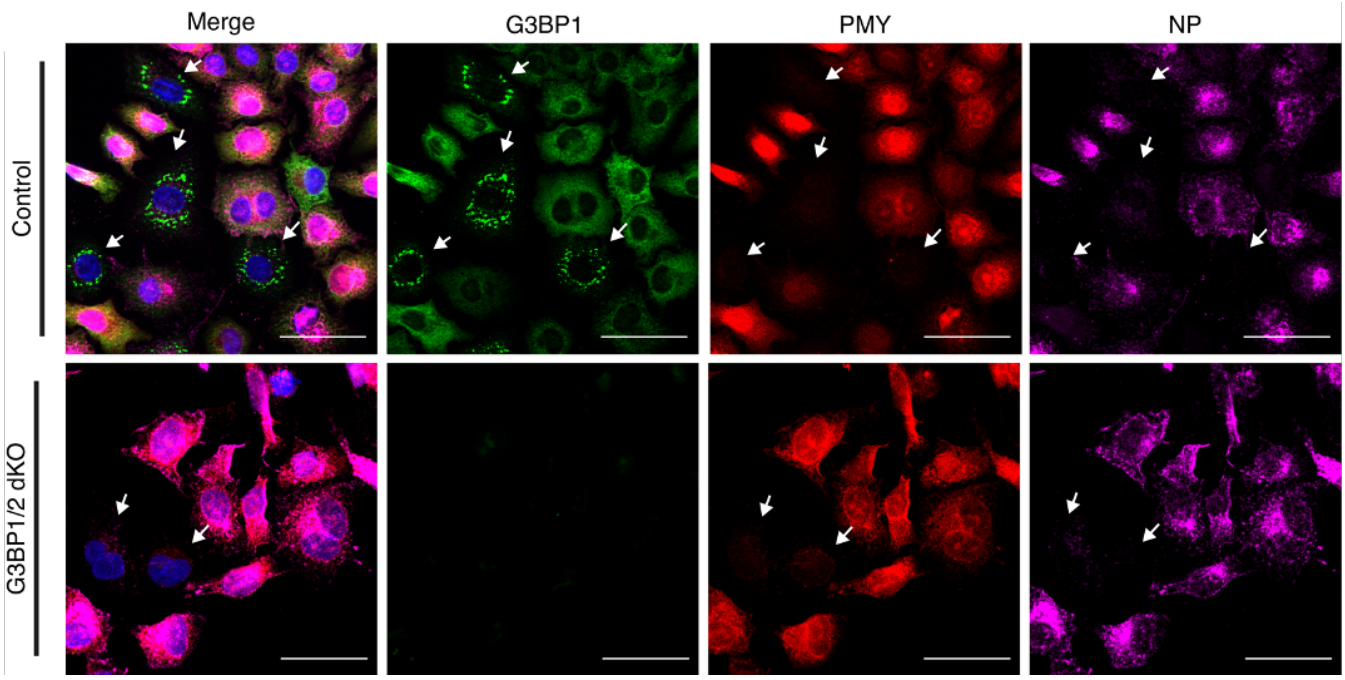

Figure 4.17. G3BP1 (green) for stress granule detection and PMY (red) for translation in control and G3BP1/2 dKO cells infected with SeV cbVG-high (SeV NP, magenta) at MOI 3 $TCID_{50}$/cell 24 hpi.

4.4. Discussion

The immunostimulatory ability of cbVGs together with published data demonstrating how stress granules are involved in inducing and sustaining the immune antiviral response [99, 101, 102, 104] led us to hypothesize that cbVGs induced stress granules to aid with activation of the antiviral response. However, using a G3BP1/2 dKO cell line that successfully impeded the formation of stress granules, we observed no differences in the induction of the antiviral immune response relative to the control cell line. This applied to both the transcriptional and the translational level of IFN and ISG expression (**Figure 4.3, 4.5**). A broader transcriptome analysis confirmed that inhibition of stress granules during infection does not hamper the antiviral immune response (**Figure 4.2**). Certain genes were downregulated in the single G3BP1 or G3BP2 KO which indicate SG-independent roles for these proteins during infection. Indeed, G3BP1 is reported to have roles involving the antiviral response [114]. We also determined if the effect the cellular stress response had on the global antiviral response was dependent on the translation inhibition that occurred upstream of stress granule formation. For this, we used the PKR KO system to look at how expression of antiviral genes and proteins were affected. Similar to the G3BP1/2 dKO system, we observed no differences in IFN and ISG expression in both RSV and SeV infection (**Figure 4.6, 4.7**), suggesting that the cellular stress response does not impact the overall antiviral immune response during RSV or SeV infection.

By performing live-cell imaging of G3BP1-GFP expressing cells infected with a reporter SeV, we uncovered interesting facts about the dynamic formation and disassembly of stress granules. First, we observed that cbVG-induced stress granules are dynamic and form

asynchronously throughout the infection (**Figure 4.8**). Although we began observing stress granule positive cells after 8 hpi, the number of stress granule positive cells increased over time (**Figure 4.8**). We could also see some cells disassembling stress granules throughout the infection (**Figure 4.9**). These data likely explain why not all cbVG-high cells are stress granule positive when we look at a singular time point 24 hpi (**Figure 2.7**). Although we do not have a working tool in our lab to perform RNA FISH in live cells, we suspect that all cbVG-high cells form stress granules at some point during the infection, but these are not all captured in snapshot immunofluorescence experiments.

Throughout our studies, we observed a drastic reduction in viral protein level in stress granule positive cells (**Figures 4.9, 2.4, 4.11, 4.13**). We reasoned that the reduction in virus protein expression could be explained by the well-known function of cbVGs in interfering with the virus life cycle via MAVS signaling and expression of antiviral proteins. In contrast, we saw a reduction of virus protein levels even MAVS KO stress granule positive cells (**Figure 4.14**), suggesting that the interference in protein expression observed in stress granule positive cbVG-high cells is regulated by activation of the stress response itself. Indeed, we observe drastic translation reduction at a single cell level in stress granule positive cells infected with cbVG-high virus (**Figure 4.15, 4.16**). These data implicate translation inhibition and stress granule formation as a previously undescribed mechanism of cbVG-mediated virus interference. We do not see differences in *RSV G* mRNA in control and PKR KO cells (**Figure 3.4**), suggesting PKR activation and translation inhibition does not interfere with virus transcription and instead, interferes with the virus at the translational level due to the translation arrest accompanied by stress granule formation. We cannot, however, discard a

potential additional role for cbVGs in directly interfering with the virus by competing with the virus polymerase, thereby reducing replication, transcription, and translation. However, our group has previously shown this mechanism of interference is minimal [150]. Finally, detection of stress granules in cells several days after infection extends the role of translation inhibition and stress granules formation to later phases of the infection (**Figure 4.10**). It remains unknown if and which other proteins are affected by cbVG-dependent translation inhibition. Although we cannot rule out that a reduction on ISG protein expression occurs specifically in stress granule positive cells, this potential reduction does not affect the global antiviral immune response during the infection, contradicting reports of a requirement for stress granules for the initiation of antiviral immunity [101, 107, 108, 151].

4.5. Procedures

Recombinant Sendai virus rCantell-miRF670 rescue

To create the pSL1180-rCantell plasmid, the complete viral genome of the SeV Cantell strain and the necessary regulatory elements were inserted into the pSL1180 vector using SpeI and EcoRI restriction enzymes in the following order: T7 promoter, Hh-Rbz, viral genome, Ribozyme, and T7 terminator. A miRF670 gene was then inserted between the NP and P genes in the pSL1180-rCantell plasmid to create the pSL1180-rCantell-miRF670 plasmid. The non-coding region between the NP and P genes was used to separate the NP, GFP, and P genes. Additional nucleotides were inserted downstream of the miRF670 gene to ensure that the entire genome followed the "rule of six". The NP, P, and L genes of Cantell were cloned into the pTM1 vector to generate the three helper plasmids. All plasmids were validated by sequencing. The recombinant virus rCantell-miRF670 was produced by co-transfecting pSL1180-rCantell-miRF670 and the three helper plasmids. BSR-T7 cells were transfected with

a mixture of plasmids containing 4.0 µg pSL1180-rCantell-miRF670, 1.44 µg pTM-NP, 0.77 µg pTM-P, and 0.07 µg pTM-L using Lipofectamine LTX. After 5 h, the medium was replaced with infection medium containing 1 µg/ml TPCK and the cells were incubated at 37 °C. The expression of miRF670 was monitored daily using fluorescence microscopy. At 4 days post-transfection, the cell cultures were harvested, and the supernatants were used to infect 10-day-old specific-pathogen-free embryonated chicken eggs via the allantoic cavity after repeated freeze-thaw cycles. After 40 h of incubation, the allantoic fluid was collected.

Ribopuromycylation

Detection of protein translation at a single cell level was adapted from the previously described puromycylation method [152]. In brief, cells were seeded at 1 x 10^5 cells/mL confluency in 1.5 glass coverslips (VWR) a day prior infection or drug treatment. After 24 hpi or 30 min post drug treatment, the media was replaced with PMY labeling medium containing 91 µM of PMY (Sigma-Aldrich) and 45 µM of emetine (Sigma-Aldrich) in tissue culture media and incubated for 5 min at 37 °C. The cells were placed on ice and washed with 1 mL of ice-cold PBS. For PMY removal, the PBS was replaced with extraction buffer containing 0.015% digitonin (Thermo), 50 mM, Tris-HCl pH 8, 5 mM $MgCl_2$, 25 mM KCl, Halt™ Protease Inhibitor Cocktail (Thermo), 10 U/mL RNase Out (Thermo) and incubated for 2 min on ice. The extraction buffer was carefully removed and replaced with ice-cold wash buffer containing 50 mM, Tris-HCl pH 8, 5 mM $MgCl_2$, 25 mM KCl, Halt™ Protease Inhibitor Cocktail (Thermo), 10 U/mL RNase Out (Thermo). The cells were then fixed with 4% paraformaldehyde (EMS) for 15 min at room temperature. Finally, immunostaining for PMY together with G3BP1 and virus protein NP was performed following the immunofluorescence protocol.

Immunofluorescence

Immunofluorescence was performed as described in Chapter 2. Antibodies used: SeV NP (clone M73/2, a gift from Alan Portner, directly conjugated with DyLight 594 or 647 *N*-hydroxysuccinimide (NHS) ester (ThermoFisher)), RSV NP (Abcam catalog number ab94806), G3BP (Abcam catalog numbers ab181150 and ab56574), Puromycin (Merck, catalog number MABE343).

Imaging analysis

Stress granule quantification was performed using Aggrecount automated image analysis as previously described [130]. CTCF was analyzed using Fiji software. In brief, cell boundaries were defined with adjusted thresholds using the G3BP1 signal. Then, the CTCF was calculated using the formula: Integrated Density – (Area of selected cell x Mean fluorescence of background).

RNA extraction and PCR/qPCR

RNA extraction and qPCR were performed as described in Chapter 2. Reverse and forward primers were used for genes: *IL-29* (CGCCTTGGAAGAGTCACTCA and GAAGCCTCAGGTCCCAATTC); *ISG56* (GGATTCTGTACAATACACTAGAAACCA and CTTTTGGTTACTTTTCCCCTATCC); *IRF7* (GATCCAGTCCCAACCAAGG and TCTACTGCCCACCCGTACA) and *RSV G* (AACATACCTGACCCAGAATC and GGTCTTGACTGTTGTAGATTGCA).

Western blots

Western blots were performed as described in Chapter 2. Antibodies used for western blot: Antibodies used for western blot: IFIT1 (Cell Signaling catalog number CS 12082S), IRF7

(Cell Signaling catalog number CS 4920S), RIG-I (Santa Cruz catalog number sc-98911, α-tubulin (Abcam catalog number ab52866).

Statistics

Statistics were calculated using GraphPad Prism. Version 9

Chapter 5

Conclusions

5.1. Introduction

An RNA virus is comprised of a community of viral particles that differ in shape and protein composition, and that contain different versions of the virus genome [33]. The fast evolution and adaptability of RNA viruses allows for selection of specific members of the virus community that will provide a benefit to the virus to ensure survival and spread depending on the host it infects. This feature not only makes RNA viruses evolutionarily successful biological entities, but it also broadens the depth of RNA virus research and how it relates to the host it infects. Fully understanding what each community member of an RNA population does to shape the outcome of an infection through the virus-virus or virus-host interactions will allow us to develop better and safer therapies to reduce the disease burden caused by RNA viruses, globally.

A relevant example of the importance of studying RNA viruses as a whole community rather than a single version of the genome is the discovery of non-standard viral genomes as key components of the population that greatly shape the outcome of an infection [41]. Our advancement on non-standard viral genome knowledge has led to the development of research focused on their use as therapeutics to treat RNA virus infections [44, 153, 154]. The major role that non-standard viral genomes play in interfering with the virus life cycle allow researchers to use non-standard viral genome particles to potentially treat RNA virus infections by reducing virus replication and alleviating disease burden [154, 155]. And although these therapies are currently under development, the premise of these therapies only considers the tip of the iceberg, as recent years of research has shown that non-standard viral genomes role during infection extend beyond their ability to interfere directly with the virus replication.

Within the non-standard viral genomes, the most understood type are cbVGs, which are commonly generated during negative-sense single-stranded RNA virus infections, *in vitro* and *in vivo.* cbVGs drive key virus-host interactions by triggering activation of major RNA sensors in the cell that induce the MAVS signaling pathway [48, 49]. By triggering this pathway, cbVGs induce antiviral immune signaling, inflammation and cell survival [40]. The evolutionary selection of cbVGs within the virus population suggest the interactions cbVGs have with the host benefit the virus. Indeed, activating the antiviral immune response, which eventually leads to a reduction of virus replication, can ensure the infected cell does not reach high levels of virus replication that can potentially kill it. At a systemic level, by inducing overall inflammation, cbVGs can modulate uncontrolled levels of virus replication that would otherwise lead to the death of the host. Stimulation of the immune response also leads to development of symptoms in the host that can allow spread of the virus to new hosts.

Interestingly, cbVGs enhancement of cell survival which leads to establishment of persistent infections also depends on MAVS signaling [56]. The coupling of antiviral immune signaling, and cell survival suggests both processes evolved to be dependent on each other to ensure both always happen in the same cell. In this way, cbVGs can lead to a reduction in virus replication by activating the antiviral immune responses to prevent that excessive replication kills the cell, and through the same signaling pathway, ensuring the survival of the cell by activating a survival mechanism. Survival of the infected cell then leads to persistent infections that allow the virus to be maintained in the host for longer periods past the acute phase of the infection.

The work presented in this dissertation shows yet another process activated by cbVGs that was previously unidentified. cbVGs induce a stress response that involves translation inhibition and formation of stress granules. Activation of this pathway through PKR leads to translation inhibition and reduced levels of viral protein expression in stress granule positive cells. More importantly, induction of this stress response does not depend on MAVS signaling. These data demonstrate the ability of cbVGs to induce cellular pathways independent on their immunostimulatory ability and suggest activation of both pathways evolved separately. Overall, this work highlights the range of virus-host interactions that cbVGs trigger and demonstrate the importance of fully understanding how these interactions shape the outcome of an infection. Elucidating all the ways in which cbVGs shape the outcome of an infection will allow us to better harness their potential to use for therapeutic purposes.

5.2. Discussion and Future Directions

The relationship of a virus and the formation of stress granules is complex, where some viruses induce stress granule formation while others inhibit their formation [119]. Contradictory evidence also shows variability within one same virus [119]. This is observed during RSV infections, where evidence suggests that RSV can block the stress response through the virus nucleoprotein that inhibits PKR phosphorylation of eIF2α [83] and through sequestration of the O-linked N-acetylglucosamine (OGN) transferase (OGT) into inclusion bodies, which is a factor important for stress granule formation [146]. Additionally, the trailer promoter region of the RSV genome was also shown to subvert stress granule formation [145]. Opposing evidence demonstrates that RSV induces stress granules, and this formation increases the replication of the virus [121]. Similar conflicting and opposing data exist for SeV infections [98, 102]. The evidence presented in this dissertation demonstrating that cbVGs induce the stress response offers an explanation to the conflicting evidence regarding stress granule formation during RNA virus infections. cbVGs are key interactors with the host cell and yet the cbVG contents in virus stocks used routinely in many laboratories across the field are not reported, nor evaluated. Lack of knowledge in cbVG contents during an RNA infection can lead to misinterpretations of the phenotypes being studied.

Here, we show that cbVGs trigger PKR signaling, leading to translation inhibition and stress granule formation during both RSV and SeV infections. This translation inhibition leads to a reduction of viral protein expression that extends to later phases of the infection. Induction of this pathway does not require MAVS signaling, showing that cbVGs induce both mechanisms independently. The uncoupling of both mechanisms is interesting because activating either

pathway leads to the same outcome: to interfere with the virus life cycle. cbVGs activation of the stress response could have evolved as a compensatory mechanism to MAVS signaling to ensure that control of the virus occurred even in the absence of immune stimulation. The reverse could also be said, where stimulation of the stress response preceded the selection of MAVS stimulation as a new mechanism of viral interference. Studying the relationship between the stress and immune responses in lower vertebrates or invertebrates could shed a light into how activation of these two pathways evolved. Nevertheless, the evolutionary selection of cbVG generation and the many ways in which they induce virus interference suggests that the process of interference is important for the virus to survive.

The stress response activated during virus infections is an antiviral response that has shown to affect viruses in different ways. The distinction between translation inhibition and stress granule formation is important to note because although they accompany each other, the roles they have during infection can be different. Access to the translation machinery is essential for the virus and, intuitively, inhibiting translation is a mechanism in which the cell can combat the infection. However, the formation of stress granules has also shown to have antiviral roles independent on the translation inhibition that precedes it. This has been shown in viruses that interfere with stress granule formation downstream of eIF2α phosphorylation [156], where stress granules associate with RNA sensors to detect viral RNA and induce the IFN response and overall antiviral immunity [101, 102]. This is what led us to explore the relationship between cbVGs and stress granule formation as both had overlapping roles in inducing the antiviral immune response.

Surprisingly, when we inhibit the formation of stress granules by knocking out both G3BP1 and G3BP2, we saw no effect in the overall antiviral immune response (chapter 4). This was true at the transcriptional level, where no differences in global mRNA levels of IFN and ISGs were observed, and at the translational level, where we saw no differences at the protein levels of ISGs. These data demonstrate that formation of stress granules is dispensable for the global antiviral immune response. The contradiction of these data with the literature could be explained by the way in which stress granules were inhibited. An important piece of evidence we found is that knocking out G3BP1 alone was not sufficient to inhibit stress granule formation during infection. This was unexpected because, based on the literature, G3BP1 KO cells are often used to study the role stress granules play during infection. In our studies, only when knocking out both G3BP1 and G3BP2 could we see inhibition of stress granules using TIAR staining as a proxy for stress granule formation.

Because we always had a G3BP1 single KO control in all our experiments, we could see the effect G3BP1 alone had in the antiviral immune response. Transcriptome analysis in RSV infected cells showed some antiviral associated genes had 2-fold decrease expression in the G3BP1 KO cell line alone. Although not significantly different, expression of IFN and ISGs showed a decreased trend as compared to the rest of the cell lines at the mRNA and protein level. The role G3BP1 has during virus infection independent on the role it has in stress granule formation was not explored in this dissertation. However, evidence in the literature has reported roles for G3BP1 directly on RLR signaling [113, 114].

To elucidate if the stress response had a role in the antiviral immune response upstream of stress granule formation, we compared activation of the IFN response together with expression levels of IFN and ISGs in control and PKR KO cells. Like the G3BP1/2 dKO system, we observed no differences in initiation of the IFN response nor levels of IFN and ISG expression in both RSV and SeV infection, suggesting that the cellular stress response does not impact the overall antiviral immune response during RSV or SeV infection. This, once again, contradicts reports in the literature. The role PKR has during virus infection is controversial. Not only is involved in inducing translation inhibition but has been described as a major receptor for NFkB signaling [64]. Additional roles include both inducing cell survival and cell death. Although we did not observe effects on the antiviral immune response in PKR KO cells and PKR KO-infected cell lines did not show major differences in cell viability during RSV and SeV infection, we cannot rule out these roles being involved during infections with other viruses. The discrepancies we see with the literature regarding stress response induction using a PKR KO system could be explained by the roles PKR could have in different infection contexts that extend beyond stress induction.

The asynchronous formation of stress granules during infection reveals interesting aspects about the role the stress response might play during infection. Although the ribopuromycylation assay only shows translation inhibition in stress granule positive cells in a single time shot, the fact that both processes are coupled allow us to use stress granules as an indicator of active translation inhibition. This way, we could assume that disassembly of stress granules follows resumption of translation and vise-versa. Through the live cell imaging analysis, we could observe formation of stress granules in cells at different timepoints during the infection, as well

as the disassembly of stress granules in some cells at later timepoints. This often correlated with reduced or increased amounts of the virus reporter protein. These data suggest that induction of the stress response by cbVGs can be switched on and/or off depending on the time of the infection at a single cell basis. It remains to be determined how this process is controlled and what are the implications for each cell in this stress granule positive cell population. Does the cell fate change depending on the time it induced stress granules and the length of activation of this response? Stress granule formation is a mechanism that functions as an intersection to determine if the cell will overcome or succumb to stress, and this is often defined by the severity and length of the stress exposure [157]. In our live imaging, we could often see increased death of stress granule positive cells at early timepoints during the infection. This was different if the cell formed stress granules later or formed stress granules for shorter times. Future work should examine how the dynamics of stress granule formation, including timing and duration, affects the fate of the cell.

The dynamic formation seen during the live cell imaging also provides further explanation regarding the ability of cbVGs to induce stress granules. By doing FISH-IFA, we show that stress granules formed almost exclusively in cbVG-high cells. However, only a percent of cbVG-high cells was stress granule positive while others were stress granule negative. These data initially suggested that only a subset of cbVG-high cells induced stress granules during the entire infection. However, the observation that some cells formed stress granules after 24hpi in the live cell imaging suggests that the population of cbVG-high cells that were stress granule negative at a 24-hour time point in the FISH-IFA assay would become stress granule positive at later times. Likewise, these cells could have also disassembled stress granules by

24 hpi, as this disassembly is also appreciated during the live-cell imaging analysis. These data highlight the importance of studying cellular processes at different timepoints during the infection and how, when possible, real-time analysis can provide information that can easily be overlooked when performing static time-shot analyses.

During RSV and SeV infection, stress granule formation occurs at a relatively late time post initial infection. During SeV infection, we can see stress granules forming at around 8 hpi and in RSV, at around 12 hpi. At these times, the antiviral innate response has already initiated, and full cycles of replication have occurred. This poses interesting questions about how activation of both pathways is being controlled. Is the cbVG accumulation threshold to activate the pathways different between MAVS and PKR signaling? Or are there cellular factors that prevent formation of stress granules earlier during infection? Is there a benefit of inducing stress granule formation at these later timepoints? Is activation based on location differences between the virus and the sensors? As for cellular factors that could be controlling activation of PKR and translation inhibition, ADAR1 is a candidate that would be of interest to look at during cbVG-high infections. ADAR1, an RNA editing protein that causes adenosine to inosine changes in RNA molecules, is an ISG often described to be an antagonist of PKR activation [158, 159]. ADAR1 knockout experiments during measles and vesicular stomatitis virus infection show increase level of PKR activity, accompanied by reduction of virus replication, and increase levels of apoptosis [160, 161]. The role ADAR1 plays during cbVG-high infections has not been studied, although some evidence suggest ADAR1 can have RNA editing activity directly on cbVGs during measles virus infection [117]. A possible explanation to the late timing of stress granule formation could be an inhibitory mechanism led by ADAR1 that prevents

activation of PKR at early times. This inhibitory mechanism could then be overcome at late times, allowing PKR activation and translation inhibition to be induced. Experiments using ADAR1-deficient cells to infect with cbVG-high viruses and looking at differences in stress granule formation could provide insights into the role ADAR1 could be playing in controlling PKR signaling. If ADAR1 is a factor controlling PKR activation and stress granule formation, an ADAR1 KO cell system could also allow us to further understand the importance of timing of the response in shaping the outcome of the infection.

We show that in stress granule positive cells, translation is inhibited and that leads to a reduction of virus protein expression. We cannot, however, rule out that host proteins are also being affected by this translation suppression. Based on the MAVS and RIG-I staining in chapter 4, figure 4.1, we could see a trend of reduced intensity of MAVS and RIG-I in stress granule positive cells compared to the rest. Reduction of MAVS expression has been explored in the context of a cbVG-high infection and it was demonstrated that upon stimulation, MAVS goes through proteosome degradation [162]. This process was shown to be important for activation of the IFN signaling pathway [162]. It would be interesting to see if translation inhibition contributes to the reduction of signaling molecules like MAVS by preventing more synthesis of the proteins after proteasomal degradation. Although we cannot rule out the possibility of stress granule positive cells having reduced levels of the ISGs analyzed in this dissertation, this reduction does not make an impact on the overall antiviral immune response that is induced early during infection.

A limitation on the design of experiments to elucidate the role the stress response played during cbVG-high infection was the low amount of stress granule positive cells we could detect at a given time. Additionally, the lack of reporter genes that are upregulated when stress granules form during cbVG-high infection prevented us from developing strategies to isolate this population of cells. This limited us to perform experiments that relied on single cell-based analyses like immunofluorescence imaging. However, this limitation led us to perform the ribopuromycylation assay where we showed that stress granule positive cells almost exclusively showed reduced levels of PMY. A potential follow-up experiment would be to develop a flow cytometry sorting strategy to isolate PMY low from PMY high cells to enrich for cells undergoing translation inhibition and stress granule formation. Sorting of these cells would allow us to do transcriptome and proteome analysis to identify pathways differentially regulated between both populations of cells. To isolate live cells, we can enrich for stress granule positive cells by sorting based on SeV miRFP670 expression levels. This method would be less ideal as some stress granule negative cells show low expression of miRFP670, most likely due to other mechanisms of interference that are activated during the infection like IFN signaling or by unsynchronized infections.

Because we now know cbVG activity in the cell extends beyond their immunostimulatory activity, we can explore other cellular processes that can be modulated by cbVGs. Some of these involve cbVGs role in the cell cycle, circadian rhythms, cell metabolism, cytoskeleton remodeling, etc. As for the role cbVGs play in inducing the stress response, some questions remain unanswered: Do cbVGs directly bind to PKR? Are the cbVG motifs that activate PKR the same as the ones that activate RLRs? What is the contribution of interference at the virus

protein translation level in the outcome of the infection? Do stress granules only form because of translation inhibition, or do they play a specific role? Do stress granules contain virus mRNA? Is the expression profile of stress granule positive cells different than the stress granule negative cells? These questions can be studied with the experimental strategies described above and through isolation of stress granules induced during cbVG-high infection.

5.3. Closing Remarks

RNA viruses have complex interactions with their host that, altogether, shape the outcome of the infection. It is now clear that specific members of the RNA virus community drive these interactions and the evolutionary selection of non-standard viral genomes highlight their importance as key modulators of the infection. It is of utmost importance to fully elucidate the cellular pathways non-standard viral genomes activate for researchers to exploit their therapeutic potential. Lack of understanding on the effects non-standard viral genomes have can hinder development of non-standard viral genomes-based therapies by causing exacerbation of the disease or long-term repercussions on the infected host. The discovery that cbVGs trigger the stress response independent on their immunostimulatory activity opens the possibility of cbVGs potential in modulating other cellular processes and highlights the versatility of cbVGs as stimulatory molecules. Finally, this work highlights the diverse mechanisms of viral interference induced by cbVGs and offers new perspectives on the strategies that, through evolutionary selection, allow viruses to successfully infect, spread and be maintained in the population.

References

1. Alvarez-Munoz, S., et al., *Key Factors That Enable the Pandemic Potential of RNA Viruses and Inter-Species Transmission: A Systematic Review.* Viruses, 2021. **13**(4).
2. Li, Y., et al., *Global, regional, and national disease burden estimates of acute lower respiratory infections due to respiratory syncytial virus in children younger than 5 years in 2019: a systematic analysis.* Lancet, 2022. **399**(10340): p. 2047-2064.
3. Branche, A.R. and A.R. Falsey, *Parainfluenza Virus Infection.* Semin Respir Crit Care Med, 2016. **37**(4): p. 538-54.
4. Waghmode, R., S. Jadhav, and V. Nema, *The Burden of Respiratory Viruses and Their Prevalence in Different Geographical Regions of India: 1970-2020.* Front Microbiol, 2021. **12**: p. 723850.
5. Lafond, K.E., et al., *Global burden of influenza-associated lower respiratory tract infections and hospitalizations among adults: A systematic review and meta-analysis.* PLoS Med, 2021. **18**(3): p. e1003550.
6. Zar, H.J., et al., *Early-life respiratory syncytial virus lower respiratory tract infection in a South African birth cohort: epidemiology and effect on lung health.* Lancet Glob Health, 2020. **8**(10): p. e1316-e1325.
7. Allinson, J.P., et al., *Early childhood lower respiratory tract infection and premature adult death from respiratory disease in Great Britain: a national birth cohort study.* Lancet, 2023. **401**(10383): p. 1183-1193.
8. Simoes, E.A.F. and A.H. Liu, *RSV prevention in infancy and asthma in later life.* Lancet Respir Med, 2018. **6**(7): p. e30.
9. Fauroux, B., et al., *The Burden and Long-term Respiratory Morbidity Associated with Respiratory Syncytial Virus Infection in Early Childhood.* Infect Dis Ther, 2017. **6**(2): p. 173-197.
10. Feldman, A.S., et al., *Toward primary prevention of asthma. Reviewing the evidence for early-life respiratory viral infections as modifiable risk factors to prevent childhood asthma.* Am J Respir Crit Care Med, 2015. **191**(1): p. 34-44.
11. Skowronski, D.M., et al., *Low 2012-13 influenza vaccine effectiveness associated with mutation in the egg-adapted H3N2 vaccine strain not antigenic drift in circulating viruses.* PLoS One, 2014. **9**(3): p. e92153.
12. Wu, N.C., et al., *A structural explanation for the low effectiveness of the seasonal influenza H3N2 vaccine.* PLoS Pathog, 2017. **13**(10): p. e1006682.
13. Broadbent, L., et al., *Respiratory syncytial virus, an ongoing medical dilemma: an expert commentary on respiratory syncytial virus prophylactic and therapeutic pharmaceuticals currently in clinical trials.* Influenza Other Respir Viruses, 2015. **9**(4): p. 169-78.
14. Del Riccio, M., et al., *Defining the Burden of Disease of RSV in Europe: estimates of RSV-associated hospitalisations in children under 5 years of age. A systematic review and modelling study.* medRxiv, 2023.
15. Heinonen, S., et al., *Infant Immune Response to Respiratory Viral Infections.* Immunol Allergy Clin North Am, 2019. **39**(3): p. 361-376.
16. Wang, X., et al., *Global burden of acute lower respiratory infection associated with human parainfluenza virus in children younger than 5 years for 2018: a systematic review and meta-analysis.* Lancet Glob Health, 2021. **9**(8): p. e1077-e1087.

17. Viguria, N., et al., *Effectiveness of palivizumab in preventing respiratory syncytial virus infection in high-risk children.* Hum Vaccin Immunother, 2021. **17**(6): p. 1867-1872.
18. Walsh, E.E., et al., *Efficacy and Safety of a Bivalent RSV Prefusion F Vaccine in Older Adults.* N Engl J Med, 2023. **388**(16): p. 1465-1477.
19. Amarasinghe, G.K., et al., *Taxonomy of the order Mononegavirales: update 2018.* Arch Virol, 2018. **163**(8): p. 2283-2294.
20. Noton, S.L. and R. Fearns, *Initiation and regulation of paramyxovirus transcription and replication.* Virology, 2015. **479-480**: p. 545-54.
21. Fearns, R. and R.K. Plemper, *Polymerases of paramyxoviruses and pneumoviruses.* Virus Res, 2017. **234**: p. 87-102.
22. Zhou, H., et al., *Structural perspective on the formation of ribonucleoprotein complex in negative-sense single-stranded RNA viruses.* Trends Microbiol, 2013. **21**(9): p. 475-84.
23. Ruigrok, R.W., T. Crepin, and D. Kolakofsky, *Nucleoproteins and nucleocapsids of negative-strand RNA viruses.* Curr Opin Microbiol, 2011. **14**(4): p. 504-10.
24. Nilsson, P., B. E.; Blanco-Melo, D.; Uhl, S.; Escudero-Pérez, B.; Olschewski, S.; Thibault, P.; Panis, M.; Rosenthal, M.; Muñoz-Fontela, C.; Lee, B.; tenOever, B. R. , *Reduced Nucleoprotein Availability Impairs Negative-Sense RNA Virus Replication and Promotes Host Recognition.* JVI, 2021. **95**(9).
25. *Transcription and replication of nonsegmented negative-strand RNA viruses.*
26. Curran, J.M., J.; Kolakofsky, D., *An N-Terminal Domain of the Sendai Paramyxovirus P Protein*

Acts as a Chaperone for the NP Protein during the Nascent
Chain Assembly Step of Genome Replication. J Virol, 1995. **69**(2): p. 849–855.
27. Smallwood, S.R., K. W.; Moyer, S. A., *Deletion analysis defines a carboxyl-proximal region of Sendai virus P protein that binds to the polymerase L protein.* Virology, 1994. **202**(1): p. 154-63.
28. Canter, D.M.P., J., *Stabilization of Vesicular Stomatitis Virus L Polymerase Protein by P Protein Binding: A Small Deletion in the C-Terminal Domain of L Abrogates Binding.* Virology, 1996. **219**: p. 376–386.
29. Steinhauer, D.A.D., E.; Holland, J. J., *Lack of evidence for proofreading mechanisms associated with an RNA virus polymerase.* Gene, 1992. **122**: p. 281-288.
30. Elena, S.F. and R. Sanjuan, *Adaptive value of high mutation rates of RNA viruses: separating causes from consequences.* J Virol, 2005. **79**(18): p. 11555-8.
31. Sanjuán, R. and P. Domingo-Calap, *Genetic Diversity and Evolution of Viral Populations*, in *Encyclopedia of Virology*. 2021. p. 53-61.
32. Poirier, E.Z. and M. Vignuzzi, *Virus population dynamics during infection.* Curr Opin Virol, 2017. **23**: p. 82-87.
33. Gonzalez Aparicio, L.J.L., C. B.; Felt, S. A, *A Virus Is a Community: Diversity within Negative-Sense RNA Virus Populations.* Microbiol. Mol. Biol. Rev., 2022. **86**(3).
34. Li, T., et al., *The shape of pleomorphic virions determines resistance to cell-entry pressure.* Nat Microbiol, 2021. **6**(5): p. 617-629.
35. Martin, B.E. and C.B. Brooke, *Flu Shows the Power of Diversity.* Cell, 2019. **176**(1-2): p. 9-10.
36. Seladi-Schulman, J., et al., *Filament-producing mutants of influenza A/Puerto Rico/8/1934 (H1N1) virus have higher neuraminidase activities than the spherical wild-type.* PLoS One, 2014. **9**(11): p. e112462.

37. Seladi-Schulman, J., J. Steel, and A.C. Lowen, *Spherical influenza viruses have a fitness advantage in embryonated eggs, while filament-producing strains are selected in vivo.* J Virol, 2013. **87**(24): p. 13343-53.
38. Lauring, A.S. and R. Andino, *Quasispecies theory and the behavior of RNA viruses.* PLoS Pathog, 2010. **6**(7): p. e1001005.
39. Leeks, A., et al., *Beneficial coinfection can promote within-host viral diversity.* Virus Evol, 2018. **4**(2): p. vey028.
40. Genoyer, E. and C.B. Lopez, *The Impact of Defective Viruses on Infection and Immunity.* Annu Rev Virol, 2019. **6**(1): p. 547-566.
41. Vignuzzi, M. and C.B. Lopez, *Defective viral genomes are key drivers of the virus-host interaction.* Nat Microbiol, 2019. **4**(7): p. 1075-1087.
42. Perrault, J., *Origin and Replication of Defective Interfering Particles*. Current Topics in Microbiology and Immunology, ed. A.J. Shatkin. Vol. 93. 1981, Berlin, Heidelberg: Springer.
43. Manzoni, T.B.L., C. B., *Defective (interfering) viral genomes re-explored: impact on antiviral immunity and virus persistence.* Future Virol, 2018. **13**(7): p. 493-504.
44. Fatehi, F., et al., *Therapeutic interfering particles exploiting viral replication and assembly mechanisms show promising performance: a modelling study.* Sci Rep, 2021. **11**(1): p. 23847.
45. Calain, P.R., L., *Functional Characterisation of the Genomic and Antigenomic Promoters of Sendai Virus.* Virology, 1995. **212**(1): p. 163-173.
46. Welch, S.R., et al., *Inhibition of Nipah Virus by Defective Interfering Particles.* J Infect Dis, 2020. **221**(Suppl 4): p. S460-S470.
47. Baum, A., R. Sachidanandam, and A. Garcia-Sastre, *Preference of RIG-I for short viral RNA molecules in infected cells revealed by next-generation sequencing.* Proc Natl Acad Sci U S A, 2010. **107**(37): p. 16303-8.
48. Tapia, K., et al., *Defective viral genomes arising in vivo provide critical danger signals for the triggering of lung antiviral immunity.* PLoS Pathog, 2013. **9**(10): p. e1003703.
49. Yount, J.S., et al., *MDA5 participates in the detection of paramyxovirus infection and is essential for the early activation of dendritic cells in response to Sendai Virus defective interfering particles.* J Immunol, 2008. **180**(7): p. 4910-8.
50. Sun, Y., et al., *Immunostimulatory Defective Viral Genomes from Respiratory Syncytial Virus Promote a Strong Innate Antiviral Response during Infection in Mice and Humans.* PLoS Pathog, 2015. **11**(9): p. e1005122.
51. Yan, N. and Z.J. Chen, *Intrinsic antiviral immunity.* Nat Immunol, 2012. **13**(3): p. 214-22.
52. Lazear, H.M., J.W. Schoggins, and M.S. Diamond, *Shared and Distinct Functions of Type I and Type III Interferons.* Immunity, 2019. **50**(4): p. 907-923.
53. Felt, S.A., et al., *Detection of respiratory syncytial virus defective genomes in nasal secretions is associated with distinct clinical outcomes.* Nat Microbiol, 2021. **6**(5): p. 672-681.
54. Xu, J., et al., *Identification of a Natural Viral RNA Motif That Optimizes Sensing of Viral RNA by RIG-I.* mBio, 2015. **6**(5): p. e01265-15.
55. Fisher, D.G., G.M. Coppock, and C.B. Lopez, *Virus-derived immunostimulatory RNA induces type I IFN-dependent antibodies and T-cell responses during vaccination.* Vaccine, 2018. **36**(28): p. 4039-4045.

56. Xu, J., et al., *Replication defective viral genomes exploit a cellular pro-survival mechanism to establish paramyxovirus persistence.* Nat Commun, 2017. **8**(1): p. 799.
57. Sidhu, M.S., et al., *Defective measles virus in human subacute sclerosing panencephalitis brain.* Virology, 1994. **202**(2): p. 631-41.
58. De, B.K. and D.P. Nayak, *Defective interfering influenza viruses and host cells: establishment and maintenance of persistent influenza virus infection in MDBK and HeLa cells.* J Virol, 1980. **36**(3): p. 847-59.
59. Kennedy, J.C.M., R. D. , *Persistent Infection with Infectious Pancreatic Necrosis Virus Mediated by Defective-interfering (DI) Virus Particles in a Cell Line Showing Strong Interference but Little DI Replication.* J Gen Virol, 1982. **58**: p. 361–371.
60. Sekellick, M.J.M., P. I, *Persistent infection. I Interferon-inducing defective-interfering particles as mediators of cell sparing: possible role in persistent infection by vesicular stomatitis virus.* Virology, 1978. **85**: p. 175–186.
61. McEwen, E., et al., *Heme-regulated inhibitor kinase-mediated phosphorylation of eukaryotic translation initiation factor 2 inhibits translation, induces stress granule formation, and mediates survival upon arsenite exposure.* J Biol Chem, 2005. **280**(17): p. 16925-33.
62. Wek, S.A., S. Zhu, and R.C. Wek, *The histidyl-tRNA synthetase-related sequence in the eIF-2 alpha protein kinase GCN2 interacts with tRNA and is required for activation in response to starvation for different amino acids.* Mol Cell Biol, 1995. **15**(8): p. 4497-506.
63. Harding, H.P.Z., Y.; Bertolotti, A.; Zeng, H.; Ron, D., *Perk Is Essential for Translational Regulation and Cell Survival during the Unfolded Protein Response.* Mol Cell, 2000. **5**: p. 897–904.
64. Garcia, M.A., E.F. Meurs, and M. Esteban, *The dsRNA protein kinase PKR: virus and cell control.* Biochimie, 2007. **89**(6-7): p. 799-811.
65. Merrick, W.C. and G.D. Pavitt, *Protein Synthesis Initiation in Eukaryotic Cells.* Cold Spring Harb Perspect Biol, 2018. **10**(12).
66. Kapp, L.D. and J.R. Lorsch, *GTP-dependent recognition of the methionine moiety on initiator tRNA by translation factor eIF2.* J Mol Biol, 2004. **335**(4): p. 923-36.
67. Pavitt, G.D.R., K. V.; Kimball, S. R.; Hinnebusch, A. G, *eIF2 independently binds two distinct eIF2B subcomplexes that catalyze*
and regulate guanine–nucleotide exchange. Genes Dev, 1998. **12**(4): p. 514-26.
68. Bounedjah, O., et al., *Free mRNA in excess upon polysome dissociation is a scaffold for protein multimerization to form stress granules.* Nucleic Acids Res, 2014. **42**(13): p. 8678-91.
69. Kedersha, N.C., M. R.; Wei, L.; Yacono, P. W.; Chen, S.; Gilks, N.; Golan, D. E.; Anderson, P. , *Dynamic Shuttling of TIA-1 Accompanies the Recruitment of mRNA to Mammalian Stress Granules.* J Cell Biol, 2000. **151**(6): p. 1257–1268.
70. Kedersha, N. and P. Anderson, *Mammalian stress granules and processing bodies.* Methods Enzymol, 2007. **431**: p. 61-81.
71. Wilbertz, J.H., et al., *Single-Molecule Imaging of mRNA Localization and Regulation during the Integrated Stress Response.* Mol Cell, 2019. **73**(5): p. 946-958 e7.
72. Novoa, I.Z., H.; Harding, H. P.; Ron, D., *Feedback Inhibition of the Unfolded Protein Response by GADD34-mediated Dephosphorylation of eIF2.* 2001. **153**(5): p. 1011–1021.

73. Berlanga, J.J., et al., *Antiviral effect of the mammalian translation initiation factor 2alpha kinase GCN2 against RNA viruses.* EMBO J, 2006. **25**(8): p. 1730-40.
74. Kim, Y., et al., *PKR Senses Nuclear and Mitochondrial Signals by Interacting with Endogenous Double-Stranded RNAs.* Mol Cell, 2018. **71**(6): p. 1051-1063 e6.
75. Kim, Y., et al., *PKR is activated by cellular dsRNAs during mitosis and acts as a mitotic regulator.* Genes Dev, 2014. **28**(12): p. 1310-22.
76. McAllister, C.S. and C.E. Samuel, *The RNA-activated protein kinase enhances the induction of interferon-beta and apoptosis mediated by cytoplasmic RNA sensors.* J Biol Chem, 2009. **284**(3): p. 1644-51.
77. Zhang, P. and C.E. Samuel, *Protein kinase PKR plays a stimulus- and virus-dependent role in apoptotic death and virus multiplication in human cells.* J Virol, 2007. **81**(15): p. 8192-200.
78. Donze, O., et al., *The protein kinase PKR: a molecular clock that sequentially activates survival and death programs.* EMBO J, 2004. **23**(3): p. 564-71.
79. Schulz, O., et al., *Protein kinase R contributes to immunity against specific viruses by regulating interferon mRNA integrity.* Cell Host Microbe, 2010. **7**(5): p. 354-61.
80. Gilfoy, F.D. and P.W. Mason, *West Nile virus-induced interferon production is mediated by the double-stranded RNA-dependent protein kinase PKR.* J Virol, 2007. **81**(20): p. 11148-58.
81. Zamanian-Daryoush, M.M., T. H.; Didonato, J. A.; Williams, B. R. G., *NF-kB Activation by Double-Stranded-RNA-Activated Protein*
Kinase (PKR) Is Mediated through NF-?B-Inducing
Kinase and IkB Kinase. Mol Cell Biol, 2000. **20**.
82. Borghese, F., et al., *The Leader Protein of Theiler's Virus Prevents the Activation of PKR.* J Virol, 2019. **93**(19).
83. Groskreutz, D.J., et al., *Respiratory syncytial virus limits alpha subunit of eukaryotic translation initiation factor 2 (eIF2alpha) phosphorylation to maintain translation and viral replication.* J Biol Chem, 2010. **285**(31): p. 24023-31.
84. Rabouw, H.H., et al., *Middle East Respiratory Coronavirus Accessory Protein 4a Inhibits PKR-Mediated Antiviral Stress Responses.* PLoS Pathog, 2016. **12**(10): p. e1005982.
85. Li, C., et al., *Foot-and-mouth disease virus induces lysosomal degradation of host protein kinase PKR by 3C proteinase to facilitate virus replication.* Virology, 2017. **509**: p. 222-231.
86. Li, S., et al., *Binding of the influenza A virus NS1 protein to PKR mediates the inhibition of its activation by either PACT or double-stranded RNA.* Virology, 2006. **349**(1): p. 13-21.
87. Gale, M.J.K., M. J.; Tang, N. M.; Tan, S.; Hopkins, D. A.; Dever, T. E.; Polyak, S. J.; Gretch, D. R.; Katze, M. G., *Evidence That Hepatitis C Virus Resistance to Interferon Is Mediated through Repression of the PKR Protein Kinase by the Nonstructural 5A Protein.* Virology, 1997. **230**: p. **217–227**.
88. Amorim, R., et al., *Zika virus inhibits eIF2alpha-dependent stress granule assembly.* PLoS Negl Trop Dis, 2017. **11**(7): p. e0005775.
89. Wang, X., et al., *Inhibition of protein kinase R activation and upregulation of GADD34 expression play a synergistic role in facilitating coronavirus replication by maintaining de novo protein synthesis in virus-infected cells.* J Virol, 2009. **83**(23): p. 12462-72.

90. Nowee, G., et al., *A Tale of 20 Alphaviruses; Inter-species Diversity and Conserved Interactions Between Viral Non-structural Protein 3 and Stress Granule Proteins.* Front Cell Dev Biol, 2021. **9**: p. 625711.
91. Yang, X., et al., *Picornavirus 2A protease regulates stress granule formation to facilitate viral translation.* PLoS Pathog, 2018. **14**(2): p. e1006901.
92. White, J.P., et al., *Inhibition of cytoplasmic mRNA stress granule formation by a viral proteinase.* Cell Host Microbe, 2007. **2**(5): p. 295-305.
93. Valadao, A.L., R.S. Aguiar, and L.B. de Arruda, *Interplay between Inflammation and Cellular Stress Triggered by Flaviviridae Viruses.* Front Microbiol, 2016. **7**: p. 1233.
94. Visser, L.J.M., G. N.; Rabouw, H. H.; de Groot, R. J.; Langereis, M. A.; de los Santos, T.; van Kuppevelda, F. J. M., *Foot-and-Mouth Disease Virus Leader Protease Cleaves G3BP1 and G3BP2 and Inhibits Stress Granule Formation.* JVI, 2019. **93**(2).
95. Visser, L.J., et al., *Essential Role of Enterovirus 2A Protease in Counteracting Stress Granule Formation and the Induction of Type I Interferon.* J Virol, 2019. **93**(10).
96. Remenyi, R., et al., *Persistent Replication of a Chikungunya Virus Replicon in Human Cells Is Associated with Presence of Stable Cytoplasmic Granules Containing Nonstructural Protein 3.* J Virol, 2018. **92**(16).
97. Kim, D.Y., et al., *New World and Old World Alphaviruses Have Evolved to Exploit Different Components of Stress Granules, FXR and G3BP Proteins, for Assembly of Viral Replication Complexes.* PLoS Pathog, 2016. **12**(8): p. e1005810.
98. Iseni, F., et al., *Sendai virus trailer RNA binds TIAR, a cellular protein involved in virus-induced apoptosis.* The EMBO journal, 2002. **21**(19): p. 5141-50.
99. Eiermann, N., et al., *Dance with the Devil: Stress Granules and Signaling in Antiviral Responses.* Viruses, 2020. **12**(9).
100. McCormick, C. and D.A. Khaperskyy, *Translation inhibition and stress granules in the antiviral immune response.* Nat Rev Immunol, 2017. **17**(10): p. 647-660.
101. Onomoto, K., et al., *Critical role of an antiviral stress granule containing RIG-I and PKR in viral detection and innate immunity.* PLoS One, 2012. **7**(8): p. e43031.
102. Manivannan, P., M.A. Siddiqui, and K. Malathi, *RNase L Amplifies Interferon Signaling by Inducing Protein Kinase R-Mediated Antiviral Stress Granules.* J Virol, 2020. **94**(13).
103. Ng, C.S., et al., *Encephalomyocarditis virus disrupts stress granules, the critical platform for triggering antiviral innate immune responses.* J Virol, 2013. **87**(17): p. 9511-22.
104. Oh, S.W., et al., *Leader-Containing Uncapped Viral Transcript Activates RIG-I in Antiviral Stress Granules.* PLoS Pathog, 2016. **12**(2): p. e1005444.
105. Sanchez-Aparicio, M.T., et al., *Subcellular Localizations of RIG-I, TRIM25, and MAVS Complexes.* J Virol, 2017. **91**(2).
106. Langereis, M.A., Q. Feng, and F.J. van Kuppeveld, *MDA5 localizes to stress granules, but this localization is not required for the induction of type I interferon.* Journal of virology, 2013. **87**(11): p. 6314-25.
107. Paget, M., et al., *Stress granules are shock absorbers that prevent excessive innate immune responses to dsRNA.* Mol Cell, 2023. **83**(7): p. 1180-1196 e8.
108. Hashimoto, S., et al., *Mumps Virus Induces Protein-Kinase-R-Dependent Stress Granules, Partly Suppressing Type III Interferon Production.* PLoS One, 2016. **11**(8): p. e0161793.

109. Lindquist, M.E., et al., *Activation of protein kinase R is required for induction of stress granules by respiratory syncytial virus but dispensable for viral replication.* Virology, 2011. **413**(1): p. 103-10.
110. Takeuchi, K., et al., *Sendai virus C protein plays a role in restricting PKR activation by limiting the generation of intracellular double-stranded RNA.* J Virol, 2008. **82**(20): p. 10102-10.
111. Pfaller, C.K., et al., *Measles virus C protein impairs production of defective copyback double-stranded viral RNA and activation of protein kinase R.* J Virol, 2014. **88**(1): p. 456-68.
112. Pham, A.M., et al., *PKR Transduces MDA5-Dependent Signals for Type I IFN Induction.* PLoS Pathog, 2016. **12**(3): p. e1005489.
113. Yang, W., et al., *G3BP1 inhibits RNA virus replication by positively regulating RIG-I-mediated cellular antiviral response.* Cell Death Dis, 2019. **10**(12): p. 946.
114. Kim, S.S., et al., *The stress granule protein G3BP1 binds viral dsRNA and RIG-I to enhance interferon-beta response.* J Biol Chem, 2019. **294**(16): p. 6430-6438.
115. Burke, J.M., et al., *RNase L promotes the formation of unique ribonucleoprotein granules distinct from stress granules.* J Biol Chem, 2020. **295**(6): p. 1426-1438.
116. Burke, J.M., et al., *RNase L Reprograms Translation by Widespread mRNA Turnover Escaped by Antiviral mRNAs.* Mol Cell, 2019. **75**(6): p. 1203-1217 e5.
117. Pfaller, C.K., et al., *Measles Virus Defective Interfering RNAs Are Generated Frequently and Early in the Absence of C Protein and Can Be Destabilized by Adenosine Deaminase Acting on RNA-1-Like Hypermutations.* J Virol, 2015. **89**(15): p. 7735-47.
118. Sanchez-Aparicio, M.T., et al., *Loss of Sendai virus C protein leads to accumulation of RIG-I immunostimulatory defective interfering RNA.* J Gen Virol, 2017. **98**(6): p. 1282-1293.
119. White, J.P. and R.E. Lloyd, *Regulation of stress granules in virus systems.* Trends Microbiol, 2012. **20**(4): p. 175-83.
120. Zhang, Q., et al., *Viral Regulation of RNA Granules in Infected Cells.* Virol Sin, 2019. **34**(2): p. 175-191.
121. Lindquist, M.E., et al., *Respiratory syncytial virus induces host RNA stress granules to facilitate viral replication.* Journal of virology, 2010. **84**(23): p. 12274-84.
122. Ruggieri, A., et al., *Dynamic oscillation of translation and stress granule formation mark the cellular response to virus infection.* Cell Host Microbe, 2012. **12**(1): p. 71-85.
123. Fernandez-Carrillo, C., et al., *Hepatitis C virus plays with fire and yet avoids getting burned. A review for clinicians on processing bodies and stress granules.* Liver Int, 2018. **38**(3): p. 388-398.
124. Williams, A.J.S.B.R.G., *Structure and Function of the Protein Kinase R*, in *Interferon: The 50th Anniversary*, S. Rallison, Editor. 2007, Springer: New York. p. 253–292.
125. Sun, Y.L., C.B., *Preparation of Respiratory Syncytial Virus with High or Low Content of Defective Viral Particles and Their Purification from Viral Stocks.* Bio-Protoc., 2016. **6**(10).
126. Genoyer, E. and C.B. Lopez, *Defective Viral Genomes Alter How Sendai Virus Interacts with Cellular Trafficking Machinery, Leading to Heterogeneity in the Production of Viral Particles among Infected Cells.* J Virol, 2019. **93**(4).

127. Genoyer, E., et al., *The Viral Polymerase Complex Mediates the Interaction of Viral Ribonucleoprotein Complexes with Recycling Endosomes during Sendai Virus Assembly.* mBio, 2020. **11**(4).
128. Zhao, Y. and J. Dong, *Effect of inactivating RNA viruses by coupled UVC and UVA LEDs evaluated by a viral surrogate commonly used as a genetic vector.* Biomed Opt Express, 2022. **13**(8): p. 4429-4444.
129. Yount, J.S., et al., *A novel role for viral-defective interfering particles in enhancing dendritic cell maturation.* J Immunol, 2006. **177**(7): p. 4503-13.
130. Klickstein, J.A., S. Mukkavalli, and M. Raman, *AggreCount: an unbiased image analysis tool for identifying and quantifying cellular aggregates in a spatially defined manner.* J Biol Chem, 2020. **295**(51): p. 17672-17683.
131. Anderson, P. and N. Kedersha, *RNA granules.* J Cell Biol, 2006. **172**(6): p. 803-8.
132. Tourriere, H., et al., *The RasGAP-associated endoribonuclease G3BP assembles stress granules.* J Cell Biol, 2003. **160**(6): p. 823-31.
133. Burke, J.M., et al., *RNase L activation in the cytoplasm induces aberrant processing of mRNAs in the nucleus.* PLoS Pathog, 2022. **18**(11): p. e1010930.
134. Sun, Y., et al., *Newcastle disease virus induces stable formation of bona fide stress granules to facilitate viral replication through manipulating host protein translation.* Faseb j, 2017. **31**(4): p. 1337-1353.
135. White, J.P.L., R. E., *Poliovirus unlinks TIA1 aggregation and mRNA stress granule formation.* J Virol, 2011. **85**(23): p. 12442-54.
136. Matthews, J.D. and T.K. Frey, *Analysis of subcellular G3BP redistribution during rubella virus infection.* J Gen Virol, 2012. **93**(Pt 2): p. 267-274.
137. Piotrowska, J., et al., *Stable formation of compositionally unique stress granules in virus-infected cells.* J Virol, 2010. **84**(7): p. 3654-65.
138. Sidrauski, C., et al., *The small molecule ISRIB reverses the effects of eIF2alpha phosphorylation on translation and stress granule assembly.* Elife, 2015. **4**.
139. Perez-Pepe, M., A.J. Fernandez-Alvarez, and G.L. Boccaccio, *Life and Work of Stress Granules and Processing Bodies: New Insights into Their Formation and Function.* Biochemistry, 2018. **57**(17): p. 2488-2498.
140. Matsuki, H., et al., *Both G3BP1 and G3BP2 contribute to stress granule formation.* Genes Cells, 2013. **18**(2): p. 135-46.
141. Li, Y., et al., *Activation of RNase L is dependent on OAS3 expression during infection with diverse human viruses.* Proc Natl Acad Sci U S A, 2016. **113**(8): p. 2241-6.
142. Dauber, B., et al., *Influenza B virus ribonucleoprotein is a potent activator of the antiviral kinase PKR.* PLoS Pathog, 2009. **5**(6): p. e1000473.
143. Heinicke, L.A., et al., *RNA dimerization promotes PKR dimerization and activation.* J Mol Biol, 2009. **390**(2): p. 319-38.
144. Rojas, M., C.F. Arias, and S. Lopez, *Protein kinase R is responsible for the phosphorylation of eIF2alpha in rotavirus infection.* J Virol, 2010. **84**(20): p. 10457-66.
145. Hanley, L.L., et al., *Roles of the respiratory syncytial virus trailer region: effects of mutations on genome production and stress granule formation.* Virology, 2010. **406**(2): p. 241-52.
146. Fricke, J., et al., *p38 and OGT sequestration into viral inclusion bodies in cells infected with human respiratory syncytial virus suppresses MK2 activities and stress granule assembly.* J Virol, 2013. **87**(3): p. 1333-47.

147. Nallagatla, S.R., R. Toroney, and P.C. Bevilacqua, *Regulation of innate immunity through RNA structure and the protein kinase PKR.* Curr Opin Struct Biol, 2011. **21**(1): p. 119-27.
148. Jayabalan, A.K., D.E. Griffin, and A.K.L. Leung, *Pro-Viral and Anti-Viral Roles of the RNA-Binding Protein G3BP1.* Viruses, 2023. **15**(2).
149. Yoo, J.S., et al., *DHX36 enhances RIG-I signaling by facilitating PKR-mediated antiviral stress granule formation.* PLoS Pathog, 2014. **10**(3): p. e1004012.
150. Sun, Y., et al., *Immunostimulatory Defective Viral Genomes from Respiratory Syncytial Virus Promote a Strong Innate Antiviral Response during Infection in Mice and Humans.* PLoS Pathog, 2015. **11**(9): p. e1005122.
151. Kang, J.S., et al., *OASL1 Traps Viral RNAs in Stress Granules to Promote Antiviral Responses.* Mol Cells, 2018. **41**(3): p. 214-223.
152. Bastide, A., J.W. Yewdell, and A. David, *The RiboPuromycylation Method (RPM): an Immunofluorescence Technique to Map Translation Sites at the Sub-cellular Level.* Bio Protoc, 2018. **8**(1).
153. Karki, B., J.J. Bull, and S.M. Krone, *Modeling the therapeutic potential of defective interfering particles in the presence of immunity.* Virus Evol, 2022. **8**(2): p. veac047.
154. Chaturvedi, S., et al., *A single-administration therapeutic interfering particle reduces SARS-CoV-2 viral shedding and pathogenesis in hamsters.* Proc Natl Acad Sci U S A, 2022. **119**(39): p. e2204624119.
155. Dimmock, N.J. and A.J. Easton, *Defective interfering influenza virus RNAs: time to reevaluate their clinical potential as broad-spectrum antivirals?* J Virol, 2014. **88**(10): p. 5217-27.
156. Humoud, M.N., et al., *Feline Calicivirus Infection Disrupts Assembly of Cytoplasmic Stress Granules and Induces G3BP1 Cleavage.* J Virol, 2016. **90**(14): p. 6489-6501.
157. Reineke, L.C. and J.R. Neilson, *Differences between acute and chronic stress granules, and how these differences may impact function in human disease.* Biochem Pharmacol, 2019. **162**: p. 123-131.
158. Gelinas, J.F., et al., *Enhancement of replication of RNA viruses by ADAR1 via RNA editing and inhibition of RNA-activated protein kinase.* J Virol, 2011. **85**(17): p. 8460-6.
159. Wang, Y. and C.E. Samuel, *Adenosine deaminase ADAR1 increases gene expression at the translational level by decreasing protein kinase PKR-dependent eIF-2alpha phosphorylation.* J Mol Biol, 2009. **393**(4): p. 777-87.
160. Li, Z., K.C. Wolff, and C.E. Samuel, *RNA adenosine deaminase ADAR1 deficiency leads to increased activation of protein kinase PKR and reduced vesicular stomatitis virus growth following interferon treatment.* Virology, 2010. **396**(2): p. 316-22.
161. Toth, A.M., et al., *RNA-specific adenosine deaminase ADAR1 suppresses measles virus-induced apoptosis and activation of protein kinase PKR.* J Biol Chem, 2009. **284**(43): p. 29350-6.
162. Castanier, C.Z., N.; Portier, A.; Garcin, D.; Bidère, N.; Vazquez, A.; Arnoult, D., *MAVS ubiquitination by the E3 ligase TRIM25 and degradation by the proteasome is involved in type I interferon production after activation of the antiviral RIG-I-like receptors.* BMC Bio, 2012. **10**(44).